Republic of Iraq
Ministry of Higher Education
& Scientific Research
University of Babylon
College of Education for Pure Sciences
Department of Physics

Linear and Nonlinear Optical Properties of Laser Dyes Doped with Metallic Nanoparticles Prepared by Pulsed Laser Ablation Method in Liquids

A Thesis
Submitted to the Council of College of Education for Pure Sciences, University of Babylon in Partial Fulfillment of the Requirements for the Degree of Doctor of philosophy in Education/Physics

By

Rusul Kadhom Mahmood Kadhom

B.Sc. in Physics
(University of Babylon, 2013)
M. E. Sc. in Physics
(University of Babylon, 2017)

Supervised by
Prof. Dr .Talib Mohsen Abbas Al-Shafai

2023 A.D. **1445 A.H.**

بسم الله الرحمن الرحيم

"فَأَمَّا الزَّبَدُ فَيَذْهَبُ جُفَآءً وَأَمَّا مَا يَنفَعُ النَّاسَ فَيَمْكُثُ فِي الأَرْضِ كَذلِكَ يَضْرِبُ اللَّهُ الأَمْثَالَ"

صدَقَ الله العَظِيم

[سورة الرعد / الآية ١٧]

Dedication

This study is dedicated wholeheartedly to Almighty Allah, thank you for the guidance, strength, power of mind, protection and skills and for giving me a healthy life.

my beloved parents, who were my source of inspiration and gave me strength when I thought about giving up, they continuously provided their moral, spiritual, emotional and financial support.

To my brothers, sister, relatives, mentor, friends, and classmates who shared their words of advice and encouragement to finish this study.

RUSUL

Acknowledgements

Praise be to Allah the Lord of all creation, who gave me health and strength to undertake the present research.

Then, I want to thank my supervisor **Prof. Dr. Talib Mohsen Abbas Al-Shafai** for the countless hours he has devoted to this thesis. Their comprehension and expertise in my research area greatly improved the content of this thesis. I am grateful, throughout this project, for their helpful comments, suggestions and constructive criticism. My research has drawn significant benefits from their informative suggestions.

A word of thanks goes to the staff members of the Department of Physics at the College of Education for Pure Sciences and to the Dean of the College of Education for Pure Sciences for their help and kind assistance.

RUSUL

Supervisor Certificate

I certify that this thesis entitled ***"Linear and Nonlinear Optical Properties of Laser Dyes doped with metallic nanoparticles prepared by pulsed laser ablation method in Liquids"*** *was prepared by the student (**Rusul Kadhom Mahmood**) under my supervision at the College of Education for pure sciences, University of Babylon in partial fulfillment of the requirements the Degree of ph . D degree in Education \ Physics*

Signature:

Name: **Dr. Talib Mohsen Abbas**
Title: Professor

(Supervisor)

Date: /9/2023.

Head of the Department Certificate

In view of the available recommendation, I forward this thesis for debate by the examining committee.

Signature:

Name: **Dr. Khalid H. Abass**

Title: Professor

(Head of Physics Department)

Date: /9/ 2023.

Contents

List of Figures

List of Tables

List of symbols and abbreviations

Symbol	Meaning	Unit
w_o	Beam waist radius	μm
z	Distance	m
λ	wavelength	nm
$R(z)$	The beam's radius of curvature	m
θ_0	the divergence angle of the laser beam	rad
f	the length of the focal distance of the lens	cm
(d_{focus})	the diameter of the spot	cm
A	Absorbance	
I	The intensity of the laser	W/m^2
I_o	Incident light intensity	W/m^2
L	the length of the optical path	cm
C_m	Molar concentration	mol/L
T	Linear transmittance	
α_o	Linear absorption coefficient	cm^{-1}
d	the thickness	cm
n_o	Linear refractive index	
c	Speed of light in vacuum	m/sec
v	Speed of light in media	m/sec
P	Polarization	w
E	The electric field	V/m
χ^1	The linear susceptibility	
χ^2	Second order nonlinear susceptibility	
χ^3	Third order nonlinear susceptibility	
n_2	Nonlinear refractive index	m^2/W
$\Delta\phi_o$	Nonlinear phase variation at the focus	rad
L_{eff}	Effective length	mm
P_{peak}	The peak power of the laser pulse	
k	the wave number $k = 2\pi/\lambda$	cm^{-1}
ΔT_{p-v}	The variance of the aperture transmittance	

β	Nonlinear absorption coefficient	m/W
W_m	Molecular weight	g/mol
W	weight	g
V	Volume	mL
C	Concentration of Matter	mol/L
C_1	Primary concentration	mol/L
C_2	New concentration	mol/L

Abbreviation	Full Name
Ag	Silver
Au	Gold
Cu	Copper
Nps	Nanoparticles
NLR	Non Linear Refraction
NLO	Nonlinear Optics
NLA	Non Linear Absorption
Nd:YAG	Neodymium-doped Yttrium Aluminum Garnet
Rh B	Rhodamine B
Rh 110	Rhodamine 110
Rh Mix	Rhodamine B +Rhodamine 110
Rh6G	Rhodamine 6G
SEM	Scanning Electron Microscope
TEM	Transmission Electron Microscope
TPA	Two Photons Absorption
UV	Ultra Violet

Abstract

In this stady, solutions of organic laser dyes (Rhodamine 110, Rhodamine B) and their mixture were prepared dissolved in organic solvents (ethanol and methanol) at different concentrations (0.01, 0.03, 0.05) mM. The linear optical properties of all the prepared solutions were studied using spectrophotometers. UV-Visible, the results showed that the values of absorbance and the values of linear optical parameter (linear absorption coefficient and linear refractive index) increase with increasing concentration, and the hight's values of dyes dissolved in methanol solvent, and that Rhodamine B dye gives the highest values compared to the other dye and the mixture.

Some metallic nanoparticles (Cu,Au,and Ag) NPs were prepared by the liquid pulsed laser ablation method, using a ND: YAK laser at a wavelength of (1064 nm), firing a laser beam with energy (300 mw) on targets of these materials placed in a specific solvent. This is to obtain a colloidal liquid with a volume of (10 ml) containing nanoparticles. Then, the nanoparticles samples were examined using transmission electron microscopy (TEM) and scanning electron microscopy (SEM) images, to ensure their nanoscale dimensions and homogeneous distribution within the colloidal solution.

Solutions of laser organic dyes and their mixture were prepared at a constant concentration of (0.05) mM, and these solutions were mixed with solutions of nanoparticles at a ratio of (1:3) in order to study the effect of these materials on the linear and nonlinear optical properties of these dyes in order to benefit from them in the field of nonlinear optics.

The results of the linear optical properties of the dye mixture solutions used in this study with the prepared nanoparticles showed that the absorbance values and the linear optical coefficients at the wavelength (532 nm) increased by adding the nanoparticles, and that the highest of these values were for the

Rhodamine B dye mixture solution dissolved in methanol solvent with Ag NPs prepared with the same type of solvent.

The nonlinear tests included the use of Z-Scan technique in both open and closed aperture cases to obtain the nonlinear absorption coefficient (β) and the nonlinear refractive index (n_2), respectively. The measurements were performed using a solid-state laser with a wavelength of (532) nm and a power of (50) mW.

The results of the nonlinear optical properties of laser organic dye mixture solutions with nanoparticles prepared in this study showed that all these solutions give nonlinear absorption (two photon absorption), and that the best value of the nonlinear absorption coefficient (β) is for pure Rhodamine 110 dye solution dissolved in ethanol solvent, which is (3.65×10^{-3} cm/mW). The results also show that these solutions are considered nonlinear materials as a de-focusing medium, and that the best value of the nonlinear refractive index (n_2) is (3.92×10^{-10} cm^2/mW) for the dissolved Rhodamine B dye mixture solution. in a methanol solvent with Ag NPs.

The results of this study showed the possibility of using all samples of pure and grafted dyes and their mixtures in various electro-optical applications as determinants of optical power. Laser organic dyes (pure and grafted) are good materials in the field of nonlinear optics and their applications due to their high nonlinear response that operates at a wide spectral range.

1.1 General Introduction

Laser dyes are Hydrocarbons unsaturated compounds where the advantage of its containing to double or triple bonds is conjugated with chains of carbon atoms. This system has the advantage of light absorbed in the wave length (200-700nm) and the transmission spectrum of absorption in the visible region. The dye laser has an important role in the history of the study and development of optical spectroscopy [1].

The dye laser provides much higher spectral brightness compared to the conventional lamp sources. The gain media of solid-state laser have a large tuning range gave a limited gain in the infrared region of the spectrum; till that time the dye laser will keep on being the workhorse for experiments requiring tunability in the visible. Consequently, much work has gone into designing and engineering dye laser sources [2].

The active medium of any dye laser is laser dye. These very often highly colored substances play the major role in the overall performance of any dye laser. Both pulse and continuous operation is possible. In addition, their unique photophysical properties make them ideal candidates for the generation of ultrashort light pulses [3].

A group of dyes are used to cover the spectral range (500-700) nm, and it is very efficient making it widely used in dye lasers. The recent development of the dye laser has opened up an important new field of applications for organic dye. The most important classes of laser dyes are xanthenes dye, depending on the end groups xanthenes has brilliant fluorescent yellow to pink to bluish red dyes characterized by the presence of the xanthenes nucleus [4].

Organic dyes are one of the materials which play an important role in the nonlinear optics field, because of the large variety of these compounds at high intensities, fast response, large nonlinear properties, and easy to process integrated into optical devices. Organic materials such as organic dyes have compatibility with other materials [5,6].

Nanotechnology represents one of the major breakthroughs of modern science, enabling materials of distinctive size, structure, and composition to be formed. For the smaller particles the percentage of surface atoms increases, leading to changes in physical and chemical properties of the materials [7].

Nonlinear optical properties have been the subject of numerous investigations theoretically and experimentally during recent years due to their applications to many branches. The nonlinear optical properties are important parameters in characterizing and determining the applicability of any material to nonlinear optical devices. There are several techniques for measuring these parameters like degenerate four waves mixing third harmonic generation and Z-Scan technique [8].

It is a sensitive and popular experimental method to measure intensity dependent of nonlinear optical (NLO) properties of materials which can rapidly measure both nonlinear absorption (NLA) and nonlinear refraction (NLR) in solids, liquids and then studying the optical limiting behavior [9,10]. Optical limiters are devices that make use of organic materials. They are used to protect the eyes and sensors. An optical limiter, in an ideal world, would transmit light linearly at low incident light but become opaque at high incident light [11].

1.2 Literature Survey

Several researches study the linear and nonlinear properties of organic dyes.

In (2010) Z. Mahdi [12] studied nonlinear optical properties of the mixed donor (C_{480}) acceptor (Rh6G). The nonlinear optical properties were measured by Z-scan technique, using Q-switched Nd: YAG laser with (1064 nm) wavelength. The obtained nonlinear properties results of the mixture (C480/ Rh6G) showed a negative nonlinear refractive index and reverse saturation absorption. Results showed that mixture of laser dyes are effective nonlinear optical materials as compared to individual laser dyes.

In (2011) G. Balaji [13] studied Nonlinear properties of Safranin O dye for applications in The optical spotter was measured using a Nd-YAG CW laser at a wavelength of 532 nm and a n coefficient was found The nonlinear refraction changes with concentration, and the dye dissolved in different concentrations in the solution showed that Nonlinearity has a thermal effect

In (2012) R. A. Ali et al .,[14] studied the spectroscopic characteristics of of laser dye RhB in ethanol and methanol solvent at concentration of (10^{-4}) M, depending on solvent polarity. The results had been indicated that . the increase in the polarity of the solvent occurs displacement in spectra towards the longer wavelengths, and also variation in quantum efficiency value as a function of increasing in solvent polarity and smallness area under the curve as in methanol where is the methanol polarity is larger than ethanol polarity.

In 2013, F. Hajiesmaeilbaigi *et al.* [15] synthesized colloidal gold nanoparticles using the technique of laser ablation. Investigations were conducted on the laser dye Rhodamine B linear and nonlinear absorption in water both with and without the addition of Au nanoparticles. The samples' emission spectra were investigated. Results demonstrate a red shift in the fluorescence emission when an Au nanoparticle-containing dye is used. The emission spectra of the samples were investigated. When an Au nanoparticle-containing dye is applied, the results show a red shift in fluorescence emission. Using the traditional Z-scan method, nonlinear absorbance in solutions of Au, Au/Rhodamine B, and Rhodamine B was measured.

In 2014, A. H. Al-Hamdani *et al.* [16]. investigated the spectrum characteristics absorption and fluorescence of Rhodamine B dye, which was dissolved in chloroform at various concentrations (3×10^{-5}, 8×10^{-5}, 8×10^{-4}, 5×10^{-4}, 2×10^{-4}, and 2×10^{-3}) M. The measured results showed a red shift in the fluorescence spectrum and a blue shift in the absorption spectra as the concentration increased.

In 2014, H. Kitching *et al.* [17] studied the interaction of gold and silver nanoparticles with Malachite green (MG) dye. The result of the UV-Vis spectrum showed only a small peak at (685) nm of Malachite green dye doped with gold nanoparticles while pure MG dye was found at (617) nm in relative proximity to the aggregate peak, these effects were not observed with silver nanoparticles.

In 2015, U. Majitha Parvi , *et al* [18] Studying the nonlinear optical properties of a dye Methylene Blue with Z-Scan technology, use He-Ne laser with wavelength of 632.8 nm, showed .The dye has a negative

nonlinear refraction with a large peak in the nonlinear refractive index. It has an absorption coefficient Saturable nonlinearity, as this dye has a large third-order nonlinearity compared toSome optical materials, polymers and organic materials

In 2016 G. Boudebs, et al,[19] verified that, in the presence of relatively moderate NL absorption, the recently introduced dark-field Z-scan system generally produces an optical output signal that is almost NL refractive. It has also been shown that the NL refractive indices sign can be calculated experimentally. Another purpose was to confirm the n2 values already reported using the other methodology, it is beam waist relative variation (BWRV). The measured DFZscan profiles and the theoretical curves achieve good agreement .

In 2017, S. Jeyaram, T. Geethakrishnan [20] , studied the third-order nonlinear optical properties of aqueous solutions of (Acid green 25 dye) using the Z-scan method using a continuous laser with a power of 5mW and a wavelength of 632 nm, where they found an increase in each of the modulus Nonlinear absorption and nonlinear refractive index with increasing concentration, and the negative sign of the refractive index indicates the behavior of self-defocusing and the mechanics of nonlinear absorption and nonlinear refraction refer to the behavior of Reverse Saturable Absorption (RSA) and to the thermal nonlinear effects respectively.

In (2017) L.G. Khlaif, [21] investigated by using a casting technique, a thin layer of Rhodamine B dye and TiO_2 nanoparticles doped in PMMA polymer was created. UV-Vis spectrum absorption was used as the sample. The Z-scan method was used to test the nonlinear optical characteristics

using Nd:YAG laser with a wavelength of 1064 nm. Estimates of the thin film's nonlinear refractive index (n_2) and nonlinear absorption coefficient (β) for various laser energy revealed that both values declined with increasing laser beam intensity. Additionally, the kind of was (n_2) negative nonlinear reflective and two-photon absorption**.**

In 2018, A. H. Al-Hamdani, [22] studied Rhodamine B (RB) dyes doped in poly (vinyl alcohol) (PVA) polymer films and showed nonlinear (NL) optical characteristics. To examine the impact of dye concentration on its NL characteristics, Z-scan at a constant 532 nm wavelength was utilized. While the closed aperture Z-scan exhibits a transition from positive (focusing) to negative (defocusing) nonlinearity at increasing dye concentration, the open aperture Z-scan shows a reverse saturable absorption behavior (positive type) of NL absorption (NLA) coefficient (β) in the RB+PVA matrix. With an increase in dye concentration, the NL refractive index, NLA coefficient, third-order susceptibility, and second order hyper polarizability all increase.

In 2019 J. Dong, et al.[23] synthesized gold nanoparticle (AuNPs) using Turkevich process. The morphology, the effect of particle size and size distribution of the AuNPs were studied in detail. The size of the (AuNPs) was optimized from (15) nm to (50) nm by reducing the molar ratio between NaCt and HAuCl4 from (2.8) to (1.5). As the molar ratio reduced, the AuNPs became more polydispersed but less spherical. AuNPs were extensively characterized for morphology, optical properties, surface chemistry, and chemical composition by using UV-visible spectrum, transmission electron microscopy (TEM), X-ray photoelectrons spectroscopy (XPS), Fourier transform infrared spectroscopy (FIIR) and Inductively coupled plasma mass spectrometry (ICP-MS). Data from the

XPS and FTIR, showed the existence of carbon, oxygen, sodium at the surface of AuNPs, these results were typical for prepared gold nanoparticles by using Turkevich process. Lastly ICP-MS tested the colloidal AuNPs samples chemical structur .

In 2020, Anitha Prakash , *et al*. [24] preparing gold nanoparticles using a laser ablation method and studying their effect on the optical properties of the dye (Neutral Red). A slight increase in the linear absorption intensity of the dye was found in the presence of gold nanoparticles. The third-order nonlinear optical properties were investigated using a single-beam Z-scan technique in the nanosecond regime. In the open-slot mode, the samples showed combined behavior of saturable absorption (SA) and reverse saturable absorption (RSA) characteristics. The study in the closed-slot mode revealed that there was a negative nonlinearity for the samples. Various nonlinear optical variables were determined, such as nonlinear absorption and refraction coefficients. They noticed that when gold nanoparticles were present, the nonlinear optical properties of the Neutral Red dye improved significantly, and this is explained on the basis of the increased effects produced by gold nanoparticles when finding results

In 2020, A. Prakash et al, [25], prepared gold nanoparticles using a laser ablation method and studied their effect on the optical properties of Neutral Red dye. Where a slight increase in the linear absorption intensity of the dye was found in the presence of gold nanoparticles. The third-order nonlinear optical properties were investigated using the single-beam Z-scan technique in the nanosecond regime. In the open aperture mode, the samples showed combined behavior of saturable absorption (SA) and reverse saturable absorption (RSA). The study in the closed aperture mode

revealed that there is a negative nonlinearity of the samples. Various nonlinear optical variables such as nonlinear absorption and refraction coefficients were determined. And they noticed that when there were gold nanoparticles, the nonlinear optical properties of the Neutral Red dye improved significantly, and this is explained on the basis of increasing the effects produced by the gold nanoparticles when finding the results.

In 2021, A.U., Habeeba, *et al*. [26] investigated the nonlinear optical of conjugated organic dyes for optical limiting applications and demonstrate a broad optical transmittance window (400-600 nm) with absorption peaks in the UV region. However, exhibits an altered band structure and extensive absorption in the visible domain (448 nm).

In (2022) B. A. Naser and H. Fadhel [27] studied optical nonlinearities and optical limiting behaviors for mixture of two organic laser dyes: Rhodamine B (RB) and Methyl violet (10B) dissolved in ethanol solvent at concentration (10^{-6}) M , have been measured utilizing Z-Scan setup. The measurement was completed using continuous wave(CW) diode pump solid state laser at wavelength (457 nm) and power (84mW).The closed-case Z-scans of all samples give self-defocousing phenomena. The consequences of the open-case of all samples give two photon absorption. Nonlinear optical properties of mixture dye is larger than those for single dyes. The results revealed that all samples can be a good candidate for optoelectronic and photonic applications .

In 2023 , **E. Silva, A. R. Vilchis-Nestor, *et al*.[28**] The ZnO NPs were obtained using varying concentrations of *Selaginella lepidophylla* as a chelating agent. The morphological analysis confirmed spherical shape and sizes of 19.86–27.75 nm for the

obtained ZnO. The structural analysis revealed a hexagonal wurtzite phase and high crystallinity. Additionally, bandgap values of 2.7 eV to 2.9 eV were calculated through analysis of the optical properties. Elemental analysis identified the main Zn, O and C peaks, as well as oxygen vacancies in the ZnO lattice. The UV photocatalytic performance of the ZnO NPs was evaluated through the discoloration of RhB as a model organic pollutant. The ZD4 sample demonstrated the best results with 99.7% dye removal after 180 min, showing excellent potential for other applications.

1.3 Aims of the Work

1. Study the, linear and non-linear optical properties for all samples of organic laser dyes (Rhodamine B) and (Rhodamine 110) dissolved in ethanol and methanol solvent at different concentrations .
2. Synthesis mixing of these two dyes in different ratios and different concentrations dissolved in ethanol and methanol solvent.
3. Preparing of (Au, Ag and Cu) Nps at different grain size for different solvents (ethanol and methanol) by the pulsed laser ablation method.
4. Study the effect of addition (Au, Ag and Cu) Nps on the linear optical properties (linear refractive index and linear absorption coefficient) and on the nonlinear optical parameters (nonlinear refractive index and nonlinear absorption coefficient) at constant concentration.
5. Possibility using all samples of organic laser dyes and their mixture as optical limiting.

2.1 Introduction

This chapter an outline of the background theory used in this thesis. In order to achieve this aim, we provide the linear and nonlinear optical characteristics of dye solutions comprising Rh110, Rh B, and Rh mix. The beam characteristics and its criteria discussed in detail in this chapter.

2.2 Organic Compounds

Hydrocarbons and their derivatives, which are used as active media in lasers dye and categorize as follows:

2.2.1 Saturated compounds

Organic compounds without double or triple bonds usually absorb at wavelength below 160nm, corresponding to a photon energy of 7.769 eV. This energy is higher than the dissociation energy of most chemical bonds. Therefore, photochemical decomposition is likely to occur, so such compounds are not very suitable as the active medium in lasers [29].

2.2.2 Unsaturated compounds

compounds are characterized by double or triple bonds, and these compounds absorb wavelengths above (200nm). Examples of such compound are laser dyes which usually contain double bonds (conjugeated) Rhodamine - 6G dye (R6G) , Rh 110 and Rh B which belongs to the family of Xanthenes class and the Coumarin -2 dye (C2) [29].

2.3 Organic Laser Dyes

Laser dyes are Hydrocarbons unsaturated compounds where the advantage of its containing to double or triple bonds is conjugated with chains of carbon atoms. This system has the advantage of light absorbed in the range (200-700) nm and the transmission spectrum of absorption in the visible region**.** It can be used as a laser medium in a dye laser [30]. Dye lasers entered

the field of scientific research at a time when many of laser active materials had already been found. Some properties of dye lasers which have attractive in different respects [31].

Dye laser considered as the most important materials because it is one of the most effective laser sources due to their important contribution in the technology and science field, and using it in several applications such as optics, electronics, non-linear optics, dyes chemistry, local area communication networks, and sensors [32].

Organic dyes are one of the materials which play an important role in the nonlinear optics field, in particular, it has a great impact on information technology and industrial applications, addition, the organic materials such as organic dyes have compatibility with other materials [33].

The Rhodamine dyes are an known series of dyes, e.g., the first member of the series, rhodamine B was synthesized (1887). All of the rhodamines are based structurally on xanthenes, which contain chromophore with amino or hydroxyl groups meta to the oxygen. Rhodamines are commercially the most important amino xanthenes .They cover the wavelength region from (500-700) nm and are generally very efficient [34]

2.4 Dyes Classification

Normally, dyes are classified in two separate ways, either accordance to their chemical structure or according to the method of application. Around thirty different groups of dyes can be discerned based on chemical structure. Organic dyes are one of most used in dye laser and classified according to their chemical structure in to [35]:

1. Poly methane dyes: gives a laser action in near IR (0.7-1.5) mM.
2. Xanthene dyes: gives a laser action in visible region (500-700) nm.

3. Coumarine dyes: gives a laser action in blue – green region (400- 500) nm.
4. Scientillate dyes: gives a laser action in UV-region (< 400 nm).

The approximate working ranges of various laser dyes are shown schematically in figure (2.1)

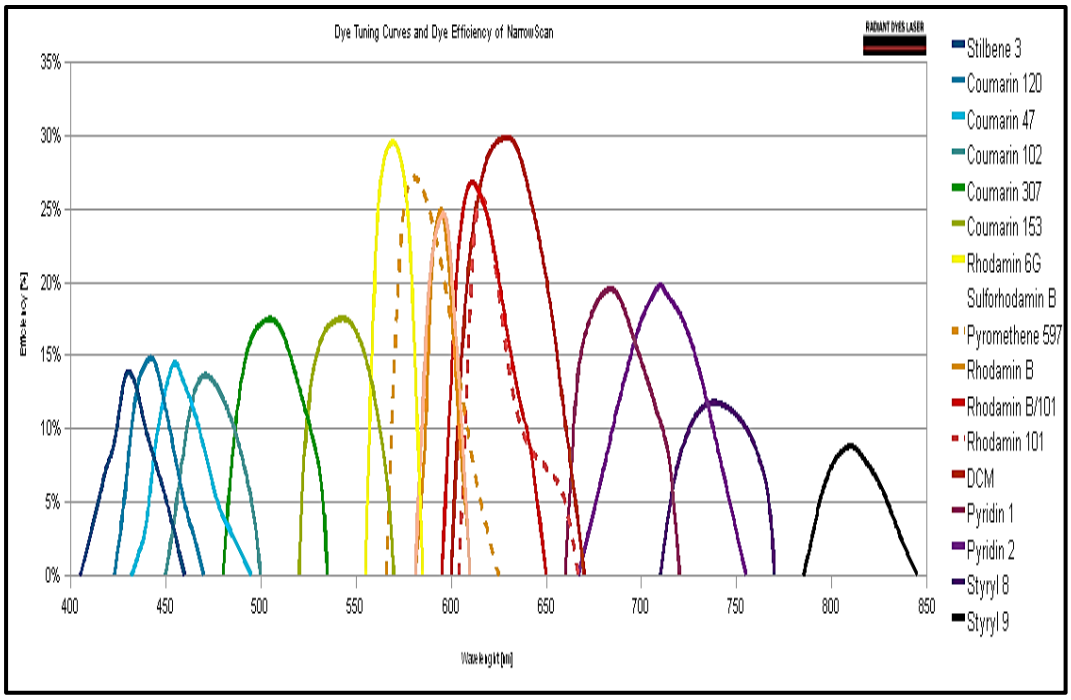

Figure (2.1): scheme Laser dyes [36].

2.5 Applications of Laser Dyes

There are many applications for laser dyes, including [37]:

1. Industrial applications of laser dyes include separation of isotopes of important radioactive elements such as Uranium. Uranium is used as fuel in the nuclear power reactors to generate electricity.
2. Medical applications of laser dyes include skin treatments, including tattoo removal, diagnostic measurements, lithotripsy and activation of photosensitive drugs for photodynamic therapy, etc.

3. Optical communications.
4. Image processing .
5. Switching.
6. 3D data storage and optical limiting

2.6 Parameters Effecting on Properties of Laser Dye

There are many factors that affect the laser properties of the dyes. The solid laser active medium, the liquid and the gas are generally affected by the design conditions of the laser system. In liquid laser active circles, special factors are affected by the concentration of the solution, the type of solvent, the viscosity of the solution and its acid, and all the influencing factors affect the electronic structure i.e the distribution of the electrons of the effective medium at its energy levels, the molecular electronic energy transitions, molecular oscillatory energy, which changes the wavelength ranges of the emission spectra in the active medium, especially the laser pigments, and this has led to the possibility of synthesis (change wavelength) of the dyes [38].

2.6.1 Concentration effect

The concentration is one of most important parameters that has influence on the organic dyes, where in a very dilute samples, dye dissolves completely into monomers. In such kind of dye solutions, the intrinsic absorption of the dye molecules is affected by dye-solvent interaction. Dyed interaction is negligible because of the large average distance between the dye molecules in dilute solution. By increasing dye concentration dimer or higher aggregates are formed. Increasing the dye concentration leads to red shifts, that may be caused by changes in the environment of dye molecules, such as changes in polarity or polarizability. This leads to interactions between neighboring molecules, which lowers their excited state energy and produces a red shift in the spectra. At high concentrations the dye-dye interaction gains

be importance since the mean distance between dye molecules becomes small and this leads to deviation from theBeer-Lambert law [39].

2.6.2 Solvent polarity effect

Solvent polarity is the most significant property which can alter the position of the absorption or emission band of molecules by solvating a solute molecule or any other molecula species introduced into the solvent milieu. On the other hand, the fluorescent dye molecules are complex organic molecules which might carry charge centers and are thus prone to absorption changes in different media [40]. Among the numerous ways of determining excited state dipole moment with electro optical methods, the solvent-shift method is the simplest and the most widely used. The observation of solvent induced shifts of electronic bands of molecules has been used extensively in order to study the changes in electronic distribution in excited states of solute molecules. The dipole moments of a molecule in the ground state and excited state depend on the electron distribution in these states. A change of solvent is accompanied by a change in polarity, dielectric constant and change in polarizability of the surrounding medium. Thus, the change of solvent affects the ground state and the excited state differently [41].

2.7 Rhodamine 110 Dye

The chemical formula of the Rh 110 is $C_{20}H_{15}N_2O_3Cl$. This character belongs to the family of type Rhodamine, xanthan class dyes, where this family is distinguished by efficient manufacture and the excellent chemical stability of the light. Figure (2.2) shows the chemical structure of Rhodamine 110 [42].

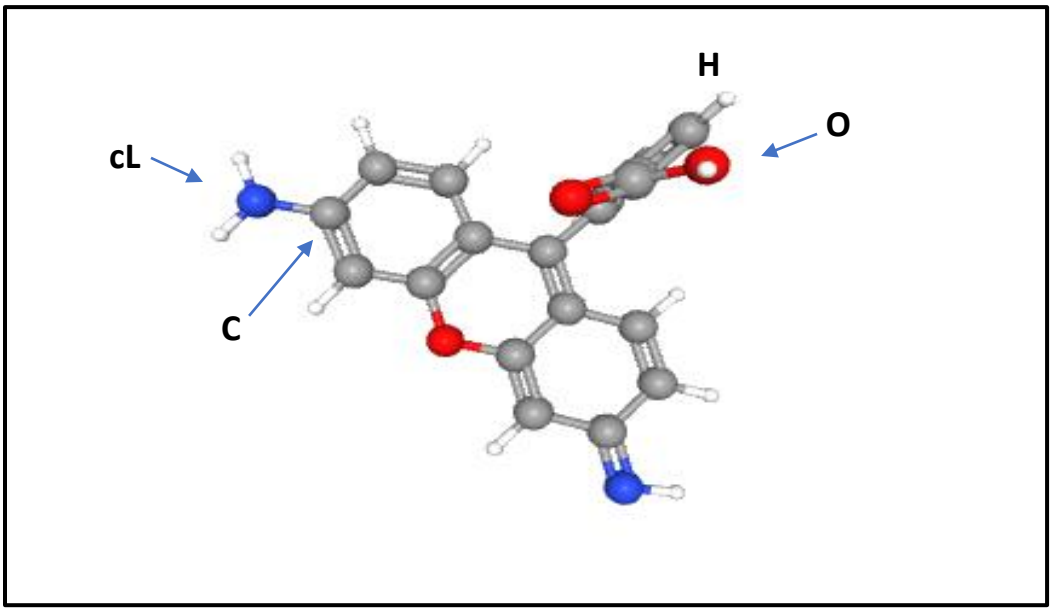

Figure (2.2) : Chemical Structure of Rhodamine 110 [42].

2.8 Rhodamine B Dye

Rhodamine B is a kind of xanthine dye. It is one of the most common spectroscopic parameters Figure (2.3) depicts the molecular structure of this dye [43,44].Rhodamines and xanthene amino acids are commonly employed in technology and research for lasing, as well as in thermochemistry as fluorescent labels and probes for the analysis of diverse substances (biological and non-biological) [45].

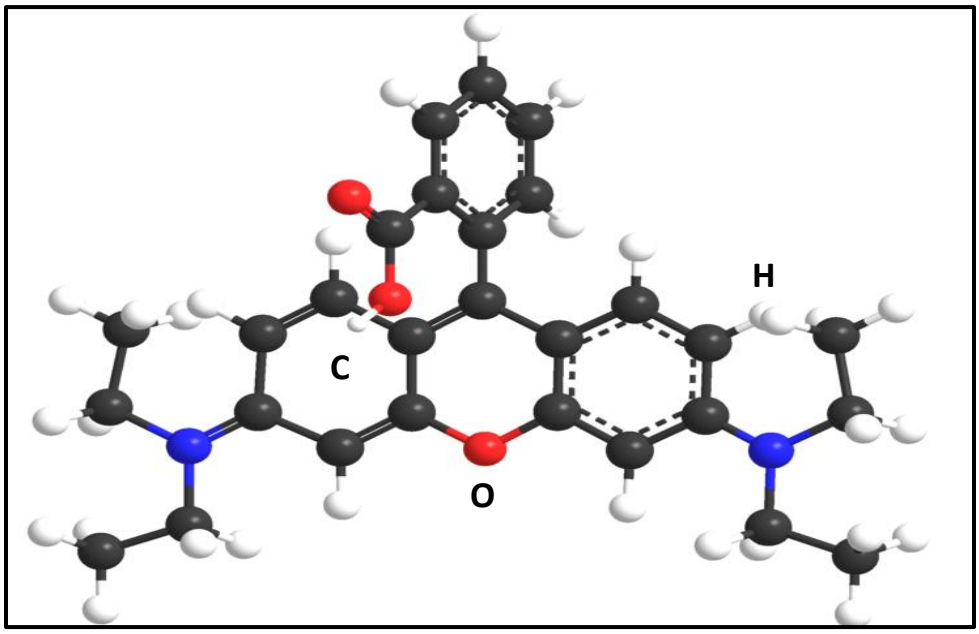

Figure (2.3): Structure of Rhodamine B types [43,44].

2.9 Ethanol Solvent

The chemical formula of the ethanol Solvent (C_2H_6O), and it is a colorless, volatile liquid with a moderate, distinct odor. it's a polar solvent. Ethanol is a versatile solvent and a chemical that is utilized in the production of organic molecules [46,47]. Figure (2.4) depicts the chemical structure of ethanol.

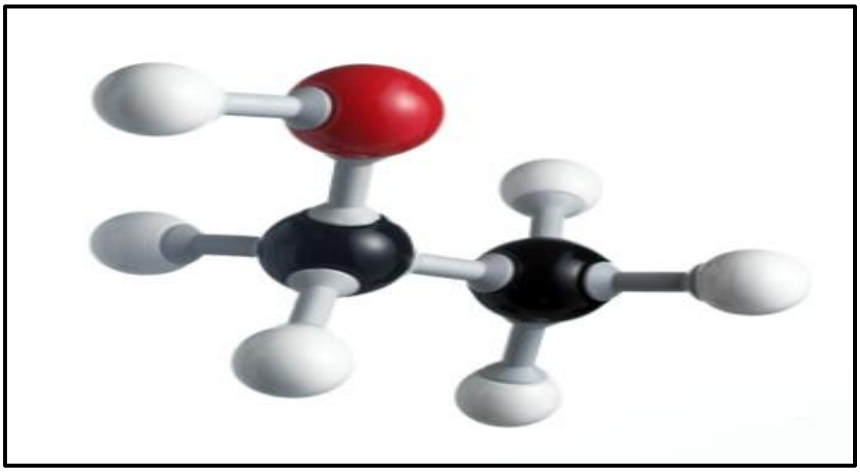

Figure (2.4): Ethanol molecule structure [48].

2.10 Methanol Solvent

The chemical formula of the methanol Solvent (CH_3OH), methanol is the most fundamental aliphatic alcohol. The functional hydroxyl group determines the reactivity of this typical representative of this class of compounds. Methanol is a clear, colorless, polar liquid that is miscible with water, alcohols, esters, and the vast majority of organic solvents; it is only marginally soluble in fat and oil. Methanol dissolves numerous inorganic compounds, particularly salts, due to its polarity [49]. Figure (2.5) shows the Methanol molecule structure.

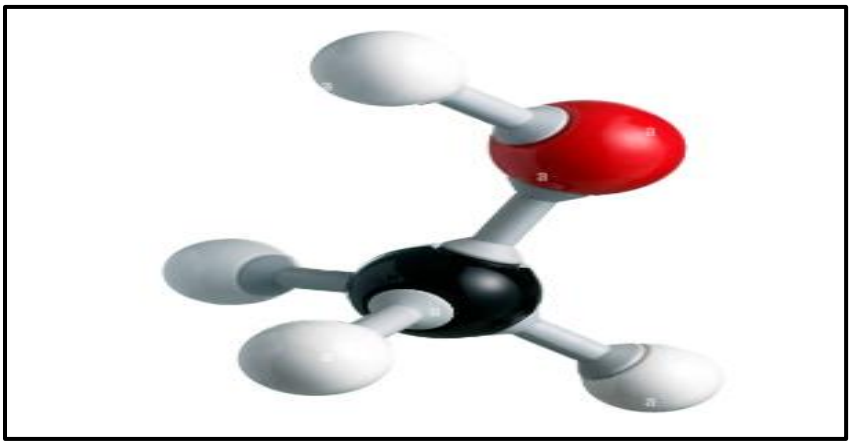

Figure (2.5): Methanol molecule structure [50].

2.11 Nanomaterials

Nanomaterials are nano-science and nanotechnology cornerstone. Science and technology in nanostructure is a broad and interdisciplinary area of research and development activity that has grown explosively throughout the world in recent years. It already has a major commercial effect, which will surely increase in the future [51, 52]. A nanometer is one millionth of a millimeter approximately 100,000 times smaller than the diameter of a human hair. The properties of nanometer-dimensional

materials differ materially from those of atoms and bulk materials. Such discrepancies are responsible for three major factors, high surface volume ratio, quantum size effect and electrodynamic interactions. All nanoparticles, because of their chemical components, have extremely high surface area to volume ratios [53,54].

The structure of the nanoparticles surface governs many of the physical properties of the nanoparticles, such as solubility and stability. The particle dimensions in the nanometer size regime make them ideal candidates for surface nanoengineering and practical nanostructure manufacturing [55, 56]. Nanomaterials are important because on this scale unique optical, magnetic, electrical and other properties are shown, in electronics, medicine, and other areas, these products have the potential for great impacts [51, 52].

Noble metal nanoparticles exhibit brilliant colors due to the resonance absorption of the surface plasmon. Examining the absorption of surface plasmon resonance is part of the big active research area to investigate properties on the nanometer scaling [57]. Nanomaterials can be divided into three categories by type, one size (e.g.surface films), two sizes (e.g. threads or fibers) and three sizes (e.g. particles). Nanomaterials have nanotechnology applications and show various physical and chemical properties from normal chemicals (i.e. nano silver, carbon nanotube, fullerene, photocatalyst, carbon nano, silica). Nano-materials with a wide range of applications in the fields of electronics, fuel cells, batteries, livestock, food and medicines [58]. Figure (2.6) shows the scheme Classification of nanomaterials with regard to dimension [59].

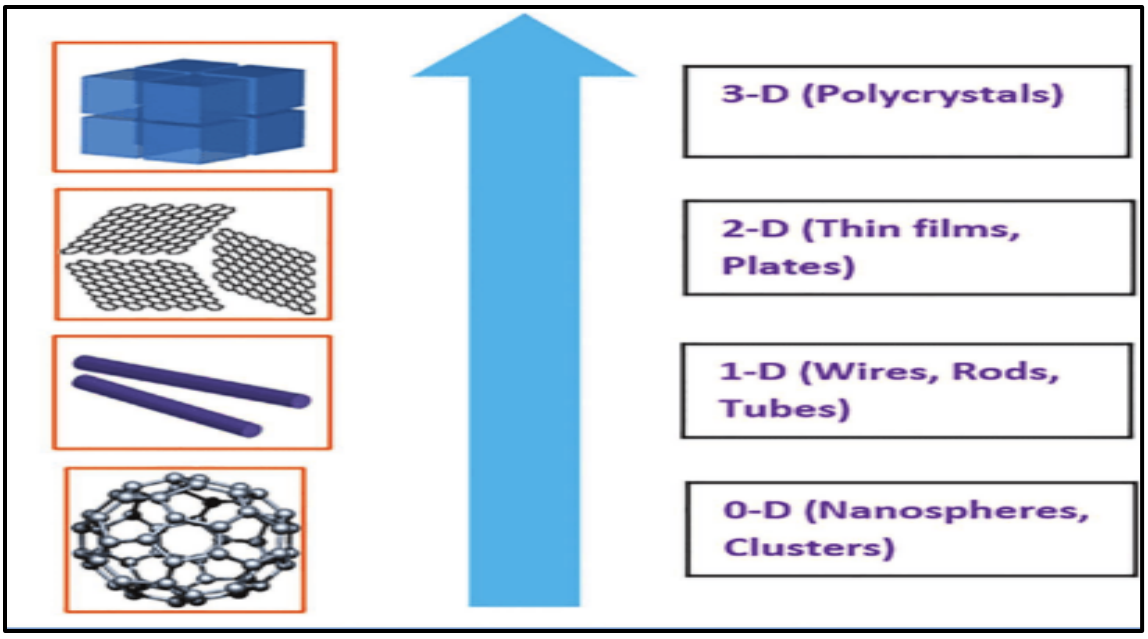

Figure (2.6) : The scheme Classification of Nanomaterials with Regard to Dimension [59]

2.12 Nanostructure

Rapidly growth of nanotechnology is related to infinite applications of devices, systems and structures, by controlling size, shape and structure at nanometer scale [60]. Materials at this scale provide many advantages, depending upon the size, shape, structure and method of preparation [61]. Particles of different types and materials at the range between (1) to (100) nm can be classified according to agglomeration of atoms and molecules as shown in Figure (2.7) into:

1. zero-dimensional (0D) nanomaterials all the dimensions are measured within the nanoscale (no dimensions are larger than 100 nm). Most commonly, 0D nanomaterials are nanoparticles. [62].
2. one-dimensional nanomaterials (1D), one dimension is outside the nanoscale. This class includes nanotubes, nanorods, and nanowires. [62].

3. two-dimensional nanomaterials (2D), two dimensions are outside the nanoscale. This class exhibits plate-like shapes and includes graphene, nanofilms, nanolayers, and nanocoatings. [62].
4. Three-dimensional nanomaterials (3D) are materials that are not confined to the nanoscale in any dimension. This class can contain bulk powders, dispersions of nanoparticles, bundles of nanowires, and nanotubes as well as multi-nanolayers [62].

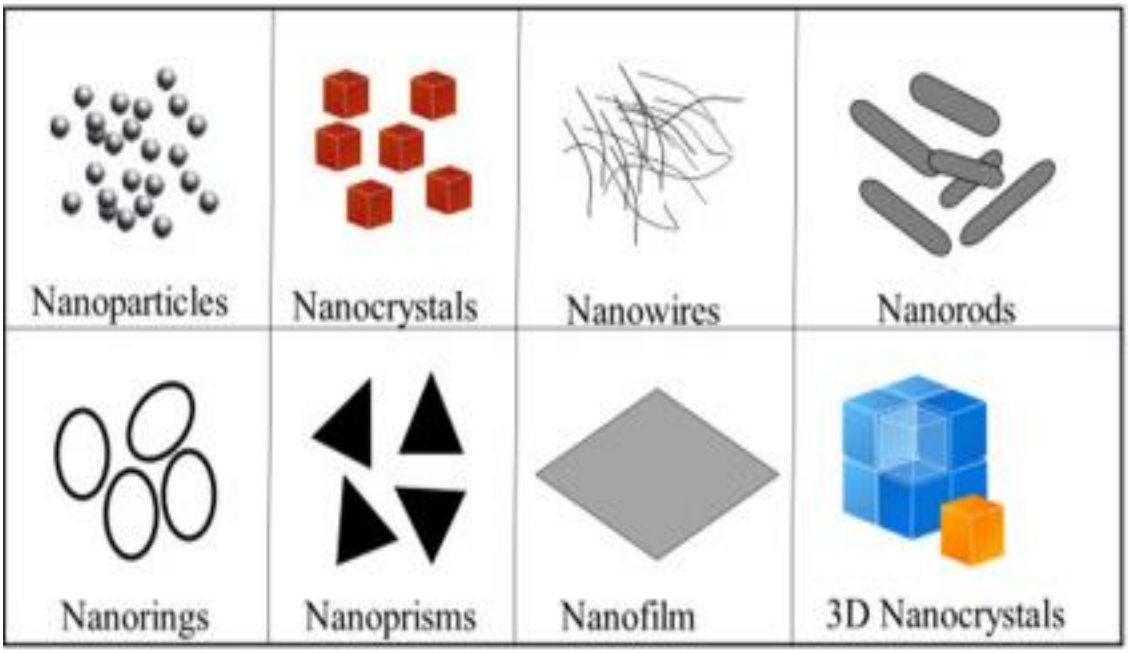

Figure (2.7): Nanoparticles classified according to their dimensions [63].

Agglomerate state of nanoparticles occurs over short distances due to van der Waals force; this agglomeration affects the chemical and the electromagnetic properties of nanoparticles [64].The agglomeration process depends on the type of nanoparticles, conditions of synthesis method and concentration of nanoparticles in solvent [65]. Agglomeration process can be avoided by several processes such as coating the nanoparticle surface by

another organic or inorganic substance or chemically stabilization by polishing slurries in aqueous suspension [66].The high development in nanoparticles synthesis techniques enables to synthesis different types of NPs such as spherical NPs, wire NP's [67].

Nanoparticles have larger enhancement of physical and chemical properties compared to bulk material due to their extremely large surface area to volume ratio [68]. Nanoparticles characteristics (physical and chemical properties) are based on the size, shape, structure, physical stability, and distribution of the nanoparticles, which can be investigated using different microscopic technique such as scanning electron microscopy, transmission electron microscopy and scanning electron microscopy [69].

2.13 Silver Nanoparticle (Ag NPs)

Silver nanoparticles has range size from 1 to 100 nm. While usually labeled as 'silver,' some are made up of a high percentage of silver oxide due to their high surface-to-bulk silver atom ratio. Depending on the application of the study, several shapes of nanoparticles can be constructed [70]. Silver nanoparticles are employed in a number of technologies and are used in a wide range of consumer items that benefit from their optical and conductive properties. Silver nanoparticles are used to increase the efficiency of light harvesting and to enhance optical spectrometers [71].

2.14 Gold Nanoparticles (Au Nps)

Although bulk gold is widely known for its lustrous surfaces and colors, when the metal decreases in size, there is a dramatic color difference. Due to its simple preparation and high stability, colloidal gold nanoparticles (Au NPs) are particularly interesting. Gold is a significant candidate for biological applications because of its chemical inertness [72]. However, the

parameters under control are the (Au NPs) size, shape, surface, chemical, and optical characteristics, which have uncovered some brand-new, intriguing possibilities [72].

Gold nanoparticles are known as stable, sized colloid solutions of gold atom particles. In this minuscule, (Au NPs) exhibits distinct physical and chemical properties relative to bulk gold. The most obvious example is the shift in colour from yellow to ruby red when turning bulk gold into nano-particulate gold. The height of the surface plasmon resonance (SPR) is (520) nm, and this peak is responsible for the ruby red color of standard gold colloids [73].Gold nanoparticle's optical-electronic properties are commonly studied for use in high-tech applications such as sensory sensors, and electronic conductors [74].

2.15 Copper Nanoparticles (Cu NPs)

Copper nanoparticles (Cu NPs) are particularly appealing due to their strong thermal conductivity and heat transfer capabilities. Cu NPs have a high surface area to volume ratio, a low cost of manufacture, and antibacterial activity, similar to precise metals like gold and silver, or palladium in terms of catalytic activity, optical, and magnetic characteristics. Researchers employ a variety of inert substances, including argon and nitrogen [75]. Copper nanoparticles are employed in a variety of technologies. It is possible to employ conductive pastes and inks containing (Cu) nanoparticles in place of the incredibly costly noble metals used in printed electronics, Applications and displays for transmissive conductive thin films [76].

2.16 Laser Beam Characteristics

Laser beam Characteristics explained in detail in the following paragraphs.

2.16.1 The Gaussian Beam

An electromagnetic beam with a transverse electric field intensity that follows a Gaussian function is called a Gaussian beam. The basic transverse mode, often known as TEM_{00}, is the mode on which the majority of lasers output beams with a Gaussian profile. Figure 2.8 depicts the Gaussian transverse irradiance profile of the laser beam, which is a perfect plane wave. [77]

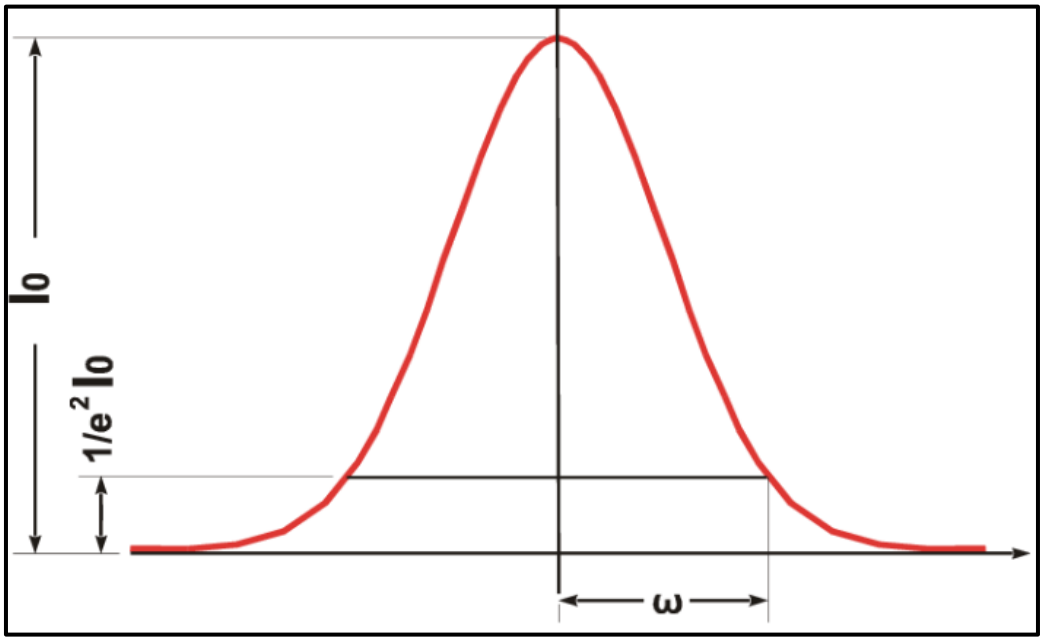

Figure (2.8): An irradiance profile for the Gaussian TEM_{00} mode [78].

2.16.2 Waist and divergence of the beam

A Gaussian beam travelling in free space will have a location size (w) at its lowest value (w_0) at a point along the beam known as the beam waist. The Gaussian profile is depicted in free space in Figure (2.9) .

The fluctuation of the spot size is given by equation. 2.1 at a distance (z) from the beam's waist for a wavelength (λ) [79].

$$W(z) = w_0 \left[1 + \left(\frac{\lambda z}{\pi W_0^2}\right)\right]^{1l2} \dots\dots\dots\dots\dots\dots\dots\dots\dots\dots \quad \dots\dots\dots (2.1)$$

The beam's radius of curvature $R(z)$ and its variation are both given by equation 2.2 [80].

$$R(z) = Z\left[1 + \frac{\pi w_0^2}{\lambda z}\right]^2 \dots\dots\dots\dots\dots\dots\dots\dots\dots\dots\dots\dots\dots\dots\dots\dots\dots\dots\dots (2.2)$$

A Gaussian beam's divergence tends to be at an angle given by equation 2.3 when it is sufficiently far from the waist [81].

$$\theta_0 \approx tan\,\theta_0 = \frac{\lambda}{\pi W_0} \dots\dots\dots\dots\dots\dots\dots\dots\dots\dots\dots\dots\dots\dots\dots\dots\dots\dots\dots\dots\dots (2.3)$$

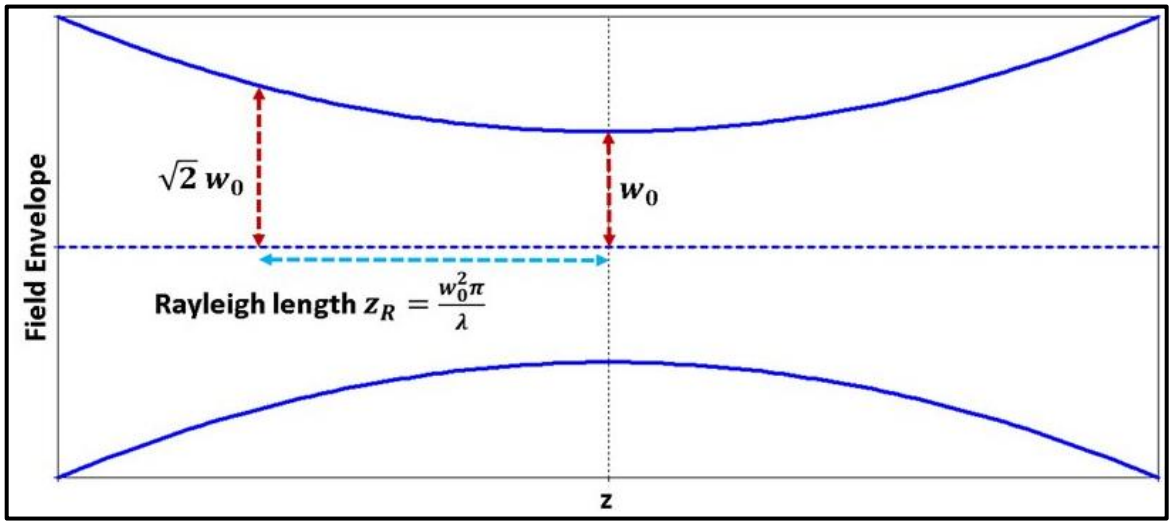

Figure (2.9): Free-space Gaussian profile [80].

When the beam is moving towards infinity, it depicts how the beam spreads. According to the aforementioned quantity, Smaller values of divergence are correlated with higher values of breadth, and vice versa [82].

2.16.3 Focusing Gaussian beam with a lens

Lenses or mirrors can photograph a Gaussian beam. The spot size (W_o) at the focal point is the same on both sides of the focusing lens when a Gaussian beam travels through it. Figure (2.10) illustrates the result of concentrating a Gaussian beam by a small positive lens, and it may be calculated by equation 2.4 [83].

$$W(z) = W_0 \left[1 + \left(\frac{f}{Z_0}\right)^2\right]^{1/2} \dots\dots\dots\dots\dots\dots\dots\dots\dots\dots\dots\dots\dots\dots\dots\dots\dots\dots\dots (2.4)$$

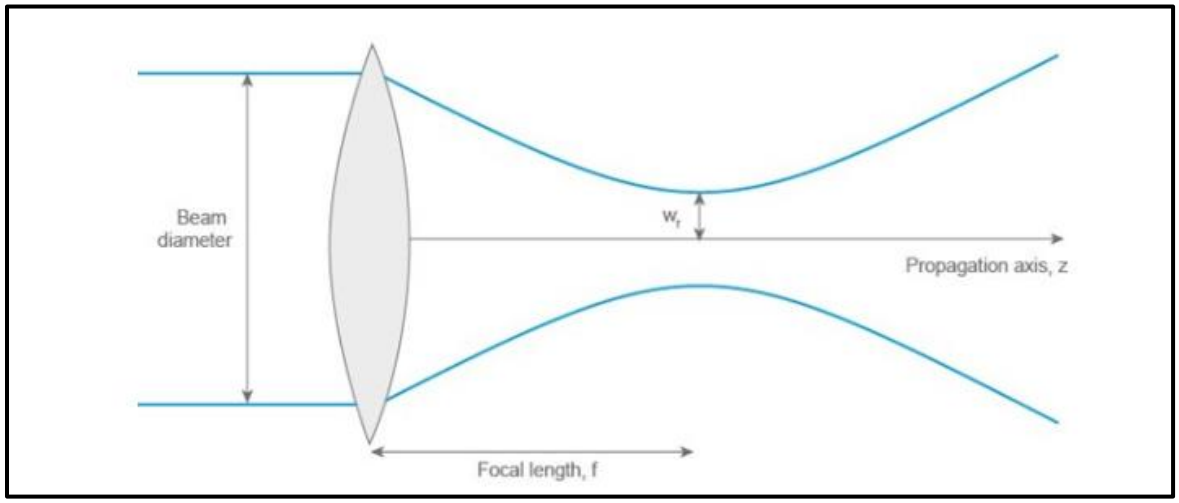

Figure (2.10): A Gaussian beam is focused using a lens [83].

Additionally, the diameter of the spot (d_{focus}) at the point of focal distance (f) from the lens, is now provided by [84]

$$d_{fous} = f\theta_0 \dots\dots\dots\dots\dots\dots\dots\dots\dots\dots\dots\dots\dots\dots\dots\dots\dots\dots\dots\dots\dots\dots\dots\dots\dots (2.5)$$

Where, f is the length of the focal distance of the lens, and θ_0 is the divergence angle of the laser beam [84].

2.17 The interaction of Laser Light with Matter

A material surface absorbs some of the laser light while reflecting other portions of it. The surface starts to get warmer as the energy is absorbed. Depending on the time frame and the purpose, there are many regimes of factors that need be taken into account. When a laser beam strikes a substance, unbound electrons absorb some of the light energy. The absorbed energy subsequently moves via the electron subsystem and is finally transmitted to the lattice, which results in the transmission of laser energy to the material [85].

Laser light's intensity results in a variety of interactions. There are two types of material interaction: linear interaction and nonlinear interaction. Nonlinear optics is a subject of science and technology that has grown out of the advantages the laser as a high-intensity coherent light source [86].

Effects of nonlinear optics are linked to changes in the material's optical constants, such as the refractive index, absorption coefficient, or both. The simplest method to handle them is to consider the interaction of the light beam with the atoms of the material as the driving force of an oscillator group operating at its natural resonance frequency [87].

2.18 Optical Properties

There are numerous benefits to studying a material's optical properties. Firstly, precise understanding of a material's optical properties over a broad range of wavelengths is necessary for its interference filters, optical fibers, and reflective coating. Secondly, the atomic structure, electronic band structure, and electrical properties of all materials may be connected to their

optical properties [88]. Linear optical qualities and nonlinear optical properties are the two categories into which organic dyes' optical properties fall.

2.18.1 The Linear Optical properties

The observation of optical characteristics in materials is the outcome of the interplay of charge nature and distribution (molecular, electronic, or ionic) within a substance with electromagnetic radiation [89]. When electromagnetic radiation strikes a material and interacts with it, a variety of processes take place. For example, some of the substance absorbs electromagnetic radiation, while other portions transmit through the material and are referred to as the transmitting ray and the reflected part, respectively [90]. To gain information on interference, it is required to understand electromagnetic radiation's transmittance, absorption, and reflectivity, structure, and type of bonds in a material. In contrast to researching the visible spectrum, which reveals the variety of real-world applications for materials, investigating the ultraviolet spectrum, for instance, displays the energy, packets, and quality of transitions inside the material [91]

One of the most important linear optical characteristics

2.18.1.1 The Absorbance

The absorbance (A), also known as optical density, is a mathematical constant that connects a sample's particle density (concentration) and sample thickness (optical path length) [91].

$$A = \log\left(\frac{I_0}{I}\right) \quad \ldots\ldots\ldots\ldots\ldots\ldots\ldots\ldots\ldots\ldots\ldots\ldots (2.6)$$

Where (I) represent the amount of light that enters the sample at the wavelength (the amount of light that is transmitted), and (I_0) is the light's

initial intensity (the light's incident intensity) before it is introduced into the sample. The possibility of absorption increases with the increase in the concentration of the material at a lower energy level and as the quantity of incoming ray photons increases. When incident rays are absorbed by a material, an electronic reaction occurs that may result in the dissolution of the material's molecules if the absorbed energy is larger than the value of the breaking down of a bond or its transfer to a higher energy level [92].

The chance of photon absorption is related to the concentration of absorbed particles in the sample and the sample thickness (the optical path and the length), The Beer-Lambert Law is an empirical connection that connects light absorption to the qualities of the medium through which the light flows. According to the law, the number of absorbing molecules in a substance is proportionate to the percentage of absorbed light in the substance. When light rays pass through a solution, an exponential function of the solute concentration controls how much light is absorbed or transmitted [93]. The equation can also be written

$$I = I_0 \ e^{-\alpha_{oP} Cm L} \ldots\ldots\ldots\ldots\ldots\ldots\ldots\ldots\ldots\ldots\ldots\ldots\ldots\ldots\ldots\ldots\ldots\ldots\ldots\ldots\ldots\ldots\ldots\ldots\ldots\ldots (2.7)$$

Where α_{oP}: indicates for the coefficient of the optical absorption, L stands for the length of the optical path., and C_m: stands for molar concentration. The equation is written [94].

$$ln \frac{I_0}{I} = \alpha_{oP} C_m L = A \ldots\ldots\ldots\ldots\ldots\ldots\ldots\ldots\ldots\ldots\ldots\ldots\ldots\ldots\ldots\ldots\ldots\ldots\ldots\ldots\ldots\ldots\ldots\ldots\ldots\ldots\ldots (2.8)$$

When using monochromatic radiation, Beer-Lambert's law can be utilized across a variety of spectral ranges, including ultraviolet, visible, and others [94].

2.18.1.2 The transmittance (T)

The proportion of incident light intensity (I) to transmitted light intensity (I_o) is known as the transmittance of the medium. Additionally, it is capable of defining the radiation energy transferred through the medium for the radiation energy impacting it. It is provided via the relationship described below [75].

$$T = \left(\frac{I_0}{I}\right) \quad \ldots\ldots\ldots\ldots\ldots\ldots\ldots\ldots\ldots (2.9)$$

In accordance with the Beer-Lambert equation, the transmittance depends as the molar concentration (Cm) and optical path length (L) of the light are both increased . Regarding the medium's permeability, it is correlated with the solution (A)'s absorbance as stated in the equation [95].

2.19 Optical constant

2.19.1 Coefficient of absorption

The percentage of the incident radiation's energy that is lost the absorption coefficient is the amount of energy absorbed in a medium related to a unit of distance in the wave's propagation direction. The energy of the photon (hυ) and the material's characteristics affect the absorption coefficient [96].

$$\log\left(\frac{I}{I_O}\right) = 2\cdot 303\, A = \alpha_0\, d \quad \ldots\ldots\ldots\ldots\ldots\ldots\ldots (2.11)$$

$$\alpha_0 = 2\cdot 303\, \frac{A}{d} \quad \ldots\ldots\ldots\ldots\ldots\ldots\ldots\ldots (2.12)$$

d: is the thickness .

2.19.2 Refractive index (n)

In a vacuum, which is a fixed quantity, light travels at a maximum speed in all of its wavelengths. In any other medium, however, this speed diminishes as it transitions between different wavelengths of material media. The refractive index of a wave is the ratio of the wavelength's speed in a

vacuum to that wave's speed in any given medium. Equation (2.13) explains this [97].

$$n = \left(\frac{C}{V}\right) \quad \ldots\ldots\ldots\ldots\ldots\ldots\ldots\ldots\ldots\ldots\ldots\ldots\ldots\ldots . (2.13)$$

where n represents the index of refractive, c is the vacuum speed of light, and v denotes the light speed in medium. The index of refraction varies with electromagnetic wave length and is not constant. Additionally, some materials have refractive indices that change depending on the direction that an electromagnetic wave travels through them, and these materials are utilized to change the polarization of these waves. The index of refraction shows a material's sensitivity to electromagnetic radiation. As the rays of the electromagnetic radiation strikes a material, they cause the charges in the material to move from their initial positions, resulting in the development of a dipole [97].

The incident wave will be transformed into vibrational energy by the created electrode dipole. As a result, the incident wave's amplitude decreases, and assuming that the energy loss due to the diodes oscillates somewhat but the delay in re-radiation slows the speed of light, the material is said to have a refractive index (n), as illustrated in equation (2.13).

As a result, it is evident that the polarization in the material generated by the fall of electromagnetic rays on it is a measure of this substance's refractive index, as a result, its refractive index (n = 1). The refractive index is generally more than one, and its value is proportional to the medium's density. There is no distinguishing unit for the refractive index. The following equation, which was used in this research's calculations after being entered into a computer software, can also be used to calculate refractive index [97].

$$n = [\frac{(4R)}{(1-R)} - (K^2)]^{\frac{1}{2}} - \frac{(R+1)}{(R-1)} \quad \ldots\ldots\ldots\ldots\ldots\ldots \quad \ldots\ldots\ldots\ldots\ldots\ldots\ldots (2.14)$$

where (n) is the index of refractive, (k); the coefficient of extinction, and (R) is the reflectivity.

2.20 Nonlinear Optical Properties

The nonlinear optics properties are the study of events that occur as a result of changes in the optical characteristics of materials as a result of intense light contact. There has been a lot of interest in nonlinear phenomena [98]. When electric fields are applied, positively charged particles move in that direction, whereas negatively charged particles move in the opposite direction. Dipole moments are created by the separation of positively and negatively charged particles, where the number of dipole moments per unit volume determines the medium's induced polarization. Electric polarization is often linearly proportional to the applied electric field (E) when the applied electric fields are small enough [99].

$$P = \chi E \ldots\ldots\ldots\ldots\ldots\ldots\ldots\ldots\ldots\ldots\ldots\ldots\ldots\ldots\ldots\ldots\ldots\ldots\ldots\ldots\ldots\ldots\ldots\ldots\ldots\ldots\ldots\ldots (2.15)$$

If the applied electric fields are strong enough to have a nonlinear dependency on them, the induced polarization, however, may be described as a power series with respect to the applied electric fields given by 2.16 [100].

$$P = \chi^{(1)} E + \chi^{(2)} EE + \chi^{(3)} \ldots\ldots\ldots\ldots\ldots\ldots\ldots\ldots\ldots\ldots\ldots\ldots\ldots\ldots\ldots\ldots\ldots\ldots\ldots\ldots\ldots\ldots\ldots\ldots (2.16)$$

$$P = P(1) + P(2) + P(3) \ldots\ldots\ldots\ldots\ldots\ldots\ldots\ldots\ldots\ldots\ldots\ldots\ldots\ldots\ldots\ldots\ldots\ldots\ldots\ldots\ldots\ldots\ldots\ldots (2.17)$$

$\chi^{(1)}$ denotes the susceptibility to linear perturbations, $\chi^{(2)}$ represents second order susceptibility to be nonlinear, and $\chi^{(3)}$ denotes third order susceptibility to be nonlinear. The term $\chi^{(1)}$ is in charge of linear refraction and absorption and is the only term that indicates the linearity between the incident electric field's induced polarization. Only non-centrosymmetric

materials, or those without inversion symmetry, contain the phrase $\chi^{(2)}$. Nonlinear optical interactions of the third order, denoted by the symbol $\chi^{(3)}$ [101].

For a few decades, nonlinear optics (NLO) has been growing as a promising field with significant applications in the fields of photonics and photoelectronics. Organic materials have substantial and quick nonlinearities, making them one of the significant classes of third order NLO materials. Many different types of organic compounds have been investigated in order to generate materials with significant third order nonlinearity [101]. Many methods, such as degenerate four wave mixing, third harmonic creation, and the Z-scan method, have been used to measure third order nonlinearity. Z-scan is the simplest approach for figuring out among these are the nonlinear refractive index and nonlinear absorption coefficient. It gives the magnitudes of the real and imaginary components of the nonlinear susceptibility, in addition to the sign of the real part. The Z-scan method may swiftly assess nonlinear refraction and nonlinear absorption in solid and liquid samples by taking use of self-focusing or self-defocusing processes in optical nonlinear materials. The two methods of Z-scan are open-aperture and closed-aperture systems [102].

2.21. Z-Scan Technique

The most alluring optical materials are organic dyes because they have strong third-order nonlinear optical characteristics. Numerous studies have been done on the NLO characteristics of organic dye molecules. There are now various experimental approaches available for measuring the third-order NLO parameters; the Z-Scan method is one of the more significant methods [103].

The basic goal of the Z-Scan approach is to calculate the intensity change in the transmitted intensity of the incident beam of a Gaussian laser through the sample as a function of the sample's distance (Z-position) from the beam focus. As shown in Figure 2.11 the transmitted beam is collected using two detector configurations: closed aperture (CA) to determine the sign and calculate the nonlinear refractive index, and open aperture (OA) to calculate the coefficient of absorption to be nonlinear [104].

Phase distortion during beam propagation changes to amplitude distortion, which is the foundation of the Z-Scan technology. The Z-Scan technique's basic operating idea is based on the sample moving from (-Z) to (+Z) along the so-called Z-axis past the focal point of a beam of a Gaussian laser. The sample is exposed to changing levels of irradiance (intensity), with the focus point providing the highest value [105].

as it moves across the concentrated beam.

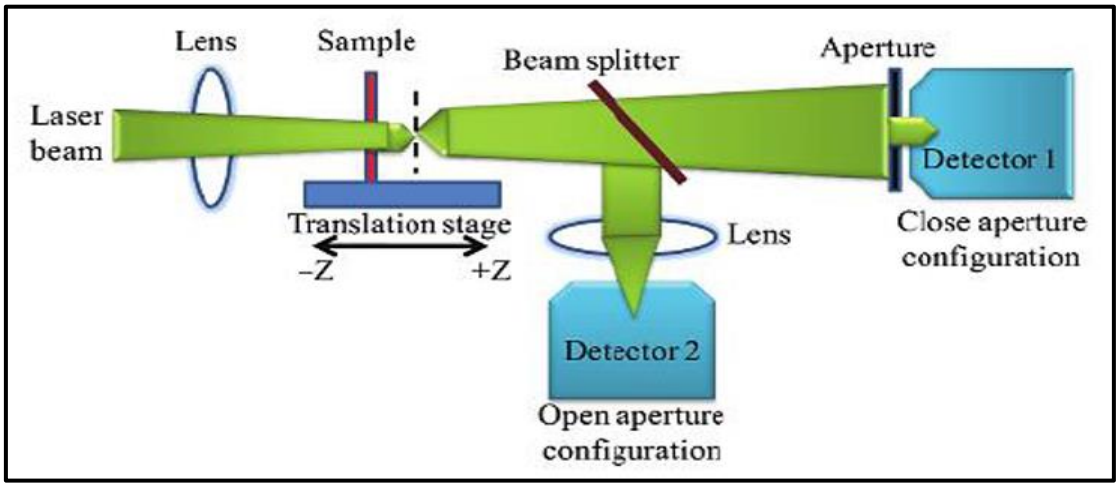

Figure (2.11): Schematics of experimental setup used for the Z-Scan with a closed and open aperture [104].

2.21.1 Closed-aperture Z-Scan

A closed aperture Z-Scan is used to quantify the change in beam intensity caused by the sample going past the focal plane of the lens (L) in Figure (2.12). The photo detector PD gathers the light that enters a far-field aperture (A) with axial centering. As shown in Figure 2.12. the sample (S) focusing by itself or defocusing by itself induces causes the index of refraction to alter, which forms a lens in sample nonlinear state and causes the change in axis intensity [106].

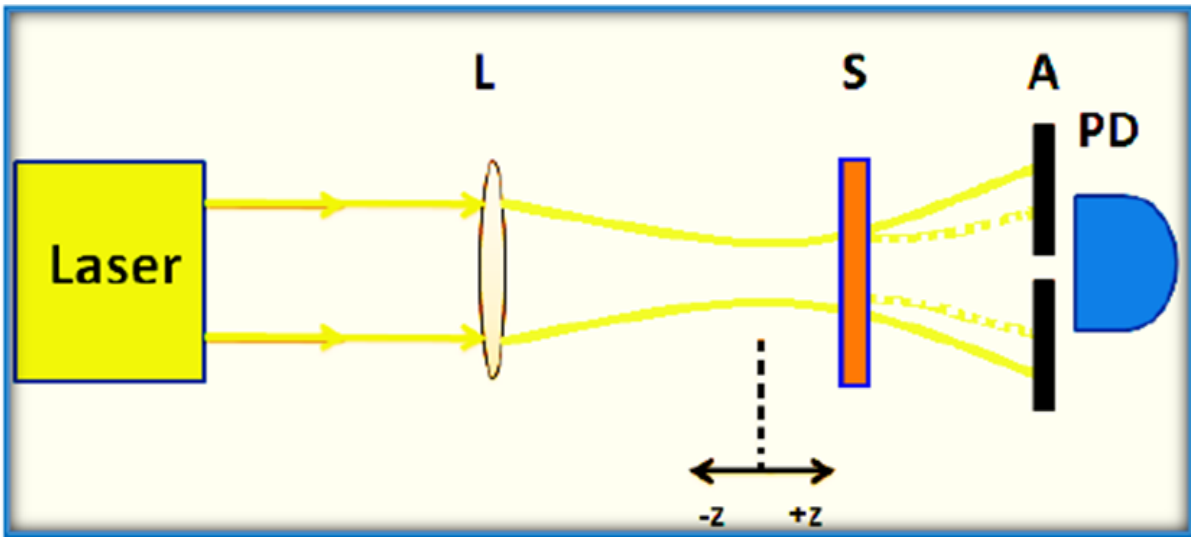

Figure (2.12): Schematics of experimental setup used for the Z-scan with a closed aperture [107].

The Z-Scan transmittance in relation to (Z) is linked to the sample's unidirectional refraction if it is constructed from a material with a negative nonlinear refraction index that is thinner than the focused beam's diffraction length. This can be compared to a telephoto lens with a changeable focal length. Small beam irradiance and negligible nonlinear refraction are observed far from the focus (Z_o). The measured transmittance in this case is constant (Z-independent). As the sample gets closer to the beam focus, the irradiance increases and the sample experiences self-lensing [108].

The link between the Z-Scan transmittance and (Z) and the sample's nonlinear refraction can be seen if a material is employed that has a nonlinear refraction index that is negative and a thickness that is shorter than the focused beam's diffraction length. This is comparable to a short different focal length lens. Away from the focus (Z_o), The irradiance of the beam is low, and the refraction of nonlinear is scarcely evident. In this case, the measured transmittance is Z-independent and constant. Sample self-lensing results from an increase in irradiance as the sample gets closer to the beam focus [108].

In the far field, the beam on the aperture will often collide with a negative self-lens in front of the focal plane, increasing the aperture position transmittance. The same self-defocusing reduces the measured transmittance and raises the beam divergence after the focal plane, causing the beam to diverge at the aperture. Since nonlinear refraction is minimal out of focus (Z > 0), the transmittance is not dependent on Z. A maximum transmittance (peak) and a minimum of the transmittance (valley) are the Z Scan characteristics of a negative nonlinearity. A curve of an inverse Z Scan (a valley and a peak) characterizes a nonlinearity of positive state. Figure 2.13 clearly shows these two cases [109].

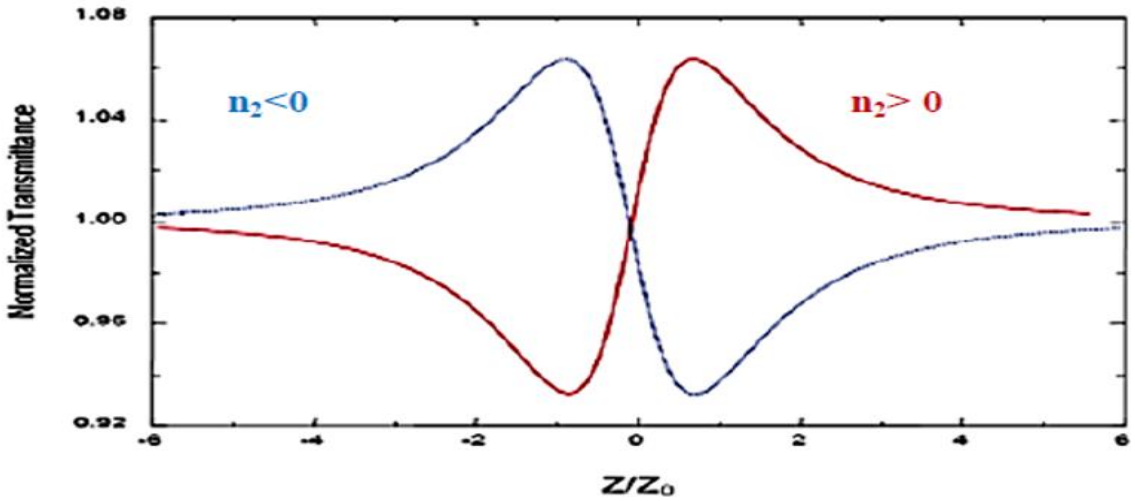

Figure (2.13): Z-Scan transmittance curves for a cubic nonlinearity [110].

To determine the nonlinear refractive coefficient using the normalized transmittance's peak to valley difference, apply the formula below [106].

$$n_2 = \frac{\Delta\,\Phi_0}{I_0 L_{eff}\,K} \quad \ldots (2.18)$$

where (I_0) is the focal point intensity, (k) is the wave number (k = 2π/ λ), and ($\Delta\,\Phi_0$) is the nonlinear phase shift [111]:

$$\Delta\,T_{P-V} = 0 \cdot 406\ \ |\Delta\,\Phi_O| \quad \ldots (2.19)$$

The sample's effective length is calculated from the difference between the normalized peak and valley transmittances, or L_{eff} [112] .

$$L_{eff} = \frac{(1-exp^{-\alpha_0 L})}{\alpha_0} \quad \ldots (2.20)$$

(L) represents the length of the sample. The focus point's intensity is governed by [113]

$$I_0 = \frac{2P_{Peak}}{\pi\omega_0^2} \quad \ldots (2.21)$$

where ω_0 is the beam radius at the focal point and is defined as the sample's peak intensity at the focus

2.21.2 Z-Scan with an open aperture

An open-aperture Z-scan examines the intensity fluctuation of a far-field beam at a photo detector (PD), which records the whole beam as it is focused by a lens (L). The intensity change is brought on by multiphoton sample absorption (S) as it passes through the waist of the beam. Figure 2.14 illustrates schematic diagrams of the experimental setup for both closed- and open-aperture Z-scan [114].

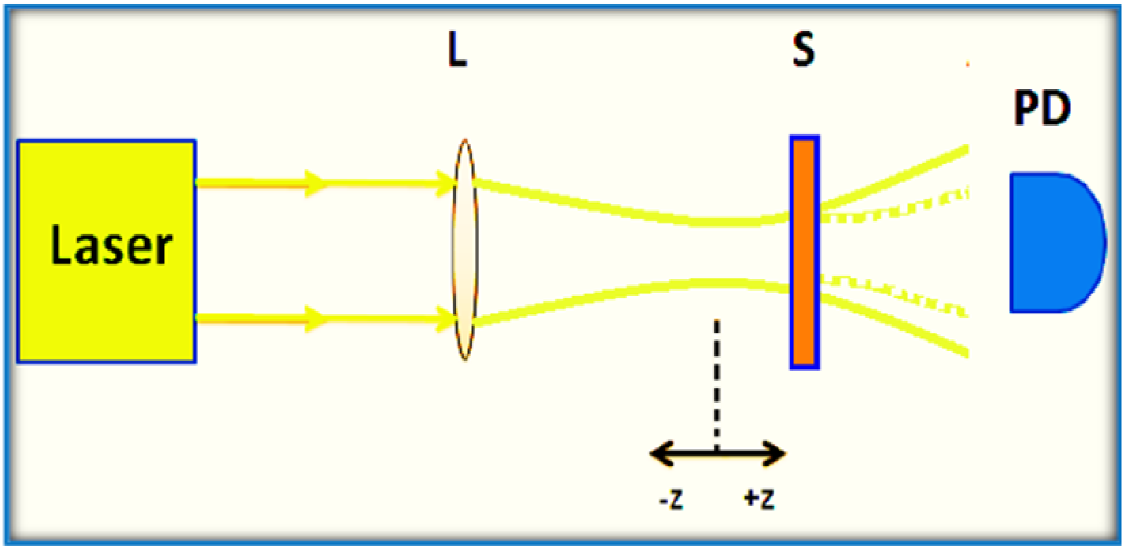

Figure (2.14) : Schematics of experimental setup used for the Z-Scan with open aperture [113].

Nonlinear refraction is obviously unresponsive to Z-scan with an open aperture, even with nonlinear absorption (thin sample approximation). With no aperture, the Z-scan signatures should be symmetric with regard to the focus (Z = 0). Where they should either have the maximum transmittance (such as during saturation of absorption) or the lowest transmittance (such as two photon absorption). In reality, such transmittance curves make it simple to determine the coefficients of nonlinear absorption. It is simple to calculate nonlinear absorption coefficient (β) using the following equation [110].

$$\beta = \frac{2\ \sqrt{2}\,\Delta T\ (z)}{I_0\ L_{eff}} \quad \ldots\ldots\ldots\ldots\ldots\ldots\ldots\ldots\ldots\ldots\ldots\ldots\ldots\ldots \ (2.22)$$

T(z) is the minimal normalized transmittance value at the focus point, (Z=0). It should be clear that the transmittance versus position graph of sample in an open aperture Z-Scan should be symmetric around the focus as shown in (Figure 2.15).

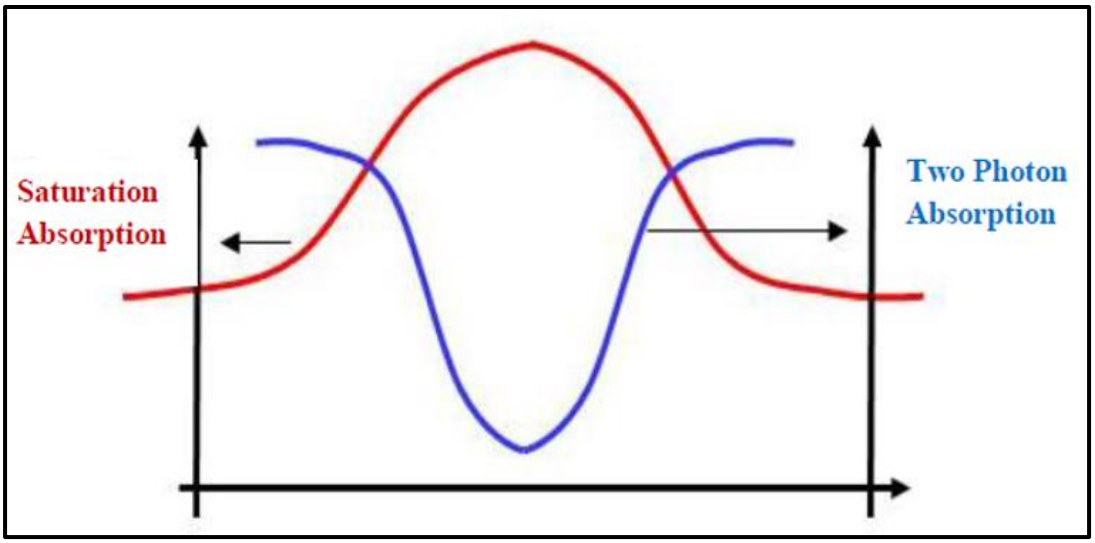

Figure (2.15): Open aperture Z-Scan curve [110].

The coefficient of nonlinear absorption (β), which determines absorption, and the nonlinear refractive index (n_2), which determines how light interacts with materials. These two variables rely on how intense a laser's electric field is. When a material is exposed to radiation, the energy of the absorbed photons enables the substance to change into the excited state from the ground state. When a substance is exposed to a high electric field, it changes its refractive index. In reality, the electric field's strength affects the index of refraction, gives the refractive index at high intensity [116].

2.22 The Nonlinear Absorption and the Nonlinear Refraction

Absorption and refraction, which are both described by the index of refraction (n) and coefficient of absorption (α), respectively, are the fundamental optical qualities involved in the interplay between matter and light. When a substance is exposed to radiation, the energy of the absorbed photons enables the transition from the ground to the excited states [117]. When a substance is exposed to a high electric field, the refractive index also changes. In reality, the strength of the electric field starts to affect the index

of refraction. The refractive index is determined at high intensity by equation (2.23) [117].

$$n = n_0 + n_2 I \quad \ldots\ldots (2.23)$$

The nonlinear refractive index (n_2) is related to the density in this case. Given that the absorption of the substance also depends on the density [118].

$$\alpha = \alpha_0 + \beta_2 I \quad \ldots\ldots (2.24)$$

Where (α_0) is the intensity-related nonlinear absorption coefficient and (β) is the linear absorption coefficient. The laser's intensity is correlated with the coefficients (n) and (α).

2.23 Nonlinear Optical Response of Organic Materials

Organic molecules have an isotropic nonlinear optical response (uniformity in all orientations). Carbons, for instance, may form two forms of covalent s-bonds and π-bonds. Because π-bonds have a larger electronic density than s-bonds, they exhibit nonlinear optical properties [119].

(NLO) are dependent on the change in polarization of the electrons in the π-bonding. As a result, the nonlinear optical properties of organic materials containing π- bonds are more numerous than those seen in saturated chemicals in the same proportion of carbon atoms. Various types of organic compounds have been explored in order to develop materials that exhibit a high degree of third order nonlinearity [120].

2.23.1 Saturable Light Absorption

Saturable absorption is a nonlinear process that can be connected to population changes in those amounts of energy that are real (as opposed to hypothetical). This happened when the relevant electronic transition became saturated (bleached) due to the nonlinear absorption coefficient ($\beta < 0$), which can develop when there is a significant light absorption between the two

levels. The ground and excited states of surface resonance were included in the two levels. Contrarily, this is a process where a material might be highly absorbing at a certain wavelength when a low-intensity beam is impressed upon it, yet an extremely intense beam (at the same wavelength) will pass through the medium with minimal change in intensity [121].

2.23.2 Two Photon Absorption (TPA)

To excite a molecule from one state—typically the ground state—to a higher energy electronic state, two photons of the same or different frequency must be absorbed simultaneously. This process is known as two-photon absorption (TPA). When the energy difference is large enough, the process of two-photon absorption occurs between the implicated molecular lower and upper states is equal to the total of the two photons' energies, similar to a saturable absorber When the nonlinear absorption coefficient $\beta > 0$, this procedure took place. This effect is shown in Figure 2.16 . The two-photon transition rate can be significantly enhanced if an intermediate level (2) is located near the virtual level shown by the dashed line in Figure 2.16 [122].

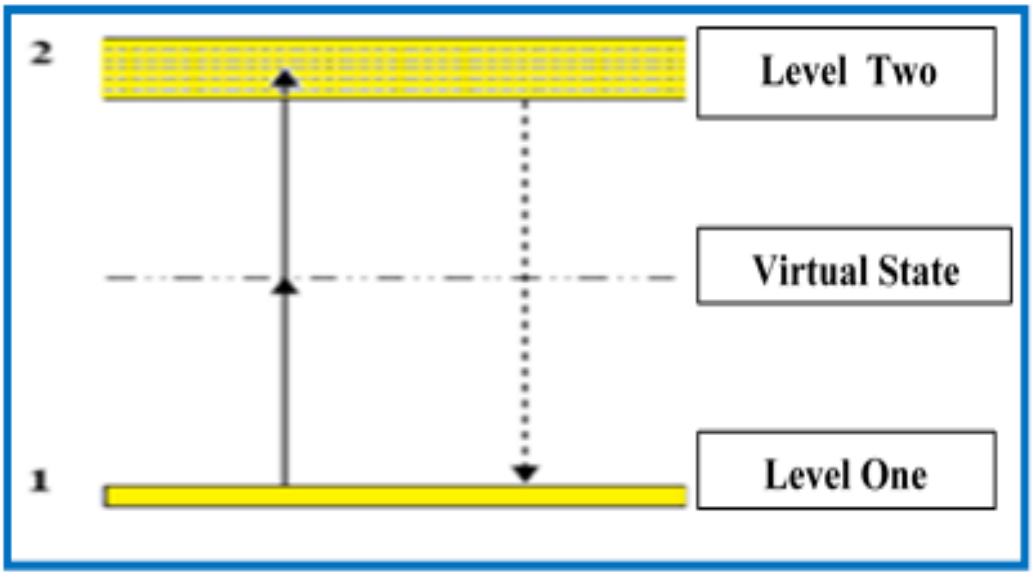

Figure (2.16) : Energy levels for the two-photon absorption process [122].

2.23.3 Kerr Effect

The nonlinear electronic polarization, which can be defined as altering the refractive index, is a nonlinear interaction of light in a material. The Kerr effect can produce a local change in the refractive index in high-intensity laser beams, causing the laser material to operate as a lens. This can cause laser beams to self-focus [123].

2.23.4 Self-focusing and Self-defocusing

Self-focusing is a nonlinear process, when the incident laser light on the material differ from in Gaussian intensity , i.e. the intensity of the pulse is higher in the center than in the flanks, as a result the refractive index will be change, so the material will acts as a lens, and the sign of nonlinear refractive index will determine whether self-focusing ($n_2>0$) when it is a positive signal or self-defocusing ($n_2<0$) when it is a negative [115]

2.24 Optical Limiting

The optical limiting effect in organic material due to reverse saturation absorption. With increasing intensity, light is absorbed in a material that has a high nonlinear impact and has an output intensity over a certain level, the output intensity gradually approaches a constant value. One can employ such a substance to restrict the quantity of optical power that enters a system. This can be employed in protective goggles, to reduce noise in laser beams, or to protect expensive or delicate equipment like sensors. Figure 2.17 depicts such a device's optimum behavior [124].

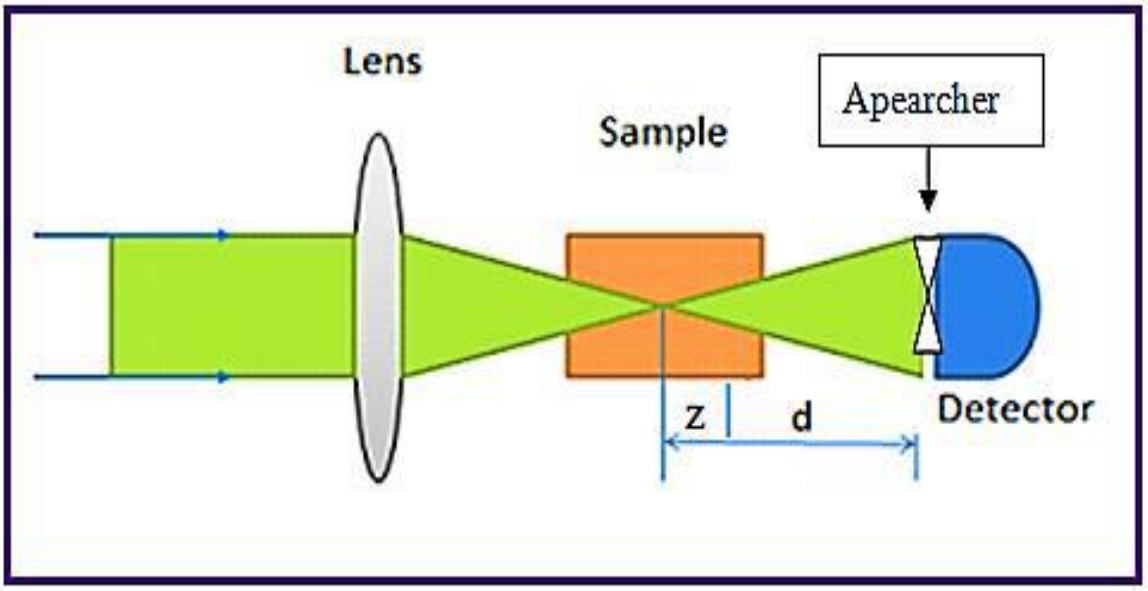

Figure (2.17): Schematic of the optical Limiting Geometry [124]

3.1 Introduction

This chapter discusses the compounds used and their solvents, the work scheme, and procedures for preparing liquid solutions (dye, nanoparticles), and the devices used in the measurements.

3.1 The Utilized Materials

3.1.1 Rhodamine 110 Dye

The Rhodamine 110 dye that is used in this research was obtained by (Sigma-Aldrich/ Germany) with high purity (99.9%). Table (3.1) shows some of the physical and chemical properties of Rh 110 .

Table (3.1): The main properties of Rhodamine 110 dye [42].

Parameters	Description
Scientific name	[6-amino-9-(2-carboxyphenyl)xanthen-3-ylidene] azanium;chloride
Productive company	Sigma – Aldrich
Appearance	Powder
Color	red
Chemical formula	$C_{20}H_{15}N_2O_3Cl$
Molecular weight	366.8 gm/mol

3.1.2 Rhodamine B Dye

The Rhodamine B dye that is used in this research was obtained by (Sigma-Aldrich/ Germany) with high purity (99.9%).Table (3.2) shows some of the physical and chemical properties of Rh B .

Table (3.2): The main properties of Rhodamine B dye [125].

Parameters	Description
Scientific name	Tetraethylrhodamine, Rhodamine o, Brilliant pink , Basic violet
Productive company	Sigma – Aldrich
Appearance	Powder
Color	Bright–red to violet
Chemical formula	$C_{28}H_{31}N_2O_3Cl$
Molecular weight	479.01 g/mol

3.1.3 Ethanol Solvent

Ethanol was utilized in present work, obtained by (Sigma-Aldrich/ Germany) with high purity (99.9%). the properties of this solvent are listed in Table (3.3).

Table (3.3): The principal characteristics of ethanol solvent [126].

Parameters	Description
Chemical formula	C_2H_6O
Molecular weight	46.07(g/mol)
Refractive index	1.3614
Dielectric Constant	24.195
Polarity	0.5771
Dipole Moment	1.70 D
Density	789 kg/ m^3
Freezing Point	-114 ^oC
Boiling Point	78.3 ^oC

3.1.4 Methanol Solvent

Methanol was utilized in present work was obtained by (Sigma-Aldrich/ Germany) with high purity (99.9%)., the properties of this solvent are listed in Table (3.4).

Table (3.4): The main properties of Methanol [127,128].

Parameters	Description
Chemical formula	CH_3OH
Molecular weight	32.05 (g/mol)
Refractive index	1.3287
Dielectric Constant	32.630
Polarity	0.6179
Dipole Moment	1.69 D
Density	0.7961(g/cm^3)
Freezing Point	–97 (C^o)
Boiling Point	64.7 (C^o)

3.1.5 Silver Nanoparticle (Ag NP_S)

The silver circular disc that is used in this research was obtained by (Central Bank of Iraq) with high purity (99.9%). The principal characteristics of (Ag) nanoparticles are shown in Table (3.5).

Table (3.5): The principal characteristics of (Ag) nanoparticles .

Parameters	Description
Productive company	Central Bank of Iraq
Form	disc
Diameter	2 cm
Thickness	2 mm

3.1.6 Gold Nanoparticles (Au Nps)

The gold tablet that is used in this research was obtained by (Central Bank of Iraq) with high purity (99.9%). The principal characteristics of (Ag) nanoparticles are shown in Table (3.6).

Table (3.6): The principal characteristics of (Au) nanoparticles .

Parameters	Description
Productive company	Central Bank of Iraq
Form	disc
Diameter	2 cm
Thickness	2 mm

3.1.7 Copper Nanoparticles (Cu NPs)

The copper tablet that is used in this research was obtained by (local markets) with high purity (99.9%). The principal characteristics of (Cu) nanoparticles are shown in Table (3.7).

Table (3.7): The principal characteristics of (Cu) nanoparticles .

Parameters	Description
Productive company	local markets
Form	disc
Diameter	2 cm
Thickness	2 mm

3.2 Scheme of the Work

Figure (3.1) shows the scheme of the main steps of the experimental part in this work.

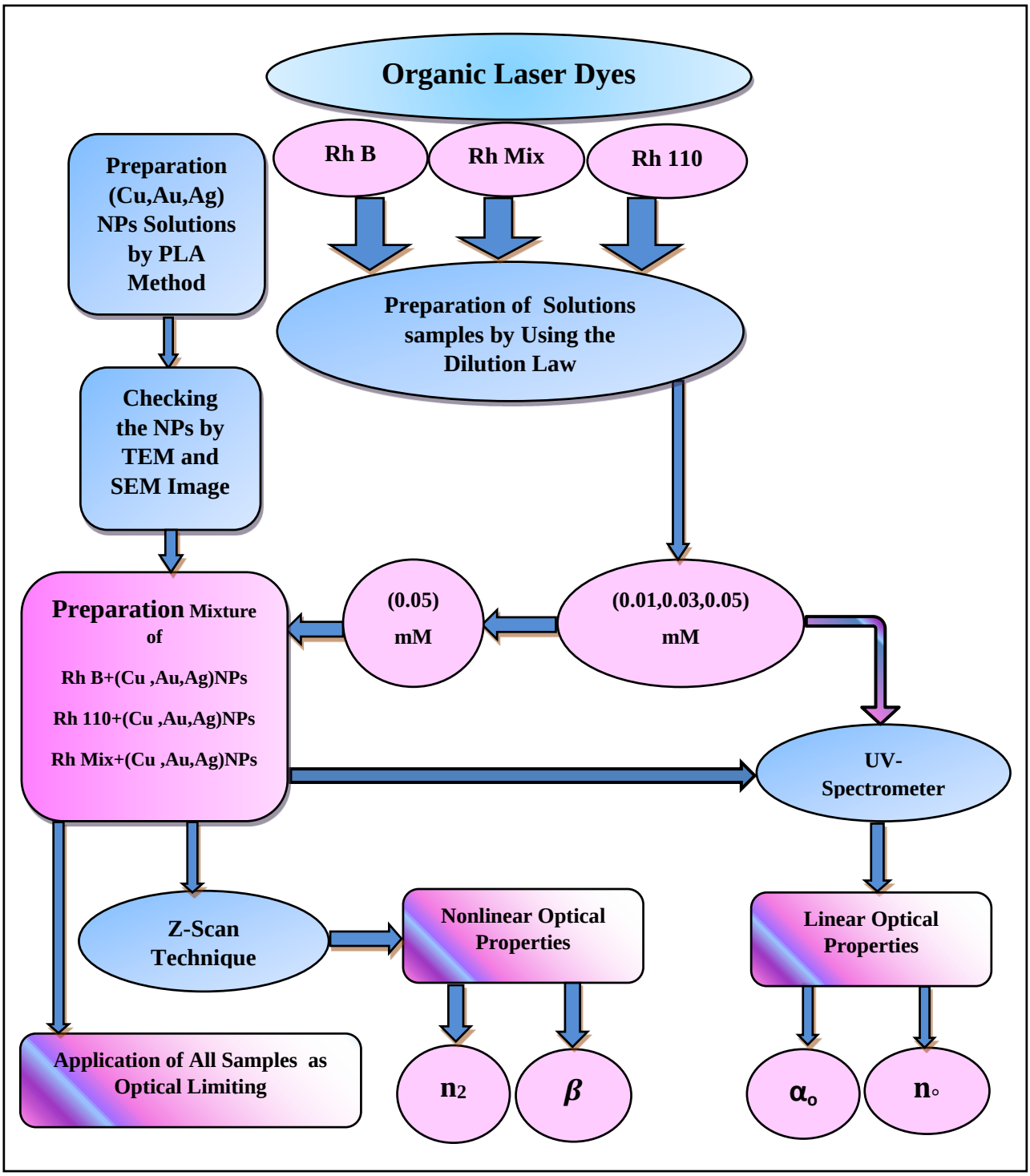

Figure (3.1): Main Steps of experimental work.

3.2. Preparation of Rhodamine 110 dye Solutions

To prepare solutions of Rhodamine 110 dye in concentration (1×10^{-3} M), in both solvents, ethanol and Methanol to dissolved (0.011g) of (Rh110) dye powder for the volume of (30 ml) of solvents used in this study and according to the relationship (3.1) [129] .

$$W = \frac{V\times C\times Mw}{1000} \quad \ldots (3.1)$$

Where W: the dye weight (in grams) needed to achieve the desired concentration.

Mw: the molecular weight of the dye employed is expressed in grams per mole. V: the volume of solvent to be added to the dye is measured (cm^3)

C: the concentration to be prepared is measured in units (M).

the prepared concentration can be diluted through the use of the following relationship (3,2) [129]

$$C_2 V_2 = C_1 V_1 \quad \ldots (3.2)$$

C_1 : the concentration of the original solution.

C_2: the Concentration after dilution

V_1: the original solution's volume.

V_2: the diluted solution's final volume.

The following concentrations were obtained (0.01,0.03, 0.05) mM as shown in Figure (3.2).

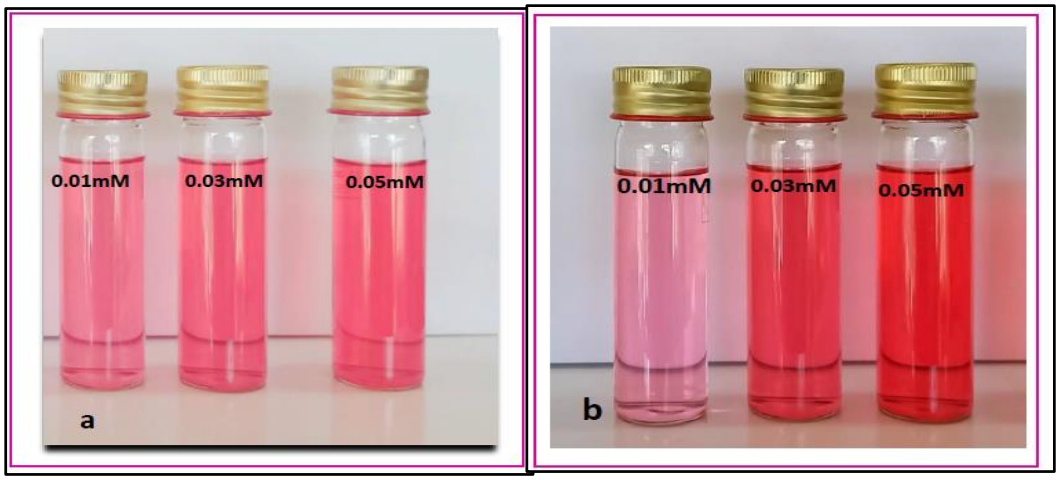

Figure (3.2): The solutions samples of Rh 110 dye at different concentrations a. ethanol solvent and b. methanol solvent.

3.3 Preparation of Rhodamine B dye Solutions

To prepare solutions of Rhodamine B dye in concentration (1×10^{-3} mM), in both solvents, ethanol and Methanol to dissolved (0.014 g) of (RhB) dye powder for the volume of (30 ml) of solvents used in this study and according to the relationship (3.1).The prepared concentration can be diluted using the relationship (3.2) The following concentrations were obtained (0.01,0.03, 0.05) mM as shown in Figure (3.3)

Figure (3.3): The solutions samples of Rh B dye at different concentrations a. ethanol solvent. and b. methanol solvent

3.4 Preparation of Rhodamine Mix (Rh110 + Rh B) dye solutions

To prepare solutions of Rhodamine Mix dye in concentration (1×10^{-3} mM), in both solvents, ethanol and Methanol , Rh110 dye dissolved in both methanol and ethanol was mixed with RhB dye dissolved in methanol and ethanol solution proportions of (1:1).The prepared concentration can be diluted using the relationship (3.2).

The following concentrations were obtained (0.01,0.03, 0.05) mM as shown in Figure (3.4)

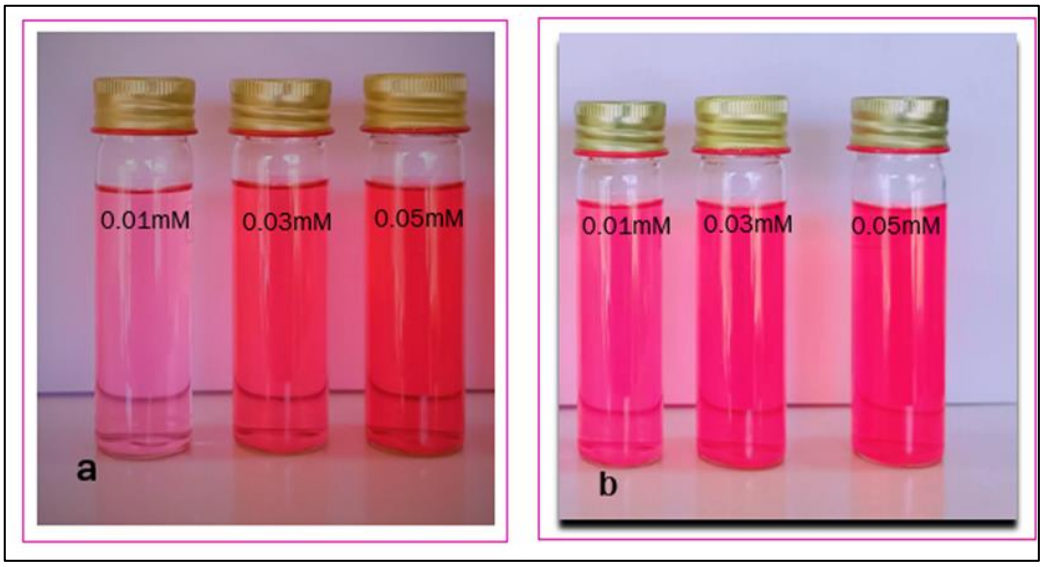

Figure (3.4): The solutions samples of Rh Mix dye at different concentrations a. ethanol solvent. and b. methanol solvent

3.5 Preparation of the Nanoparticles (NPs)

The technique of pulsed laser ablation in liquids (PLAL) has emerged as crucial for producing nanoparticles with precise geometry and size [130]. Colloidal suspensions of objects on a nanoscale scale are created in research involving PLAL stands for immersion of solid objects in pulsed laser ablation in liquid environments [131].

Synthesis of (Au, Ag and Cu) Nps were using the pulsed liquid laser ablation method to obtain a colloidal liquid for the nanomaterials used in a target form placed in a small beaker containing 10 cm methanol and ethanol.A colloidal solution of (Cu , Au and Ag) Nps was prepared, with methanol, and ethanol solvents.

Then a Nd:YAG laser beam with wavelength (1064 nm) is projected onto the plate inside the enclosure through a convex lens (10 cm), and the necessary power was (300 mJ) , to complete the process of removing gold particles, silver particles, and copper particles. I noticed in the gold particles a change in the color of the liquid to a dark red color, which indicates the formation of the nano-liquid. In the silver particles, the color of the liquid changed to a brownish-red solution, while the copper changed to a semi-transparent color.

The concentration and size of the particles depend on the number of pulses that are fired [131] . Figure 3.5 (a) represents the device used for laser ablation and (b) an experimental scheme for preparing nanoparticles. Figure (3.6):(a) the solutions samples of NPs dye at ethanol solvent (b):the solutions samples of NPs dye at methanol solvent

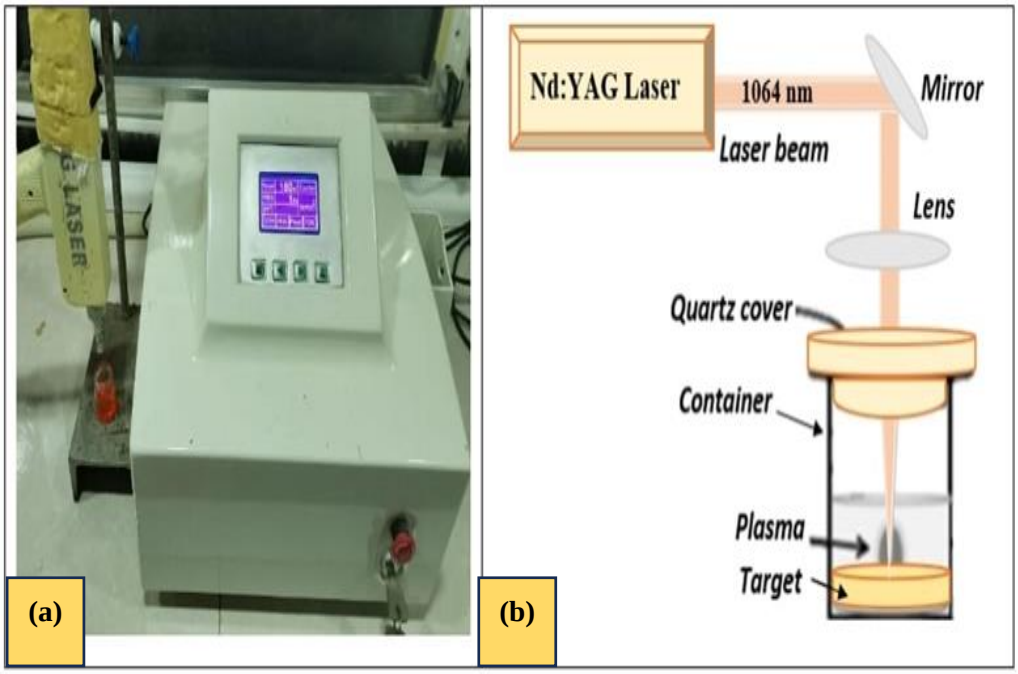

Figure (3.5): (a) the device used for laser ablation. and (b) the scheme for device.

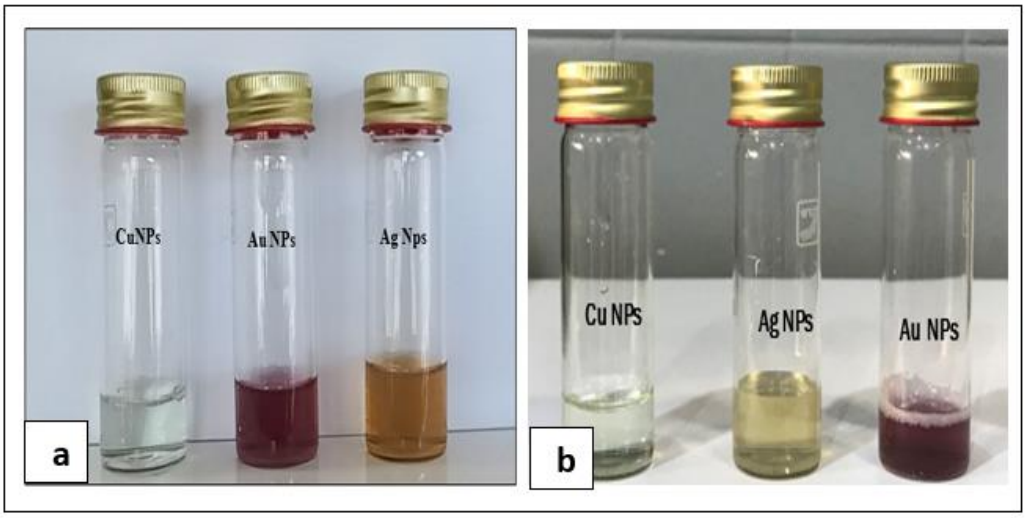

Figure (3.6): (a) the solutions samples of NPs dye at ethanol solvent. and (b) the solutions samples of NPs dye at methanol solvent.

3.6. Preparation of the (Rh 110, Rh B and Rh mix) dye Solutions with Nps

The nanomateal is prepared by taking (1 ml) of colloidal gold solution (Au Nps). dissolved in ethanol solution and added to (Rh110) at a ratio of 1:3 and stirred by magnetic stirring for (30 minutes), thus obtaining (Rh110-NPs) nanocomposite. repeat the same method for the nano silver solution and the nano copper solution. And in the same way as for the methanol solvent. In the same way as before, use it for dye-solution (Rh B) and also dye-solution (Rh Mix). Figures (3.7-3-9) show the solutions samples of (Rh 110-NPs), (Rh B-NPs) and (Rh Mix-NPs) in ethanol solvent and methanol solvents.

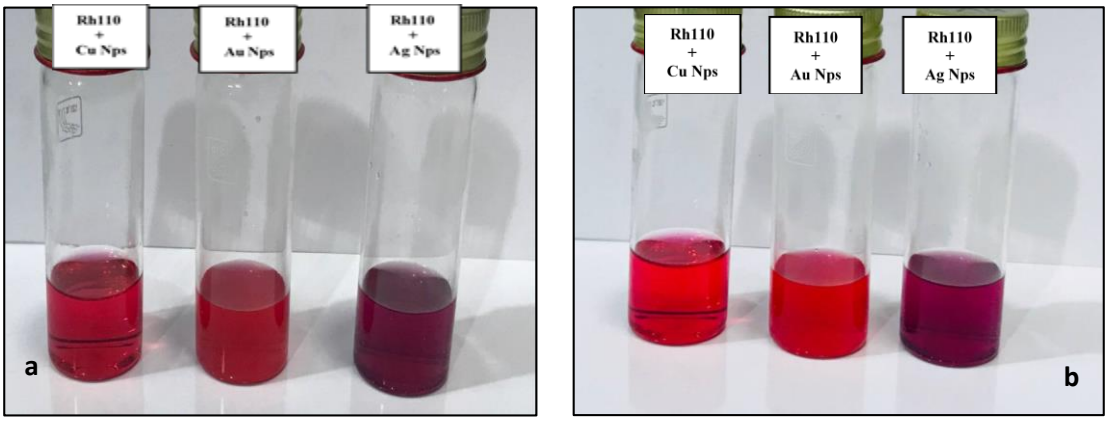

Figure (3.7) :The solutions samples of (Rh110- NPs) in a. ethanol solvent and b. methanol solvent

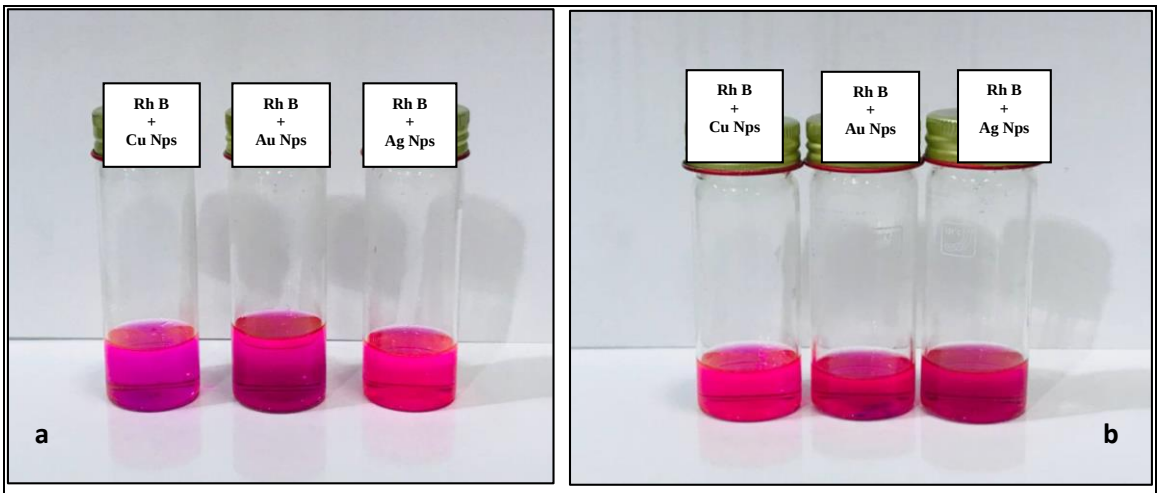

Figure (3.8): The solutions samples of (RhB- NPs) in a. ethanol solvent and b. methanol solvent

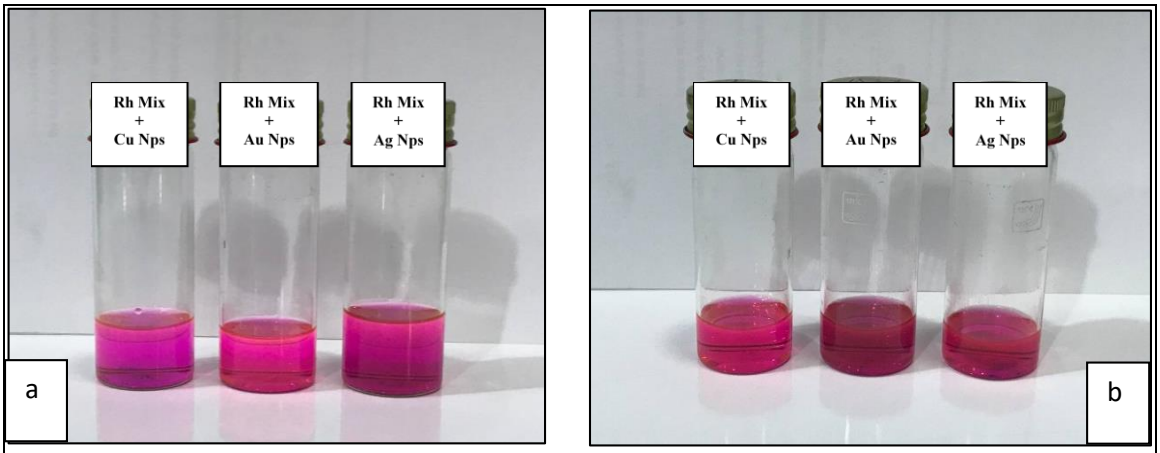

Figure(3.9): The solutions samples of (Rh Mix- NPs) in a. ethanol solvent and b. methanol solvent

3.7.The Used Devices

3.7.1 UV-Visible Spectrometer

The absorbance spectra were measured using a UV-Visible spectrophotometer type (Shimadzu-1800). This device has two light sources deuterium Lamp (190-360) nm and Tungsten Lamp (360-1100), so it covers a wide range of the electromagnetic spectrum, extending from the ultraviolet to the near infrared region. Table 3.8 shows the specifications of the device. The idea of operating the device depends on the separation of the incoming beam into two parts, one of which passes through the sample solution to be studied, while the second beam in the solvent that represents the reference beam. The device then subtracts the reference beam and registers the absorption spectrum of the sample alone. All samples were examined in the laboratory of thin films (University of Babylon / College of Education for Pure Sciences / Department of Physics), as shown in Figure (3.10).

Table (3.8): UV-Visible spectrometer characteristics.

Parameters	Descriptions
Range of wavelengths	(190-1100) nm
Scan rate for wavelengths	Maximum 1000 nm / min
Source of light	Deuterium and Tungsten Lamps
The detector	Silicon photodiode
Requirements for power	220-240V (AC)

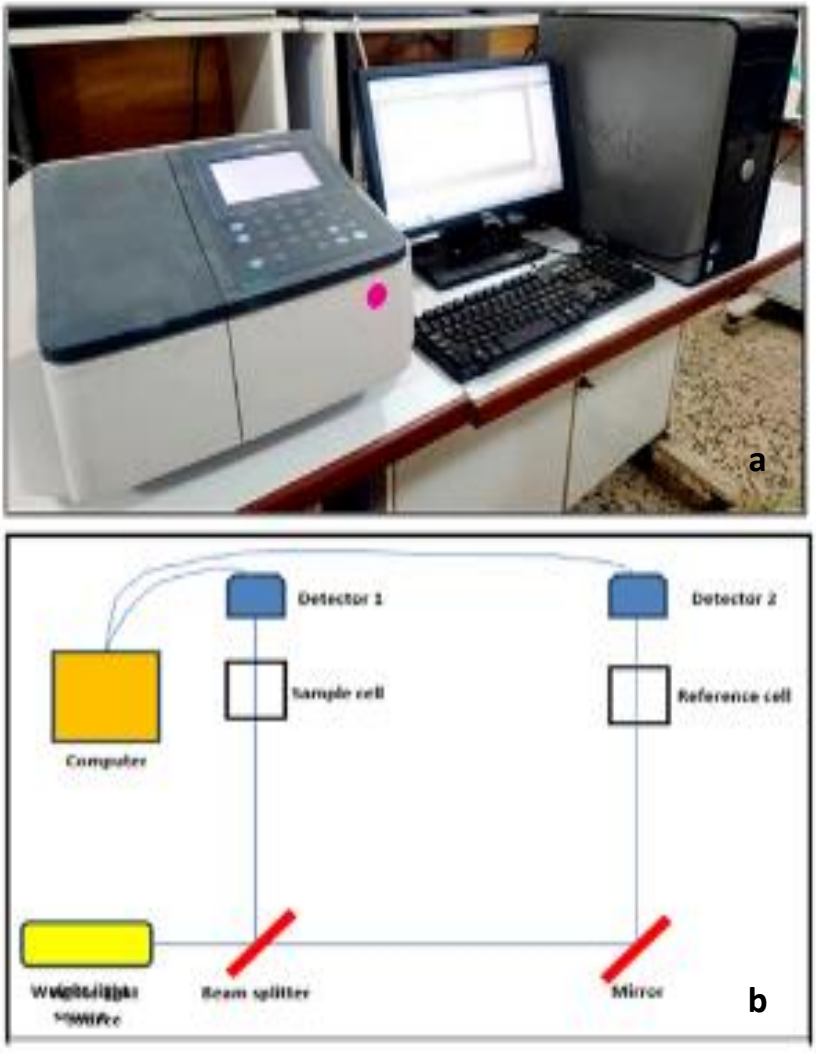

Figure (3.10): (a) UV-visible spectrophotometer and (b) the scheme for device.

3.7.2 Transmission Electron Microscope (TEM)

Transmission electron microscopy (TEM) (PHILIPS, CM 120) is used to examination the morphology of (NPs). TEM is a microscopy technique in which an electron beam is sent through a specimen to generate an image. The electrons interact with the specimen as the beam travels past it, generating a picture. An imaging gadget then magnifies and focuses the picture, such as a

fluorescent tube, a photographic film plate, or a sensor attached to a load-coupled device, such as a scintillator. Because electrons are used to edify the sample rather than light, TEM imagery offers significantly greater resolution than light-based imaging approaches. The contrast between the sample and the backdrop is crucial for efficient TEM nanoparticle imaging. Drying nanoparticles on a copper grid covered in a small layer of carbon prepares them for imaging; It is simple to photograph components with electron densities much higher than amorphous carbon. The ideal method for accurately determining particle size is TEM imaging, grain size, particle dispersion, and nanoparticle shape. Often, size accuracy is within 3% of the true number [132]. The TEM device is depicted in Figure (3.11).

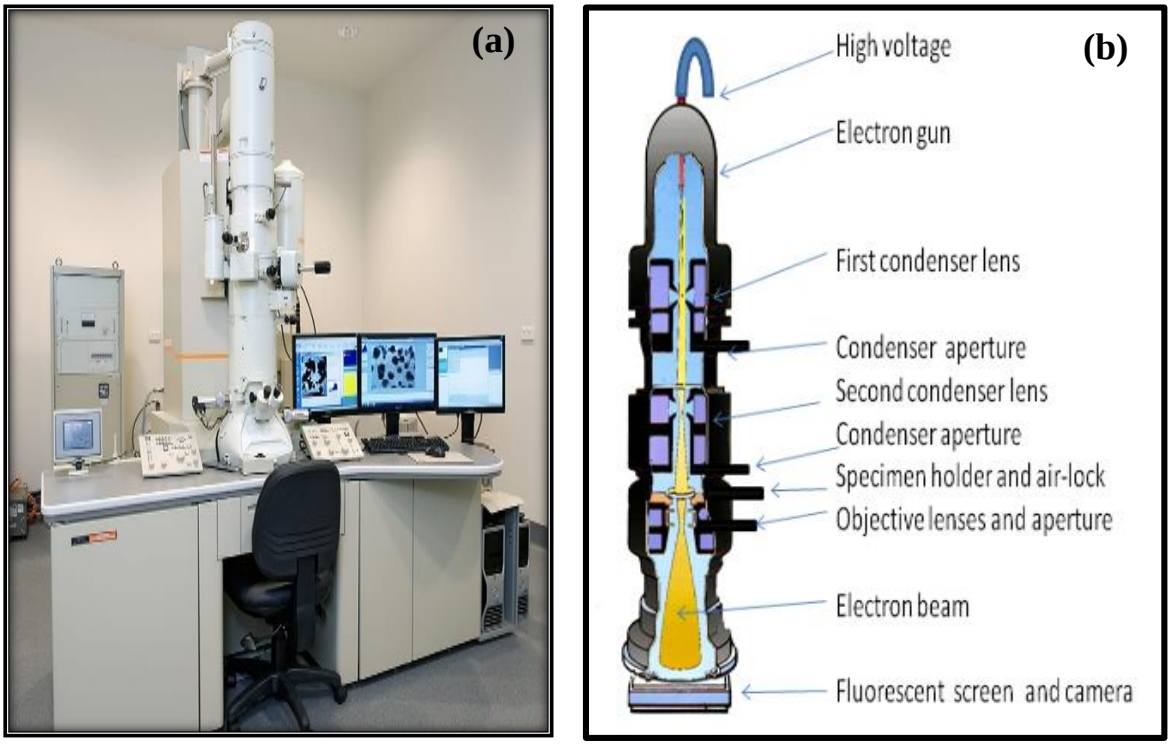

Figure (3.11): (a) The system of the TEM and (b) the scheme for device[133].

3.7.3. Scanning Electron Microscope (SEM).

Figure (3.12) shows the scanning electron microscopy device (SEM, MIRAIII, TESCAN Co.). Using SEM microscopy the information on the surface morphology of the samples and the particle size of (Au, Ag and Cu) NPs deposited on a glass substrate was determined. SEM is the technique by which electrons are often used to screen the micro-structure of a sample surface instead of light waves, thus it produces detailed images by scanning the surface of the sample and by examining the materials surface morphology. SEM is a kind of electron microscopy, which produces the sample images by focusing high-energy electrons beams. The SEM can be used to examine surface morphology, design specifics, cross section, widths and film thickness [134].

Figure (3.12): Scanning Electron Microscopy device.

3.8. Z-Scan Measurement Technique

The Z-scan results were classified as closed aperture or open aperture. solid state continuous wave (CW) diode pump laser with a wavelength of (532) nm and a laser power of (50) mW was used for each component. An enclosed-aperture Z-scan was used to measure the nonlinear refractive index, as opposed to the nonlinear absorption coefficient, which was calculated using an open-aperture Z-scan. A convex lens (f =15 cm) was employed to focus the beam. Along the Z-axis, the sample was moved. Based on the sample position, the transmittance through the sample is measured. Figure (3.13) depicts the configurations for both open and closed aperture Z-scan.

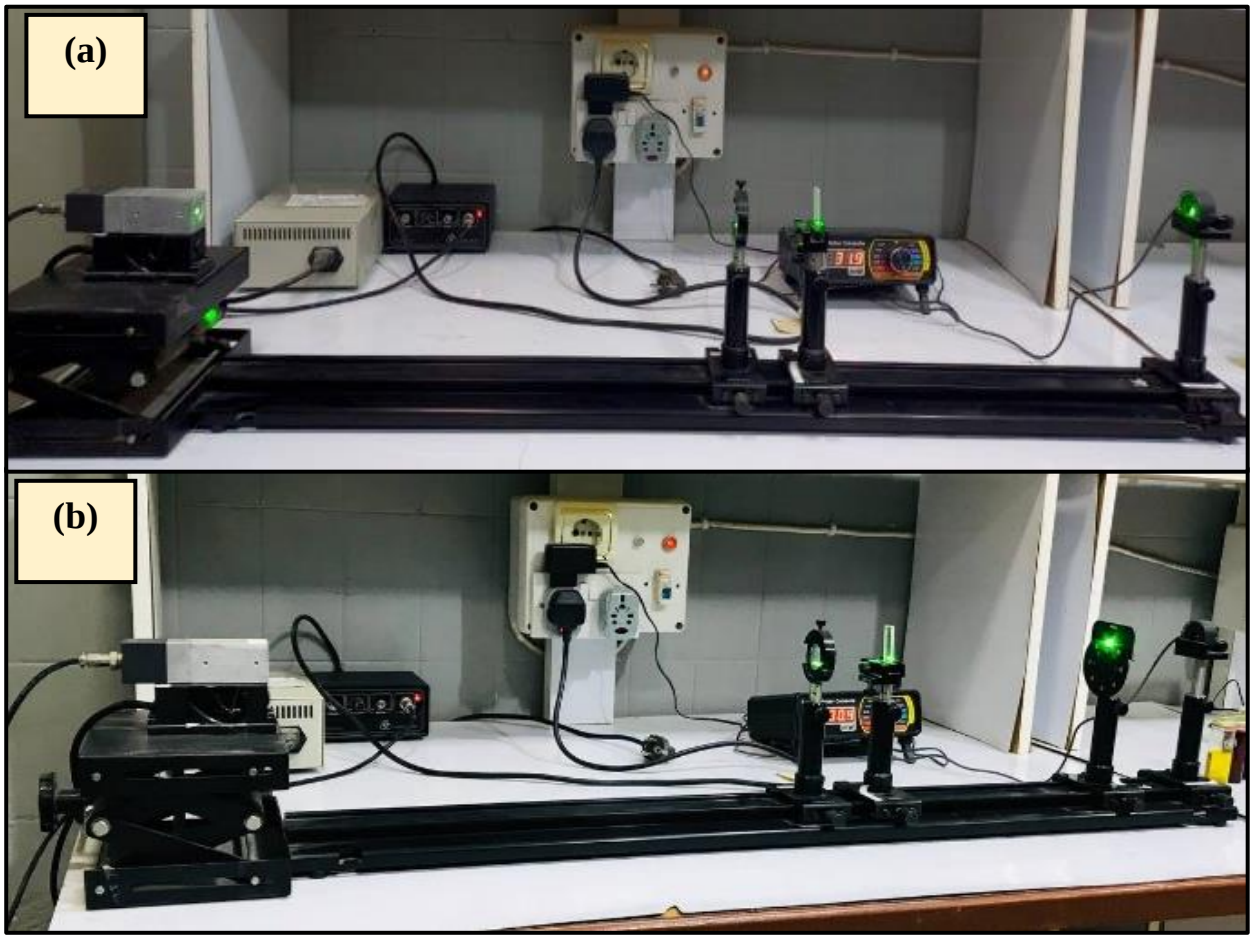

Figure (3.13): (a) open-aperture Z-scan (b) closed -aperture Z-scan.

2.11 The technique of the optical limiting

measuring output power based on input power, the optical limiting characteristics were determined. The light source was a diode laser, and the sample was placed in the focus (beam splitter) The detector monitored both the input and output power simultaneously in order to split the beam. Figure (3.14) shows how to set up an optical limiting system.

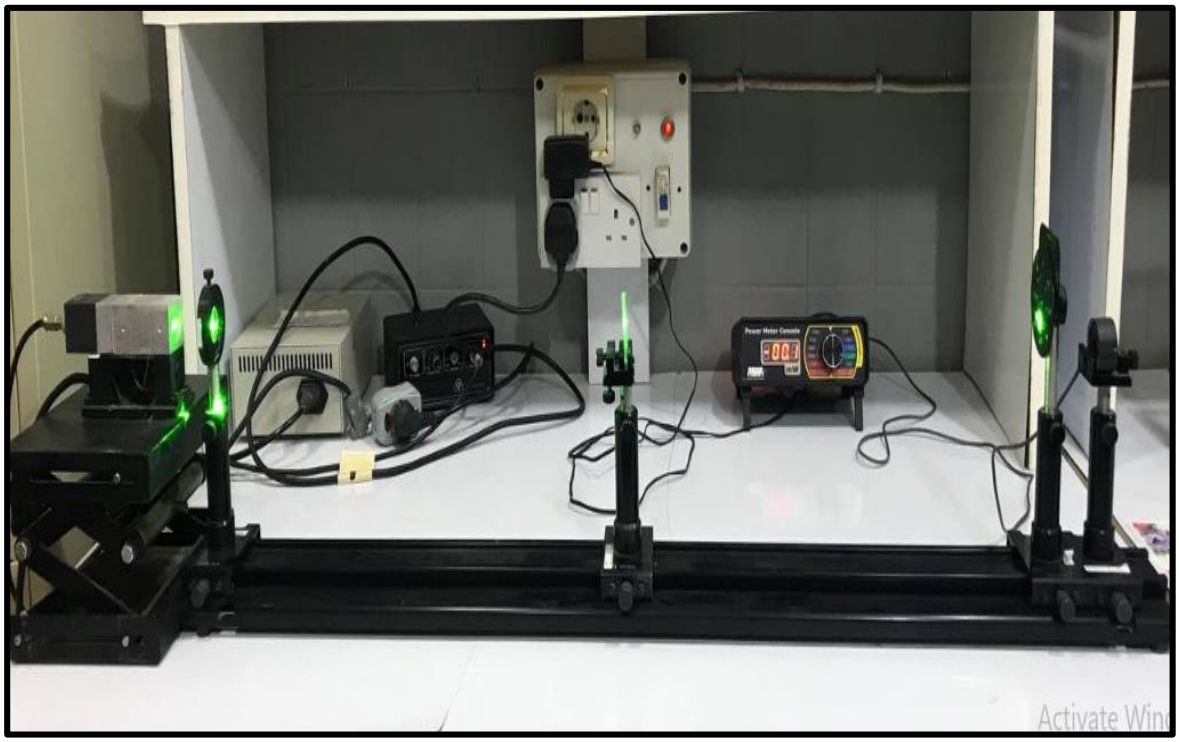

Figure(3.14): The setup of optical limiting.

4.1 Introduction

This chapter discuss the results of the absorption, transmittance, and linear and nonlinear optical properties of some laser organic dyes , used in this study (Rh B , Rh 110 and Rh mix) dyes prepared at different concentrations and dissolved in two solvents (ethanol and methanol). study and discuss the effect of adding metallic nanomaterials (Au , Cu and Ag) NPs solutions of these dye in order to obtain good linear and nonlinear optical properties. These solutions used in optical limiter applications.

4.2 The Results of TEM and SEM Images of NPs

Figures (4.1-4.3) show TEM images of (Ag,Au, and Cu) NPs prepared in this study by pulsed laser ablation in liquids (PLAL) with two organic solvents (ethanol and methanol). It is noted from these figures that all the prepared samples have nano-dimensions less than 50 nm. It is also noted that AgNPs have larger nano-dimensions than the rest of the samples and that the nanoparticles for all samples have lower nano-dimensions using methanol solvent compared to ethanol solvent. Figures (4.4-4.6) show SEM images of (Ag, Au, and Cu) NPs s, from these figures noted that all nanoparticles spread homogeneously within the colloidal liquid.

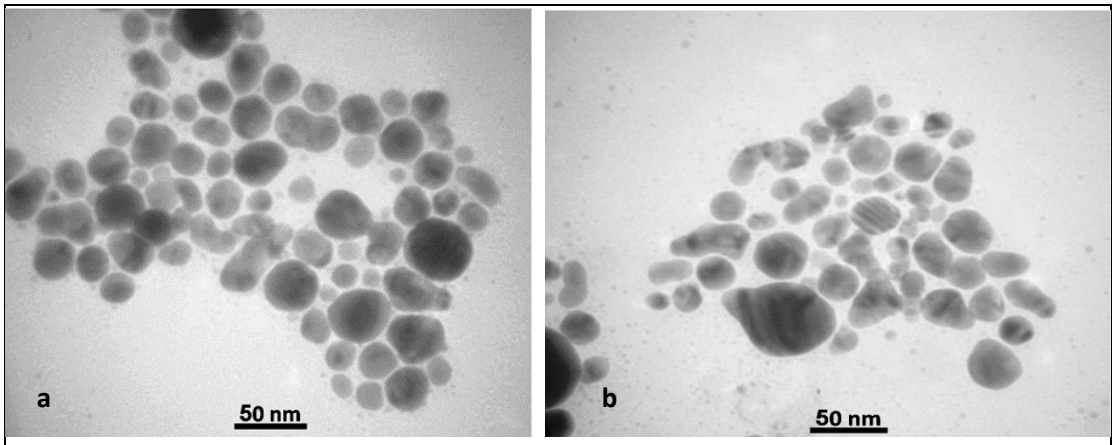

Figure (4.1): TEM images of Ag NPs in a. Ethanol b. Methanol

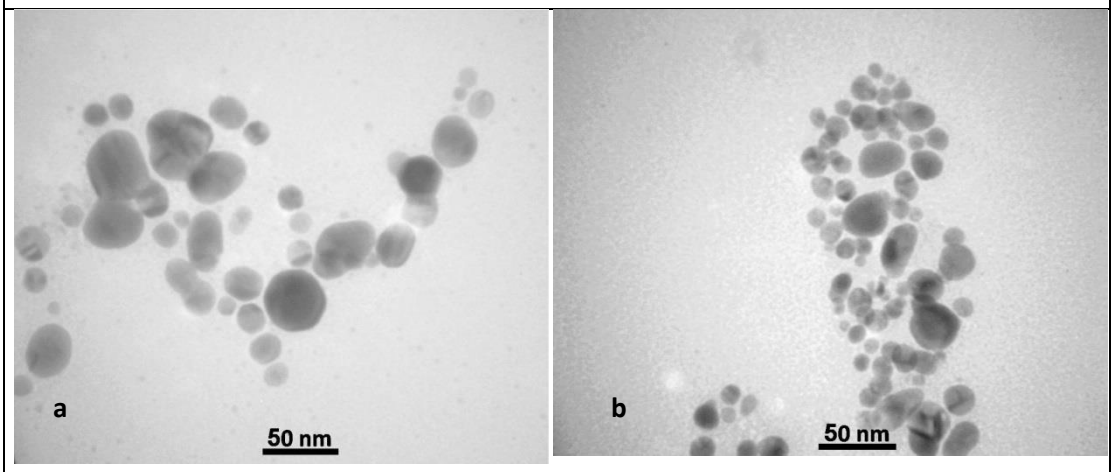

Figure (4.2): TEM images of Au NPs in a. Ethanol b. Methanol

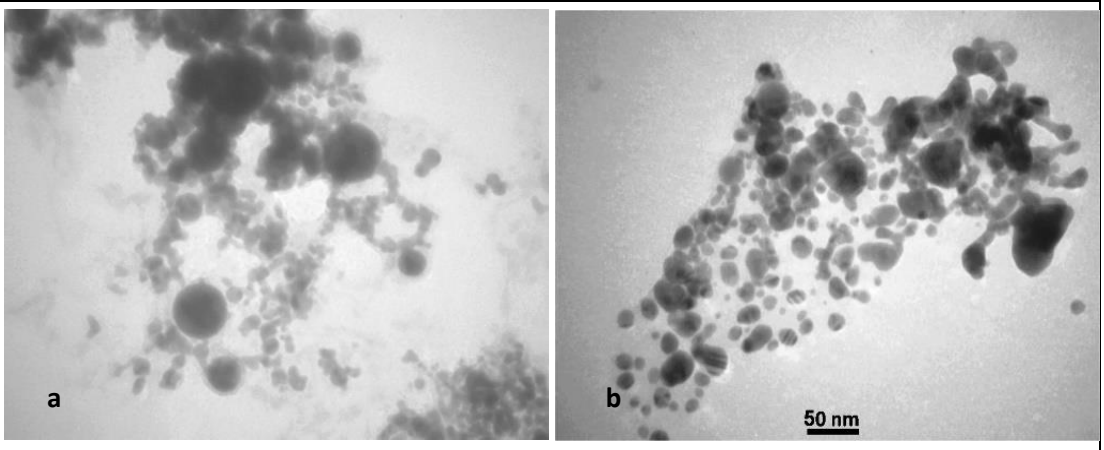

Figure (4.3): TEM images of Cu NPs in a. Ethanol b. Methanol

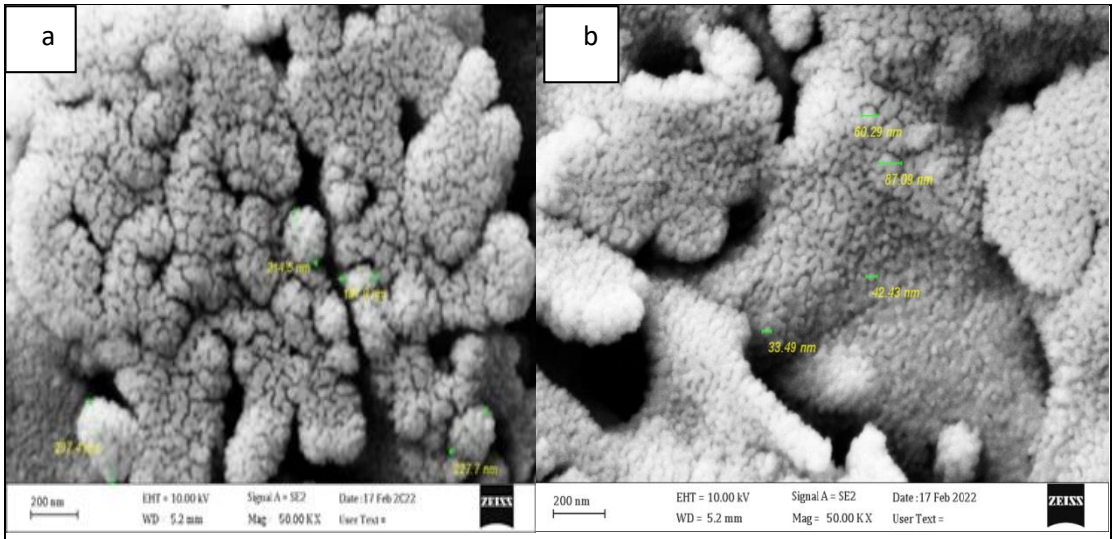

Figure (4.4): SEM images of Ag NPs in a. Ethanol b. Methanol

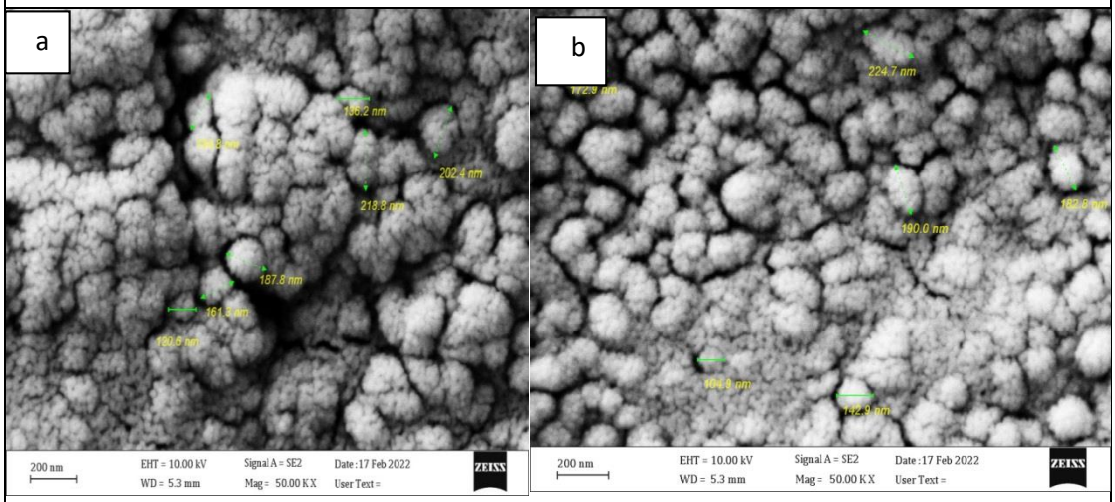

Figure (4.5): SEM images of Au NPs in a. Ethanol b. Methanol

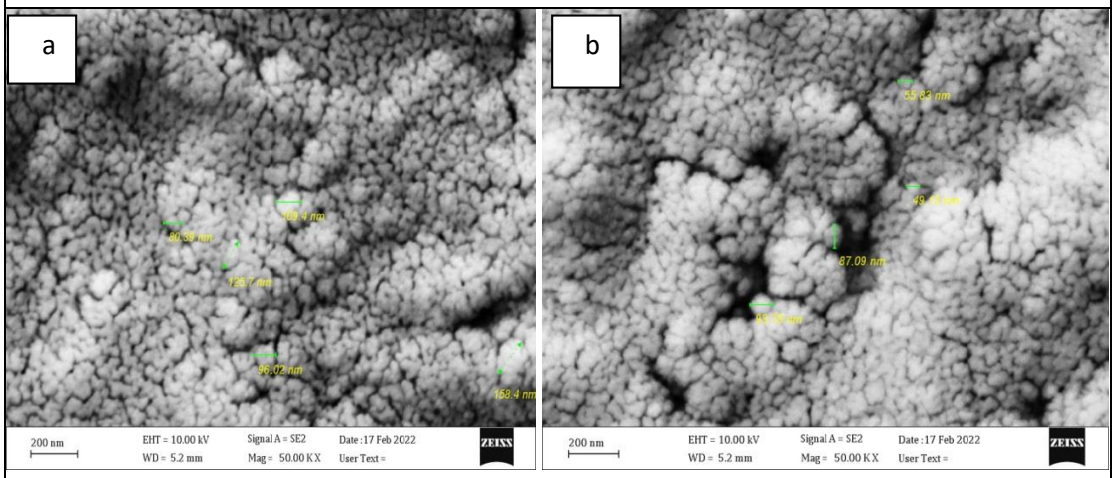

Figure (4.6): SEM images of Cu NPs in a. Ethanol b. Methanol

4.3 Linear Optical Properties

4.3.1 Absorbance and transmittance spectra of (Rh B , Rh 110 and Rh mix) dye solutions dissolved in ethanol solvent

Figures (4.7 , 4.8 and 4.9) show the absorbance spectra of Rh B , Rh 110 and Rh mix dyes solutions dissolved in ethanol solvent at different concentrations (0.01, 0.03 and 0.05) mM, which were measured using visible and ultraviolet spectrometers. It is noted from the figures that increasing the concentration leads to an increase in the values of absorbance for all dye solutions, and this is consistent with the beer-Lambert law. It is also noted that the absorbance values of Rh B are higher than the rest of the other dyes, This was overall obtained due to the increasing number of molecules per volume unit at high concentration, this in turn lead to change in energy levels result in effect of vibration field on molecules. Therefore, absorbance increased with increasing concentration as shown in Table (4-1).

From the absorbance curves, the transmittance values were calculated, as Figures (4.10 , 4.11 and 4.12) show the transmittance curves of Rh B, Rh 110 and Rh mix dye solutions dissolved in ethanol solvent at different concentrations (0.01, 0.03 and 0.05) m M , and it is noted from these figures that increasing the concentration leads to separation In the transmittance values, the reason for this is due to the increase in the absorbance values, as shown in Table (4.1).

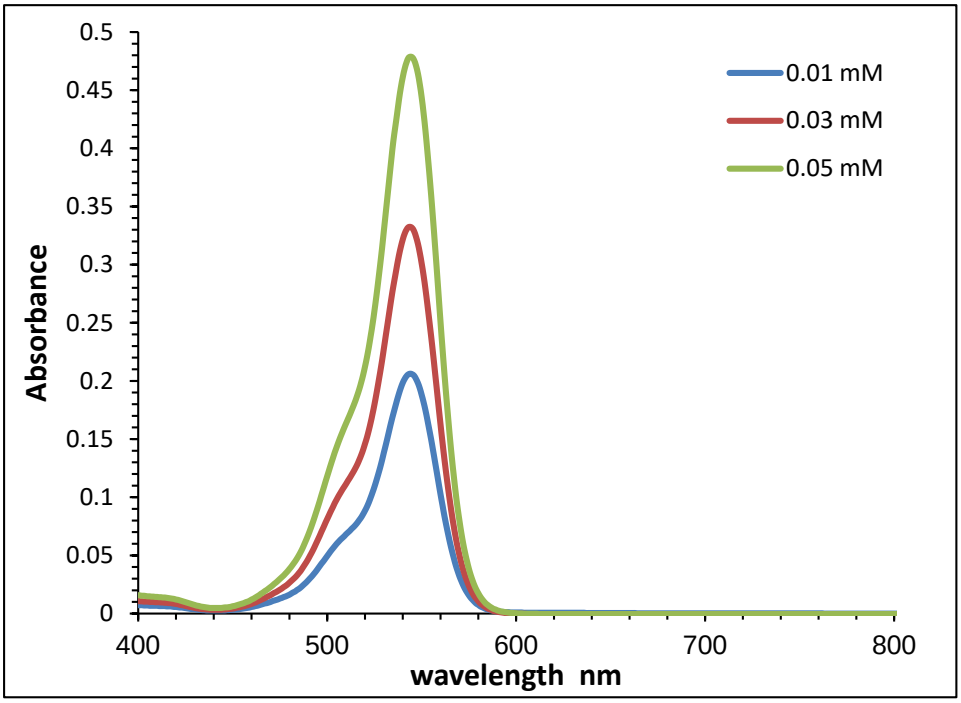

Figure (4.7) : Absorbance spectra of (Rh B) dye solutions dissolved in ethanol solvent at different concentrations.

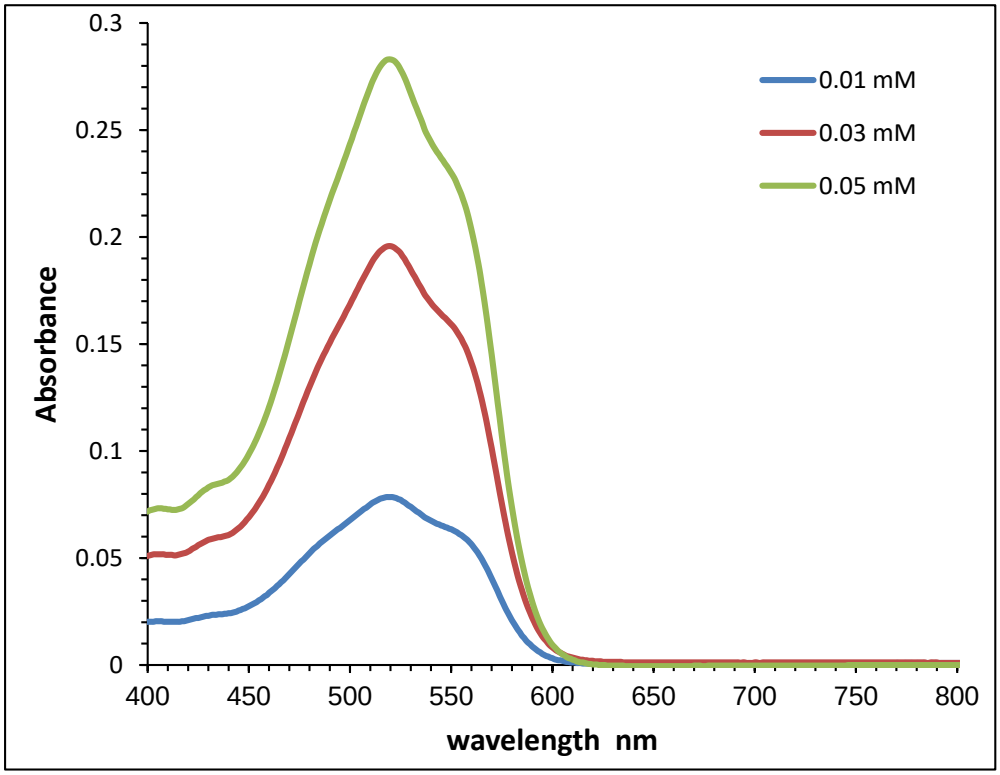

Figure (4.8) : Absorbance spectra of (Rh 110) dye solutions dissolved in ethanol solvent at different concentrations.

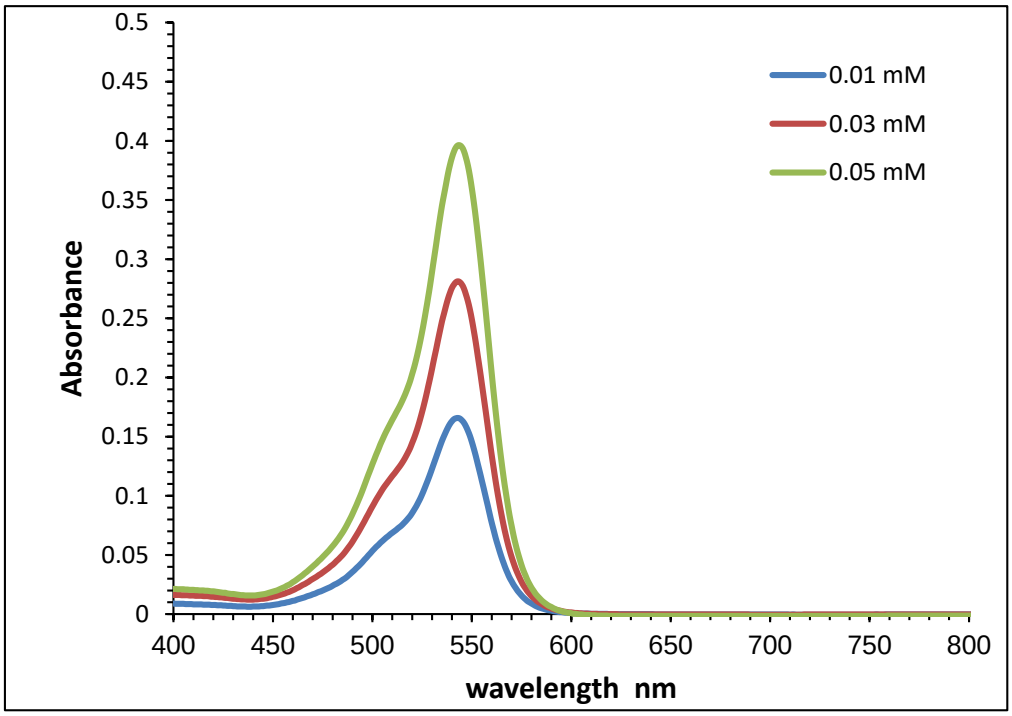

Figure (4.9): Absorbance spectra for solutions of (Rh mix) dissolved in ethanol solvent at different concentrations

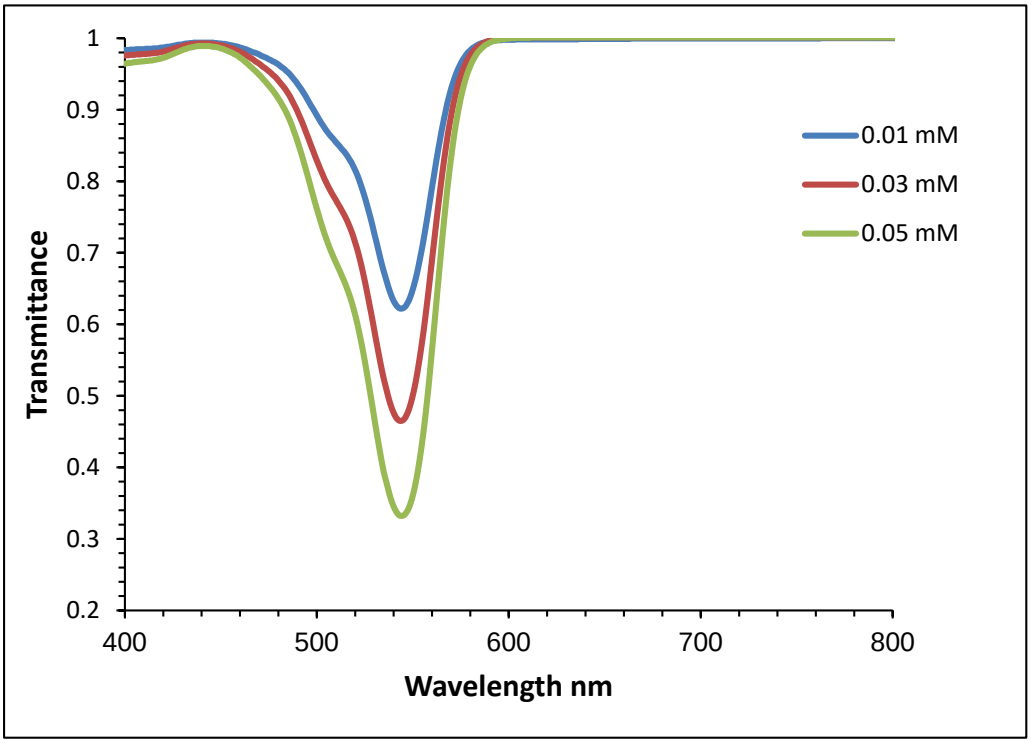

Figure (4.10): Transmittance spectra for solutions of (Rh B) dissolved in ethanol solvent at different concentrations

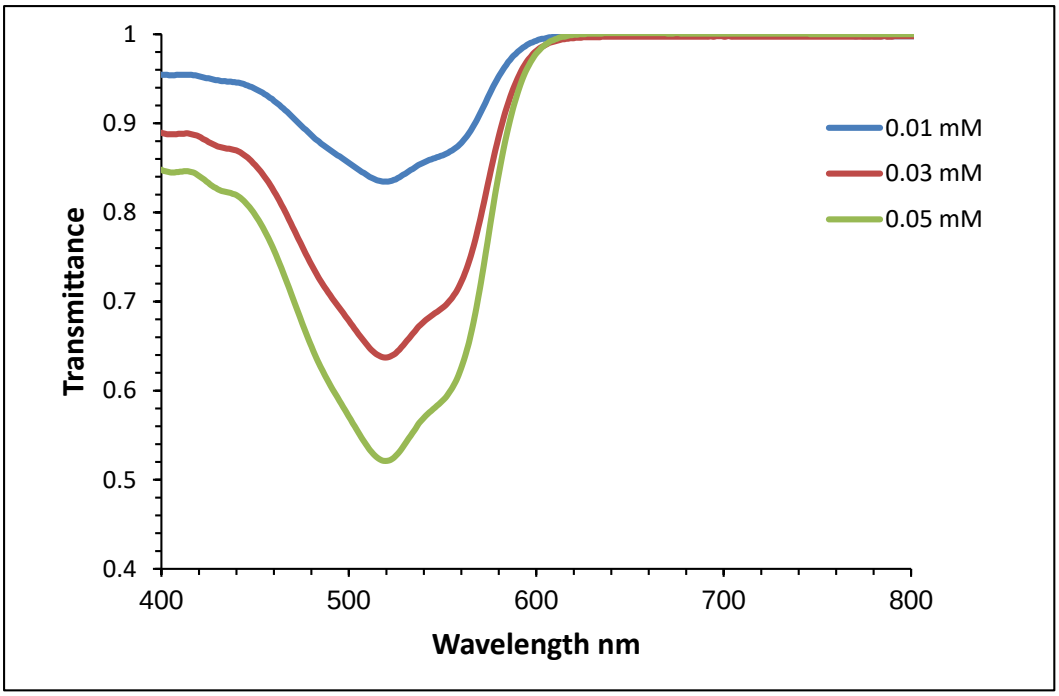

Figure (4.11): Transmittance spectra for (Rh 110) dye solutions dissolved in ethanol solvent at different concentrations.

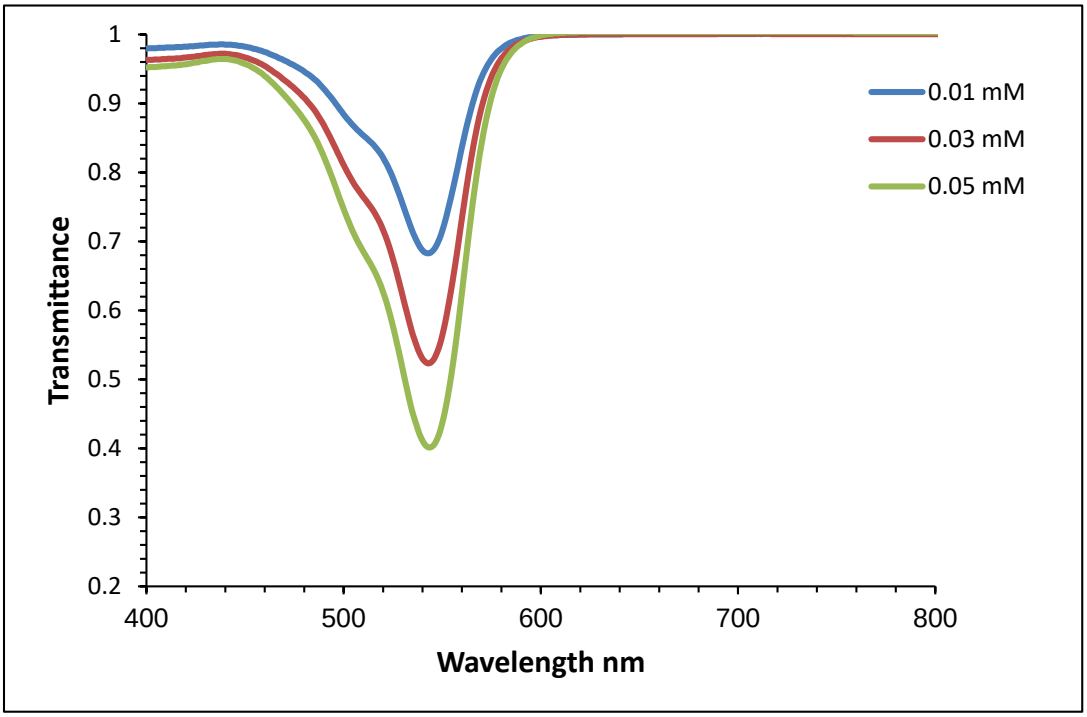

Figure (4.12): Transmittance spectra for (Rh mix) dye solutions dissolved in ethanol solvent at different concentrations.

From the absorbance and transmittance calculations, the values of the linear refractive index (n_o) and the linear absorption coefficient (α_o) were calculated for all the prepared samples. Table (4.1) shows the most important linear optical properties for solutions of dyes Rh B, Rh 110 and Rh mix dissolved in ethanol solvent and at different concentrations. different at wavelength 532 nm .

It is noted from the table that increasing the concentration leads to an increase in the values of the optical coefficients (linear refractive index and linear absorption coefficient) for all the prepared samples dye to the increase in the absorbance values.

Table (4.1): The most important linear optical properties of (Rh B , Rh 110 and Rh mix) dye dissolved in ethanol solvent at different concentrations

Samples	C (m M)	A	T	α_o	n_o
Rh B dye	0.01	0.15	0.71	0.35	1.72
	0.03	0.25	0.56	0.58	2.03
	0.05	0.36	0.44	0.83	2.15
Rh 110 dye	0.01	0.07	0.84	0.17	1.37
	0.03	0.18	0.66	0.42	1.84
	0.05	0.26	0.54	0.60	2.06
Rh mix dye	0.01	0.13	0.75	0.31	1.65
	0.03	0.22	0.60	0.51	1.97
	0.05	0.31	0.49	0.72	2.13

4.3.2 Absorbance and transmittance spectra of (Rh B , Rh 110 and Rh mix) dye solutions dissolved in Methanol solvent.

The absorbance and transmittance spectra were measured for Rh B , Rh 110 and Rh mix dyes dissolved in methanol solvent at different concentrations (0.01, 0.03 and 0.05) mM using a visible spectrometer and a violet fluorescence spectrometer. Figures (4.13 , 4.14 and 4.15) show the absorbance spectra for these solutions. It is noted from these figures that the absorbance values increased for all models compared to the same concentrations of dyes dissolved in the ethanol solvent as shown in Table (4.2). The reason for this is due to the increase in the polarity of the methanol solvent compared to ethanol.

Figures (4.16 , 4.17 and 4.18) show the transmittance spectra for solutions of dyes Rh B, Rh 110 and Rh mix dissolved in methanol solvent at different concentrations .Table (4.2) shows the most important linear optical properties of Rh B , Rh 110 and Rh mix dyes dissolved in methanol solvent at different concentrations at wavelength 532 nm .

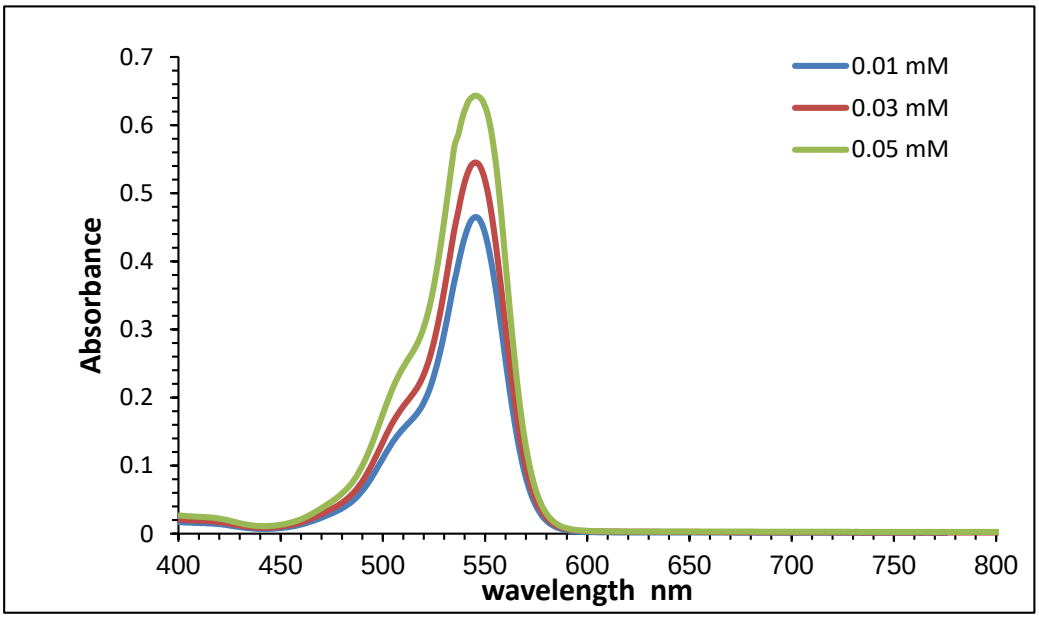

Figure (4.13): Absorbance spectra of (Rh B) dye solutions dissolved in methanol solvent at different concentrations

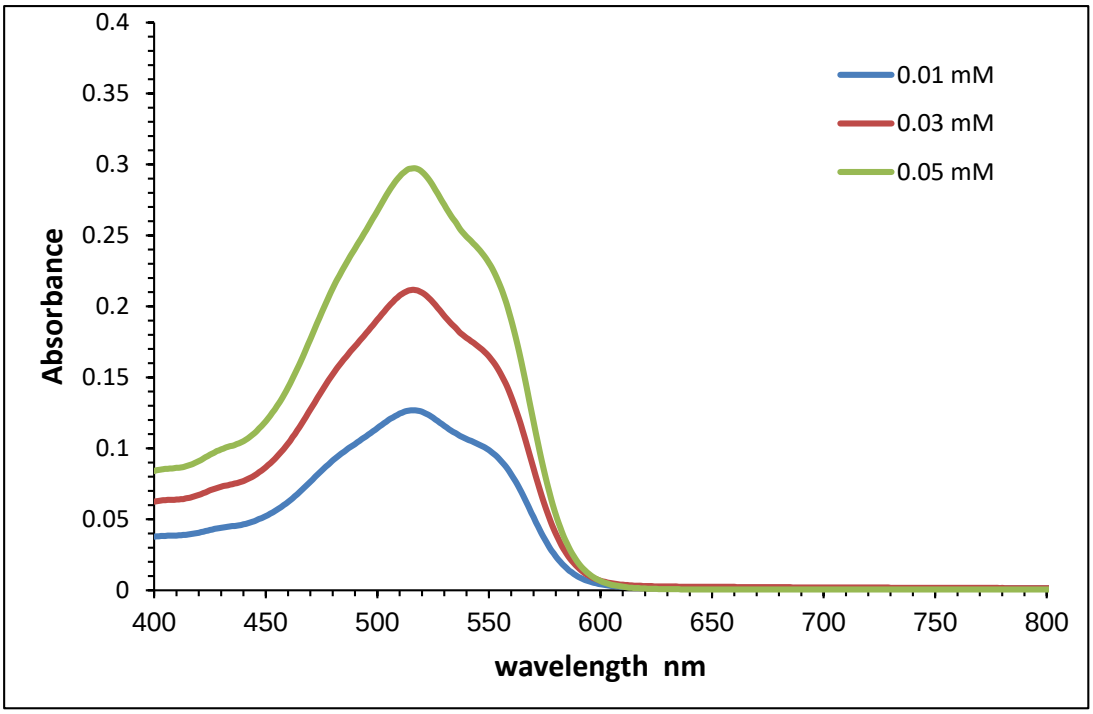

Figure(4.14): Absorbance spectra of (Rh 110) dye solutions dissolved in methanol solvent at different concentrations

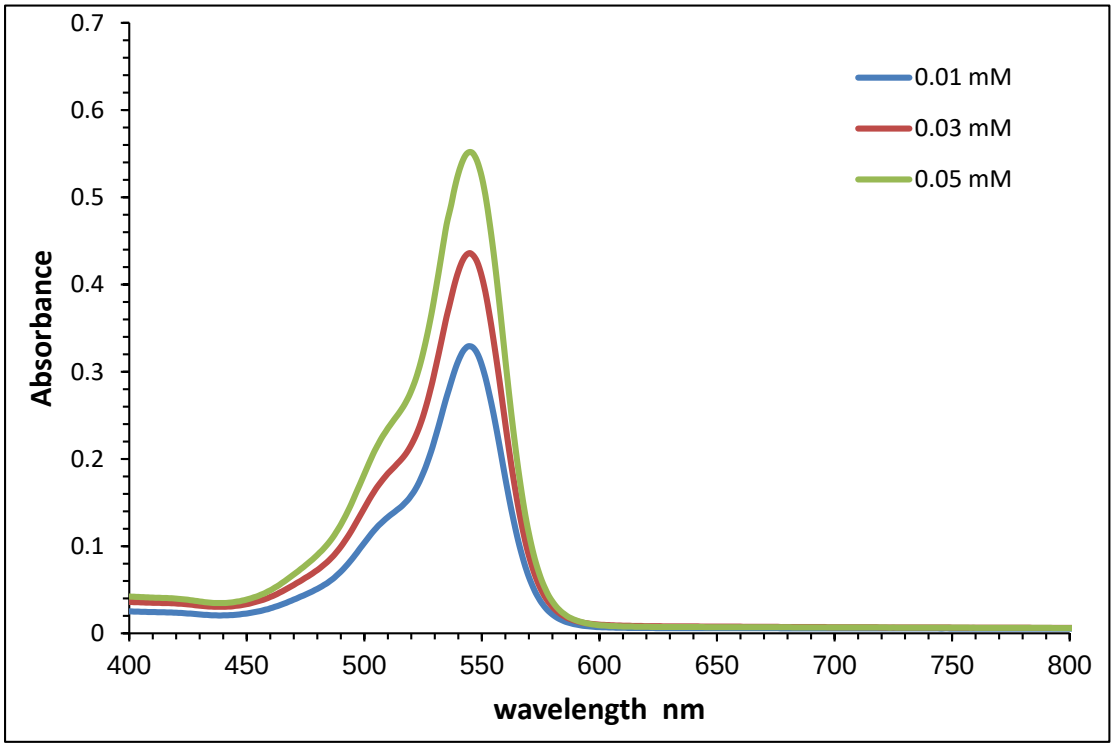

Figure (4.15): Absorbance spectra of (Rh mix) dye solutions dissolved in methanol solvent at different concentrations.

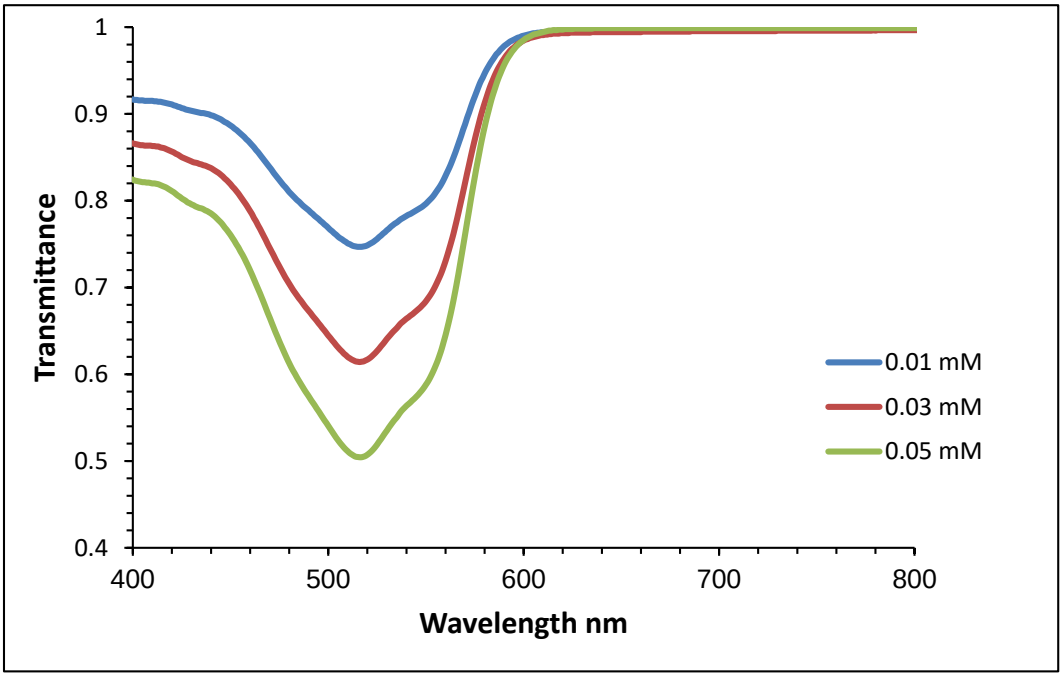

Figure (4.16): Transmittance spectra for (Rh B) dye solutions dissolved in methanol solvent at different concentrations.

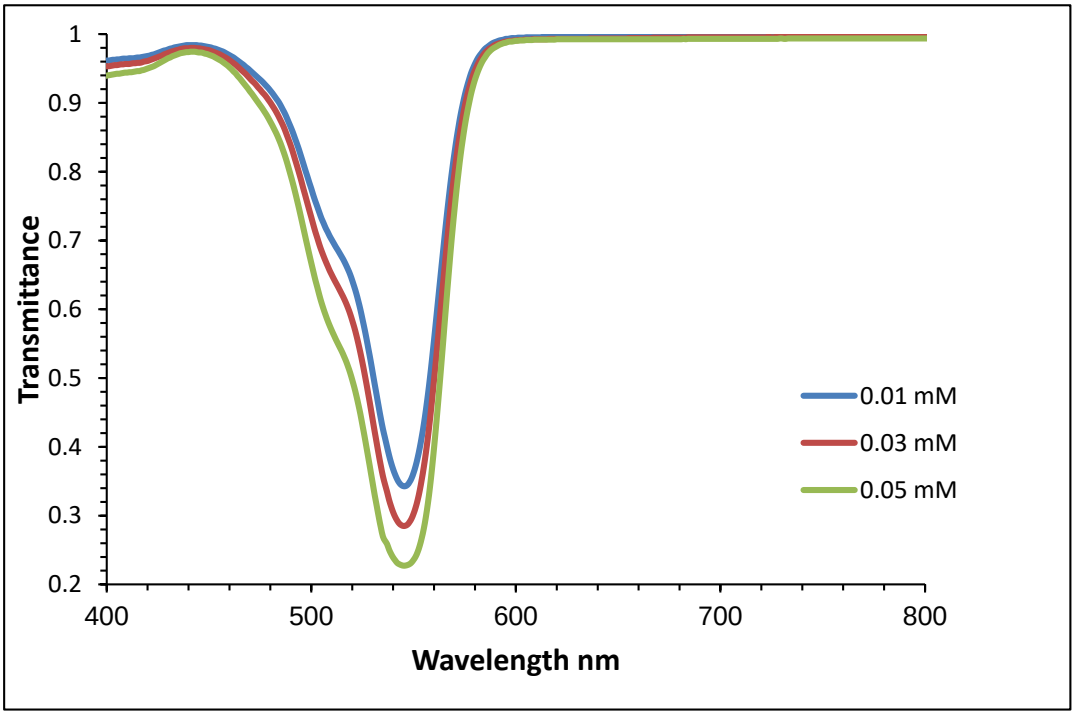

Figure (4.17): Transmittance spectra for (Rh 110) dye solutions dissolved in methanol solvent at different concentrations.

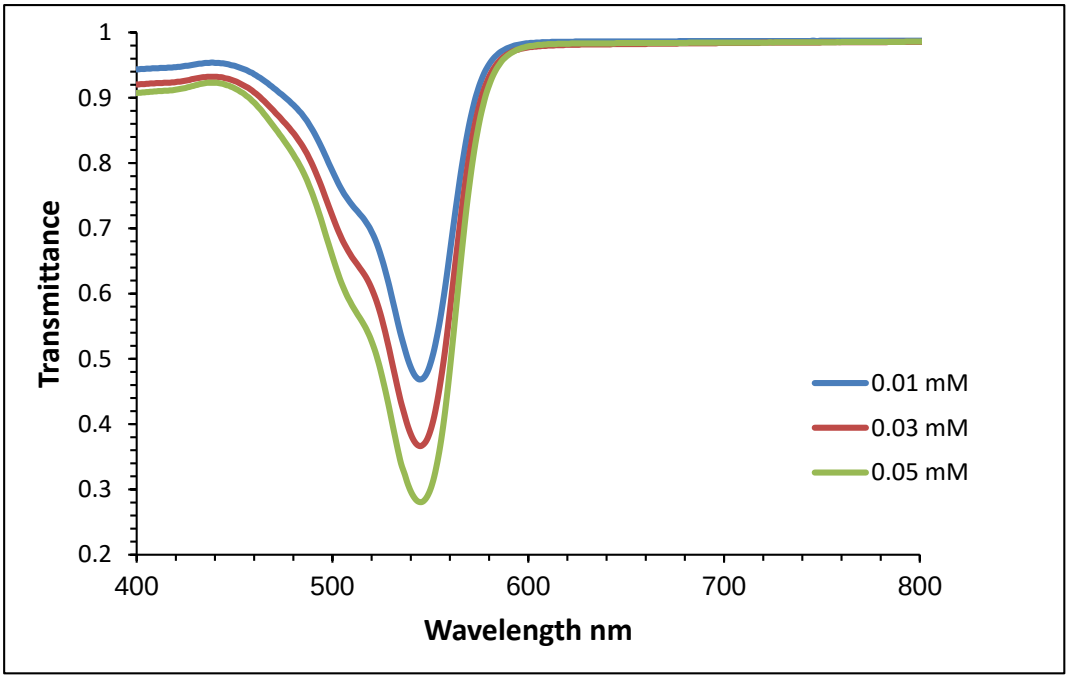

Figure (4.18): Transmittance spectra of s (Rh mix) dyes solutions dissolved in methanol solvent at different concentrations.

Table (4.2): The most important linear optical properties of (Rh B, Rh 110 and Rh mix) dyes solutions dissolved in methanol solvent at different concentrations.

Samples	C (mM)	A	T	α_o	n_o
Rh B dye	0.01	0.32	0.47	0.75	2.10
	0.03	0.39	0.41	0.91	2.17
	0.05	0.50	0.31	0.95	2.23
Rh110 dye	0.01	0.11	0.77	0.26	1.56
	0.03	0.21	0.62	0.45	1.91
	0.05	0.29	0.51	0.66	2.11
Rh mix dye	0.01	0.24	0.57	0.56	2.01
	0.03	0.32	0.47	0.74	2.13
	0.05	0.42	0.38	0.82	2.21

Through the above, it is noted that the highest concentration (0.05 mM) for all solutions used in this study gives the highest linear optical properties (linear refractive index and linear absorption coefficient). Therefore, this concentration was used to study the effect of adding some nanoparticles (Cu, Au and Ag) NPs on linear optical properties, as a volumetric ratio (1:3) of nanomaterials was mixed for these solutions.

4.3.3 Absorbance and Transmittance of (Rh B, Rh 110 and Rh mix) dyes solutions dissolved in Ethanol solvent with nanoparticles.

Figures (4.19 , 4.20 and 4.21) show the absorbance spectra of dye mixture solutions Rh B , Rh 110 and Rh mix . mixed with ethanol solvent at a concentration of (0.05) mM with nanoparticles (Cu , Au and Ag)NPs used in this study, It is noted from these figures that the highest values of absorbance are when adding Ag NPs and the lowest values when adding Cu NPs to all dye solutions. The reason for this is due to the difference in the absorbance values of these particles, which directly affected the absorbance of the mixture and this is reflected in all properties Linear optics for solutions as shown in Table (4.3). Figures (4.22 , 4.23 and 4.24) show the transmittance curves of solutions of dye mixture Rh B , Rh 110 and Rh mix , dissolved in ethanol solvent at a concentration of (0.05) mM with nanoparticles. Absorbency as shown in Table (4.3).

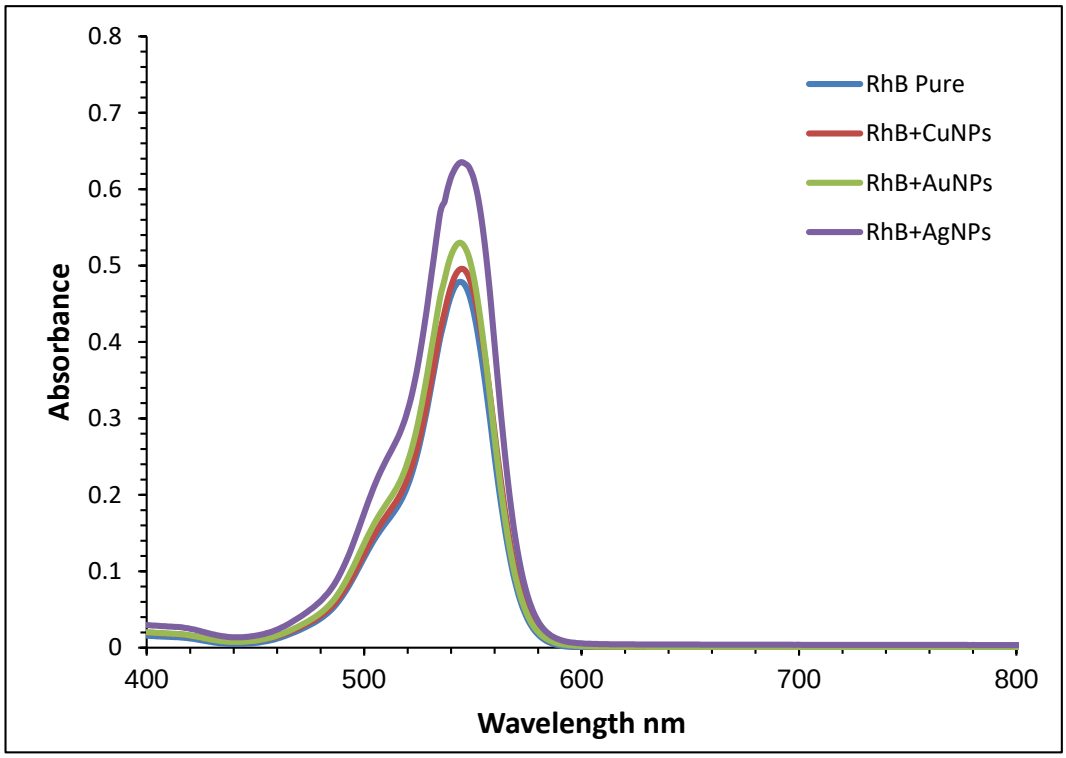

Figure (4.19): Absorbance spectra of (Rh B – nanoparticles) mixture solutions in ethanol solvent.

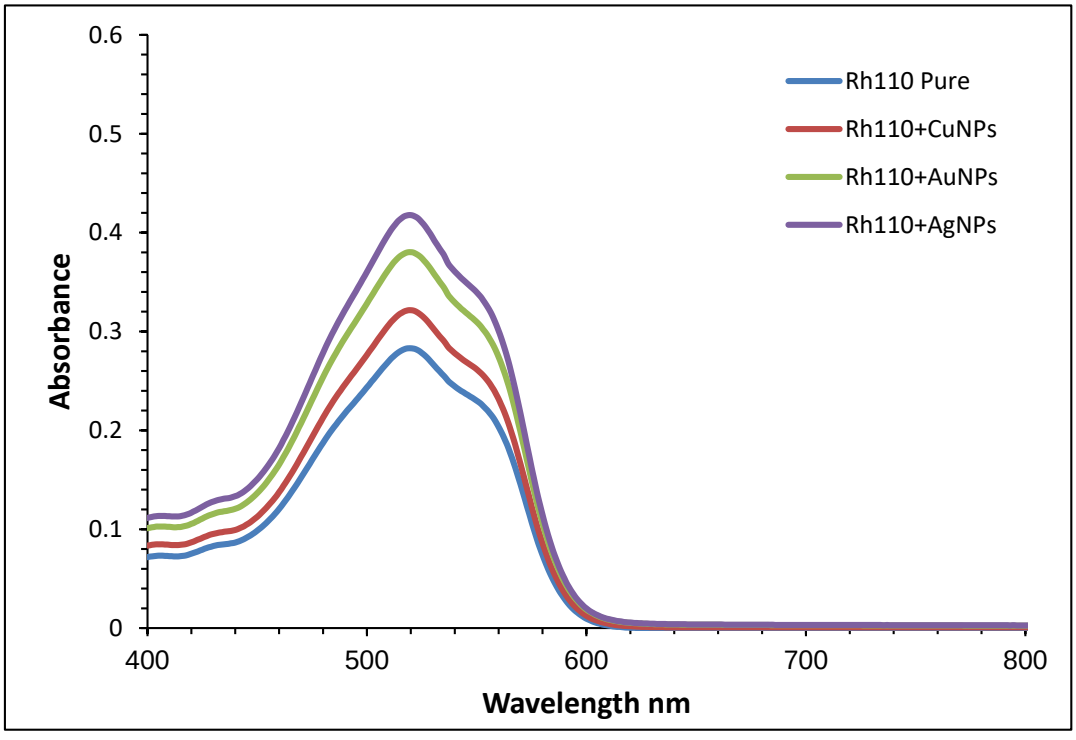

Figure (4.20): Absorbance spectra of (Rh 110- nanoparticles) mixture solutions in ethanol solvent.

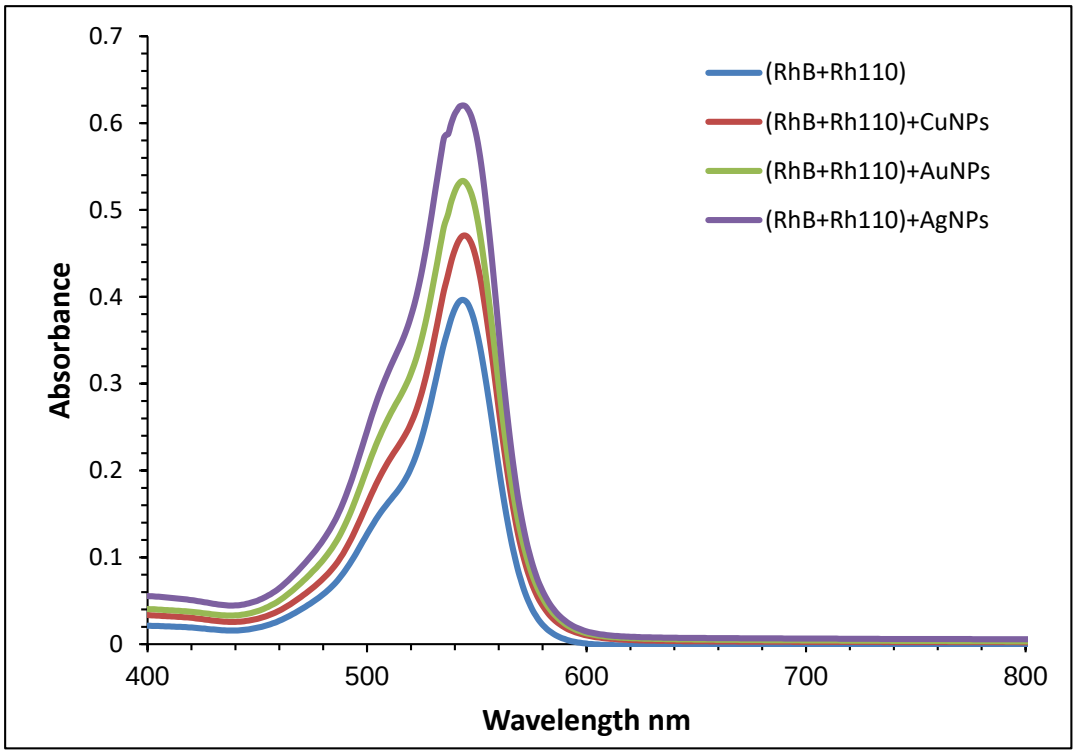

Figure (4.21): Absorbance spectra of (Rh mix - nanoparticles) mixture solutions in ethanol solvent.

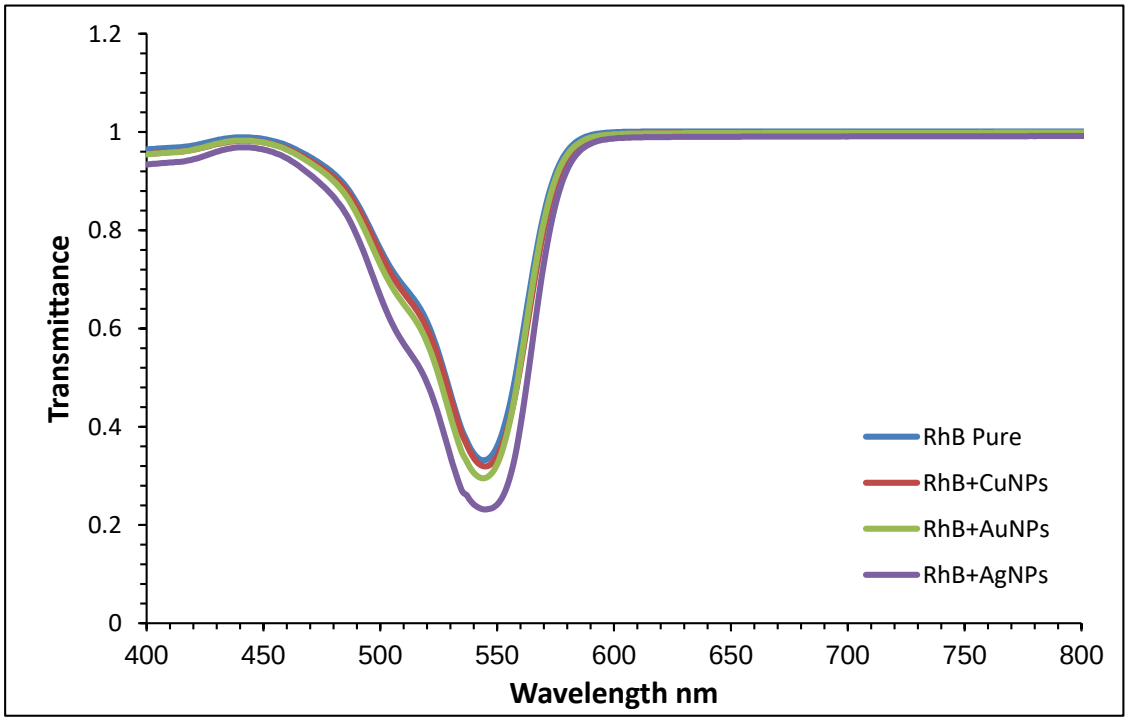

Figure (4.22): Transmittance spectra of (Rh B - nanoparticles) mixture solutions in ethanol solvent.

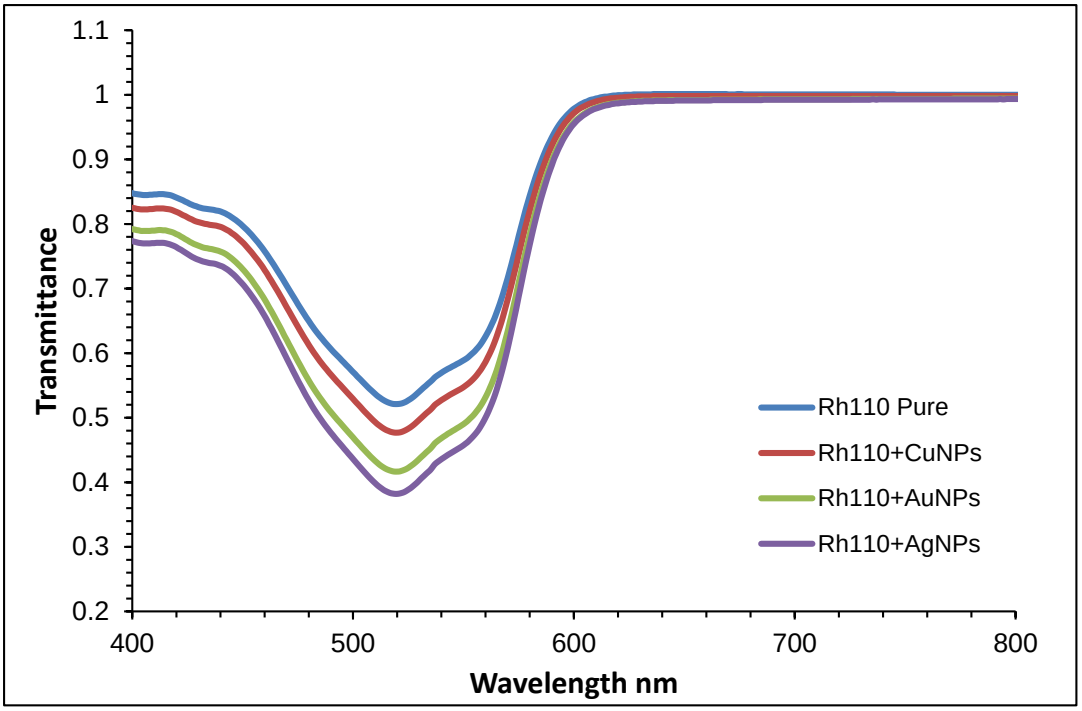

Figure (4.23): Transmittance spectra of (Rh 110 - nanoparticles) mixture solutions in ethanol solvent.

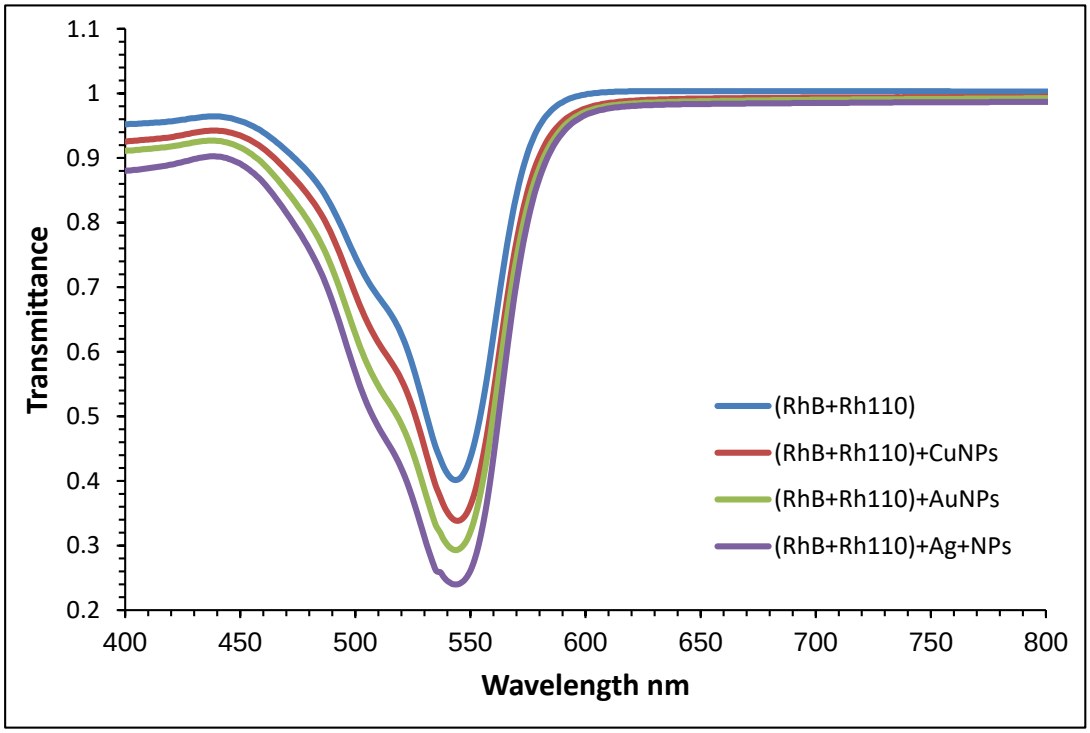

Figure (4.24): Transmittance spectra of (Rh mix - nanoparticles) mixture solutions in ethanol solvent.

Table (4.3): The most important linear optical properties of (Rh B, Rh 110 and Rh mix) dye solutions dissolved in ethanol solvent with NPs.

Sample	A	T	α_o	n_o
RhB Pure	0.36	0.44	0.83	2.15
RhB+Cu NPs	0.37	0.42	0.85	2.18
RhB+Au NPs	0.41	0.39	0.94	2.21
RhB+Ag NPs	0.54	0.31	1.17	2.25
Rh110 Pure	0.26	0.54	0.60	2.06
Rh110+Cu NPs	0.30	0.50	0.69	2.12
Rh110+Au NPs	0.35	0.44	0.81	2.15
Rh110+Ag NPs	0.39	0.41	0.89	2.18
Rh mix	0.31	0.49	0.72	2.13
Rh mix + Cu NPs	0.33	0.43	0.81	2.15
Rh mix + Au NPs	0.37	0.36	0.85	2.18
Rh mix + Au NPs	0.51	0.29	0.95	2.21

4.3.4 Absorbance and Transmittance of (Rh B, Rh 110 and Rh mix) dyes solutions dissolved in Methanol solvent with nanoparticles.

Figures (4.25 , 4.26 and 4.27) show the absorbance spectra of the dye mixture solutions Rh B, Rh 110 and Rh mix dissolved in methanol solvent at a concentration of (0.05)mM with nanoparticles (Cu , Au and Ag) NPs, It is noted from these figures that the highest values of absorbance, as in the previous paragraph, are when adding Ag NPs and the lowest values when adding Cu NPs for all dye solutions and for the same reason. It is also noted that the absorbance values for all solutions dissolved in the methanol solvent are higher than their values in the ethanol solvent Due to the polarity of the solvent, which reflects positively on the linear optical properties, as shown in Table (4.4). Figures (4.28 , 4.29 and 4.30), show the transmittance curves for solutions of dye mixture Rh B, Rh110 and Rh mix dissolved in methanol solvent at a concentration of (0.05)m M with nanoparticles. in Table (4.4).

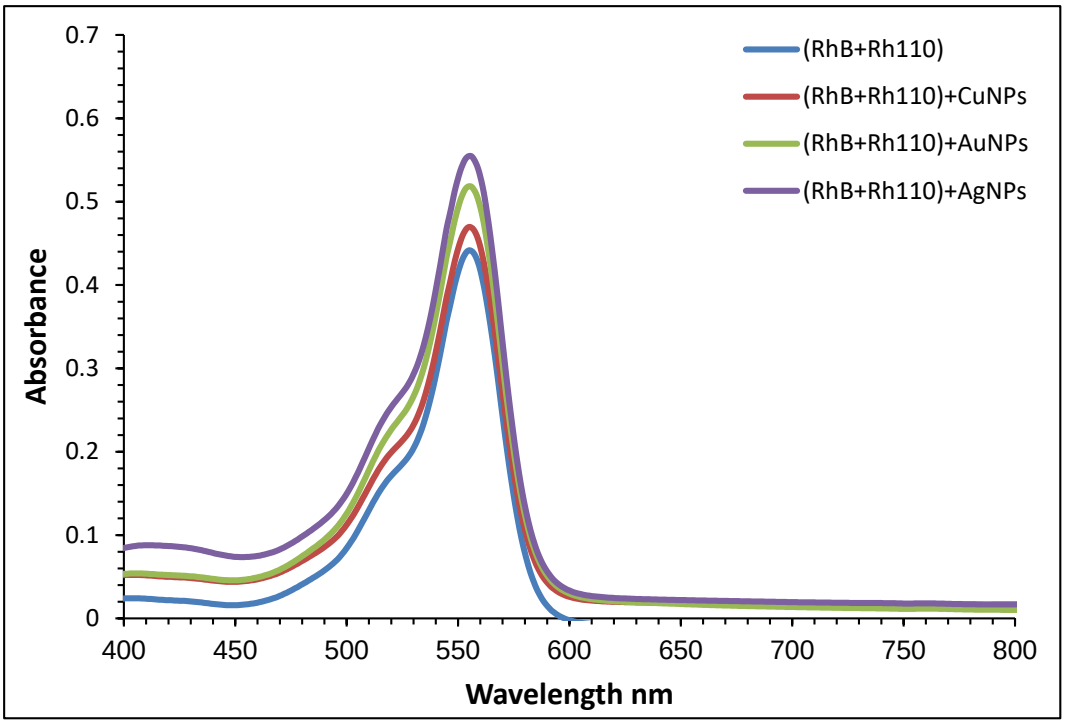

Figure (4.25): Absorbance spectra of (Rh B – nanoparticles) mixture solutions in methanol solvent.

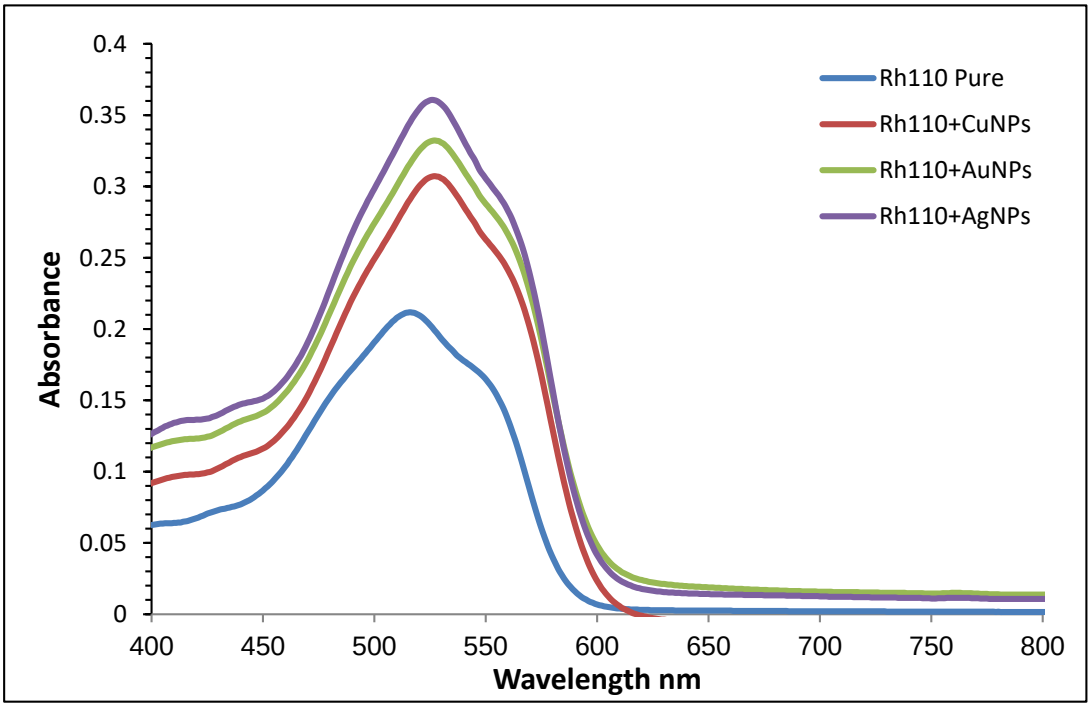

Figure (4.26): Absorbance spectra of (Rh 110 – nanoparticles) mixture solutions in methanol solvent.

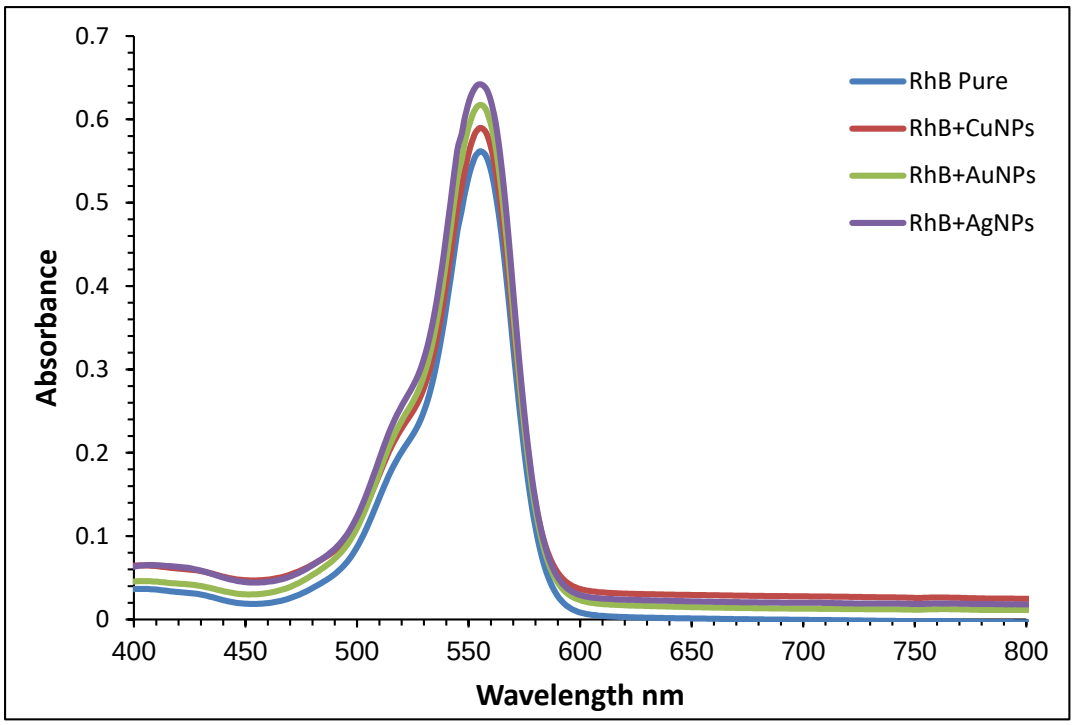

Figure (4.27): Absorbance spectra of (Rh mix - nanoparticles) mixture solutions in methanol solvent.

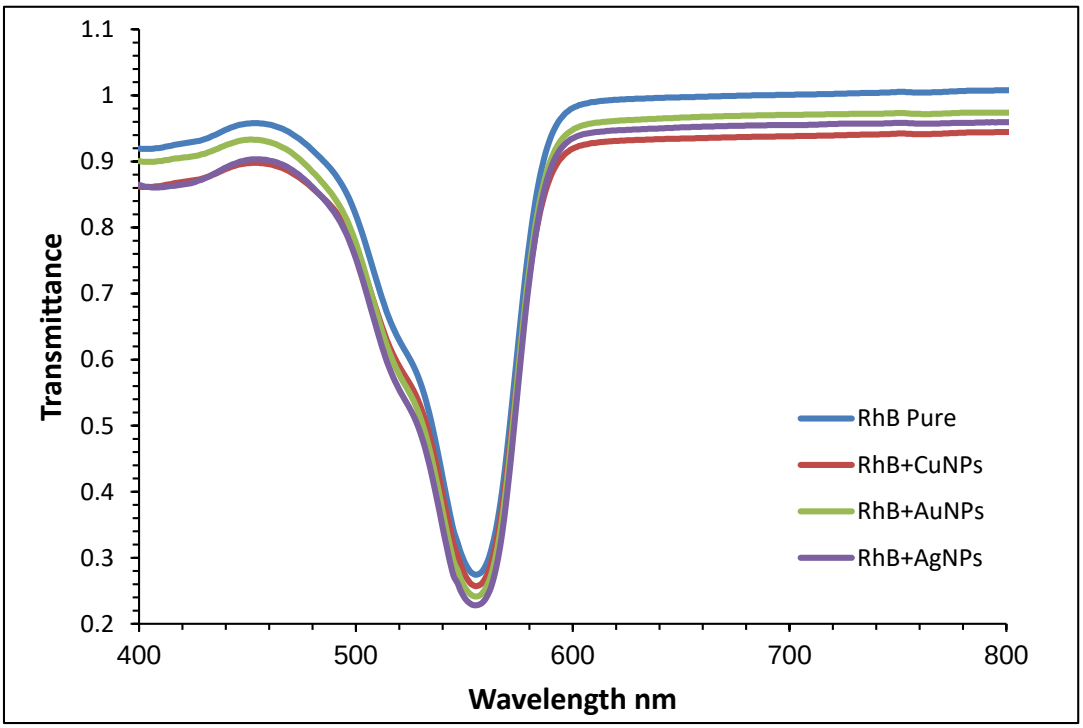

Figure (4.28): Transmittance spectra of (Rh B - nanoparticles) mixture solutions in methanol solvent.

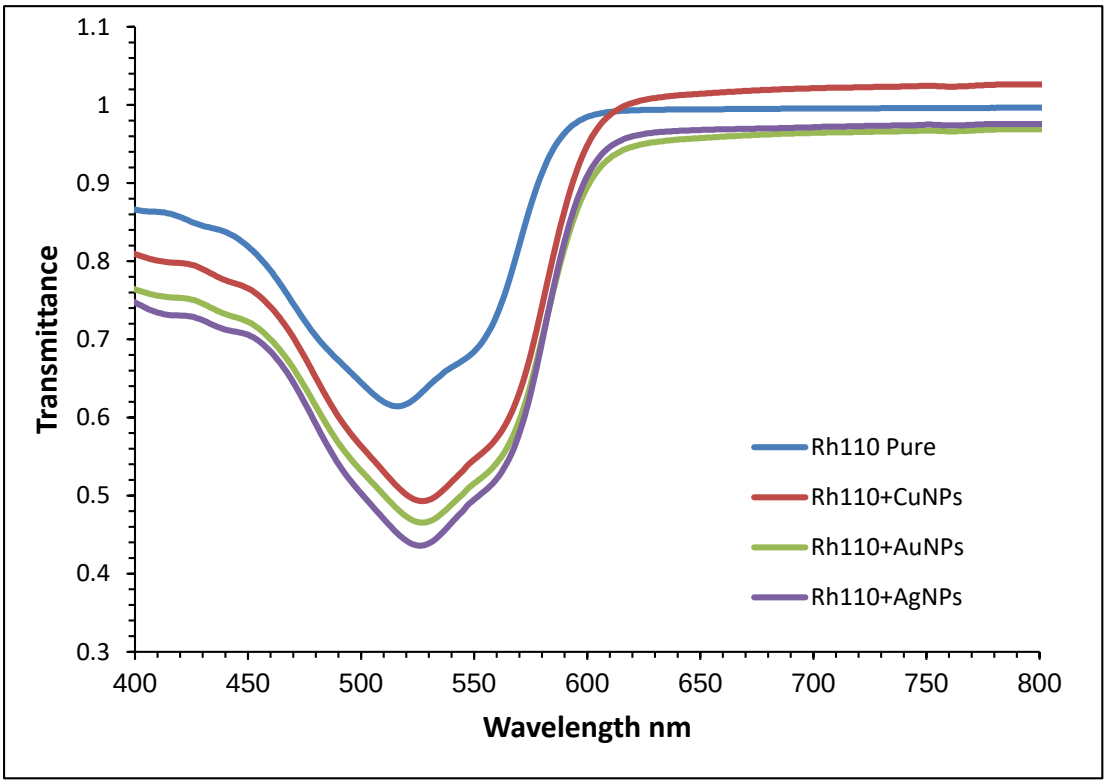

Figure (4.29): Transmittance spectra of (Rh 110 - nanoparticles) mixture solutions in methanol solvent.

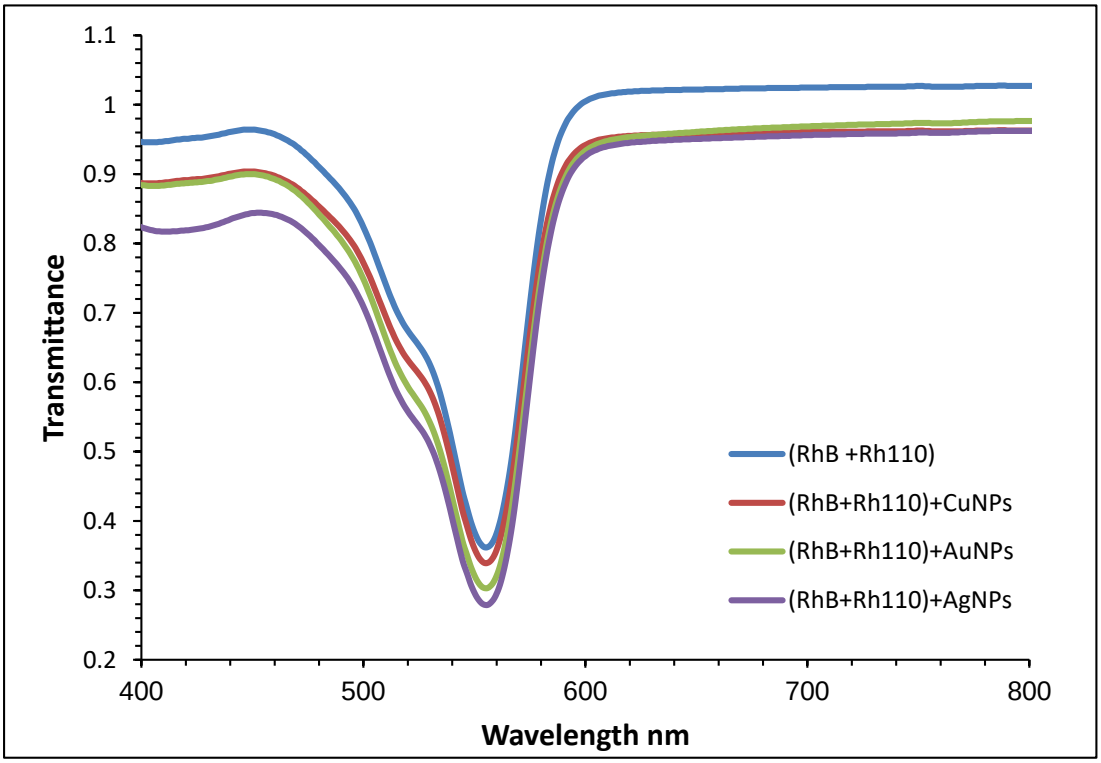

Figure (4.30): Transmittance spectra of (Rh mix - nanoparticles) mixture solutions in methanol solvent.

Table (4.4): The most important linear optical properties of (Rh B, Rh 110 and Rh mix) dye solutions dissolved in methanol solvent with NPs

Sample	A	T	α_o	n_o
RhB Pure	0.50	0.31	0.95	2.23
RhB+Cu NPs	0.52	0.28	1.23	2.26
RhB+Au NPs	0.55	0.25	1.33	2.28
RhB+Ag NPs	0.58	0.22	1.53	2.33
Rh110 Pure	0.29	0.51	0.66	2.11
Rh110+Cu NPs	0.33	0.48	0.72	2.14
Rh110+Au NPs	0.37	0.45	0.88	2.16
Rh110+Ag NPs	0.41	0.41	0.98	2.19
Rh mix	0.42	0.38	0.82	2.21
Rh mix + Cu NPs	0.45	0.35	0.93	2.23
Rh mix + Au NPs	0.48	0.31	1.12	2.25
Rh mix + Au NPs	0.51	0.29	1.18	2.29

4.4 Nonlinear Optical Properties

The nonlinear optical properties were investigated of Rh B, Rh110 and Rh mix organic dyes solutions dissolved in two solvent (Ethanol and Methanol) . All samples have been the same concentration (0.05 mM), and mixture with different nanoparticles (Cu, Au and Ag)NPs that prepared as solutions by pulse laser ablation in liquid method.

The solutions of the used organic dyes were mixed with the nanoparticles in a volumetric ratio (1:3). There are two parts were used to measure the nonlinear properties of the material by Z-Scan technique. The first part is open-aperture Z-Scan and the second part is the closed-aperture Z-Scan.

4.4.1 The nonlinear refractive index of (Rh B, Rh 110 and Rh mix) dyes solutions dissolved in Ethanol solvent with nanoparticles.

The nonlinear refractive index of Rh B, Rh 110 and Rh mix organic dyes solutions dissolved in Ethanol solvent at (0.05 mM) with different nanoparticles (Cu , Au and Ag) NPs, at volumetric ratio (1:3) were measured by closed-aperture Z-Scan technique.

The normalized transmittance of closed-aperture Z-Scan measurements as a function of distance for prepared samples dissolved in Ethanol solvent is shown in Figures (4.31, 4.32 and 4.33) the nonlinear effect region is extended from (-15) mm to (15) mm. The peak followed by a valley transmittance curve obtained from the closed aperture Z-Scan data indicates that the sign of the refraction nonlinearity is negative ($n_2 < 0$), leading to self-defocusing lensing in these samples, it agree with references [135,136].

In order to describe the Z-Scan behavior in the previous Figures, when the sample moves far from the focus, the transmitted beam intensity is low and the transmittance remains relatively constant.

As the sample approaches the beam focus, intensity increases, leading to self-lensing in the sample tend to collimate the beam on the aperture in the far field, increasing the measured transmittance at the iris position. If the beam experiences any nonlinear phase shift due to the sample as it is translated through the focal region, then the fraction of light falling on the detector will vary due to the self-lensing generated in the material by the intense laser beam. In this case, the signal measured by detector will exhibit a peak and valley as the sample is translated [137].

The position of the peak and valley, relative to the z-axis, depends on the sign of the nonlinear phase shift .Where the change in the normalized transmittance from the peak of the curve to the valley (ΔT_{p-v}) is directly proportional to the nonlinear phase shift imparted on the beam. Moreover,

if the beam is transmitted through the nonlinear medium the induced phase shift can also be either negative or positive accordingly when the medium is self- defocusing or self-focusing, respectively [138].

The magnitude of the phase shift can be determined from the change in transmittance between peak and valley (ΔT_{p-v}). After the focal plane, the self-defocusing increases the beam divergence, leading to a widening of the beam at the focus and thus reducing the measured transmittance. Far from focus (Z > 0),again the nonlinear refraction is low resulting in a transmittance Z-independent. The behavior of Z-Scan curves was agreement with reference [139]. The closed-aperture Z-Scan defines variable transmittance values, which used to determine the nonlinear phase shift $\Delta\Phi$ using equation (2.18) and the nonlinear refractive index (n_2) using equation (2.19).

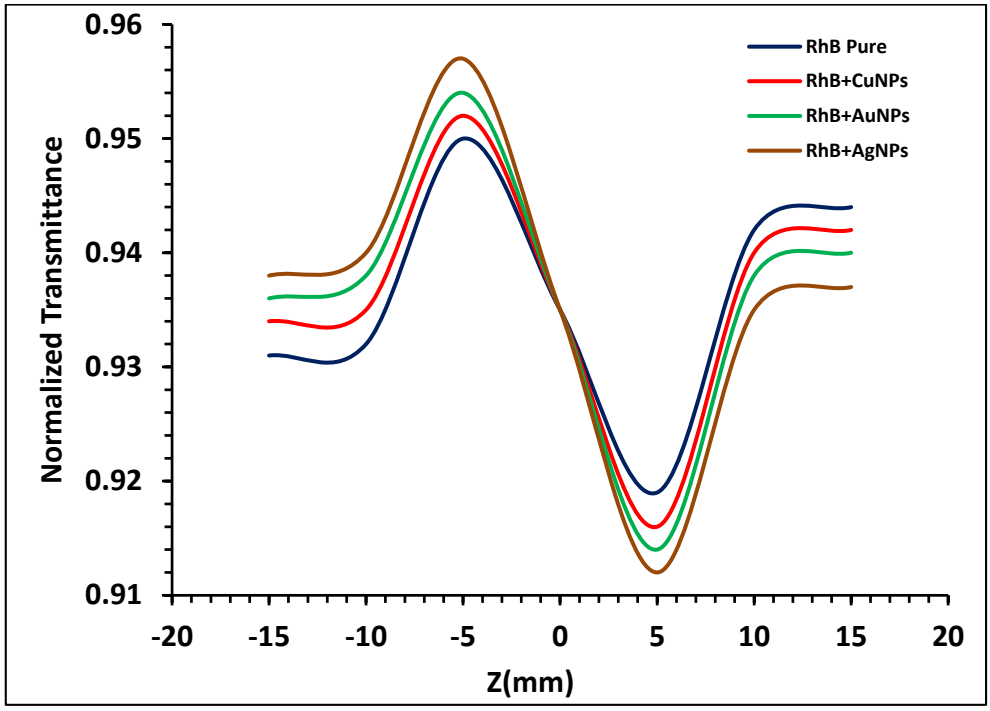

Figure (4.31): The normalized transmittance of closed-aperture Z-Scan measurements as a function of distance for Rh B dye solutions dissolved in Ethanol solvent with different nanoparticles

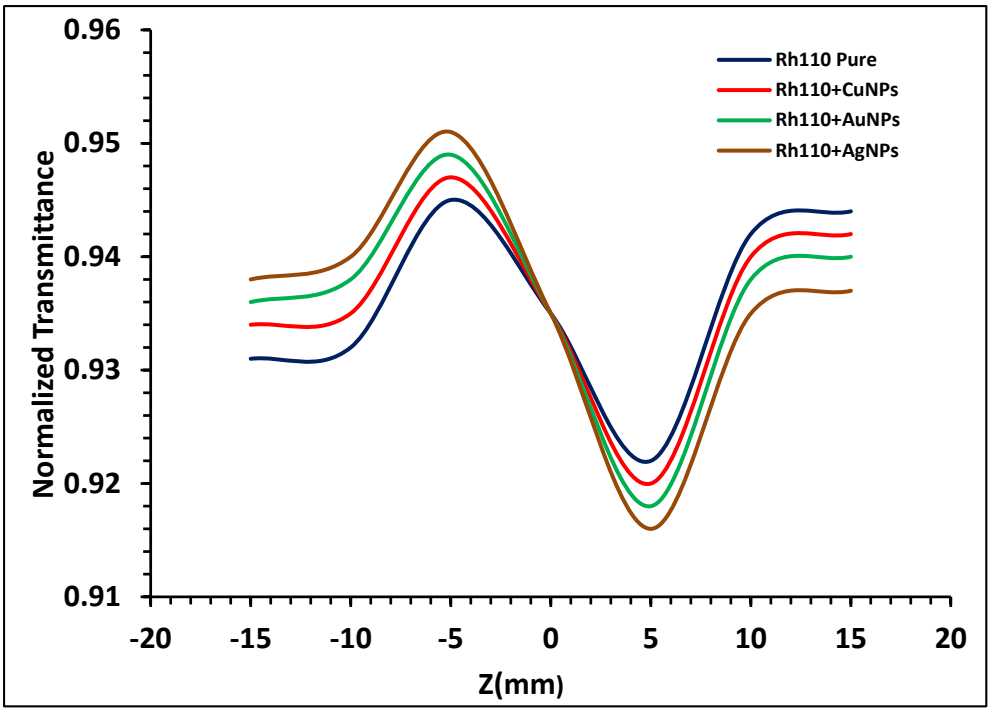

Figure (4.32): The normalized transmittance of closed-aperture Z-Scan measurements as a function of distance for Rh110 dye solutions dissolved in Ethanol solvent with different nanoparticles

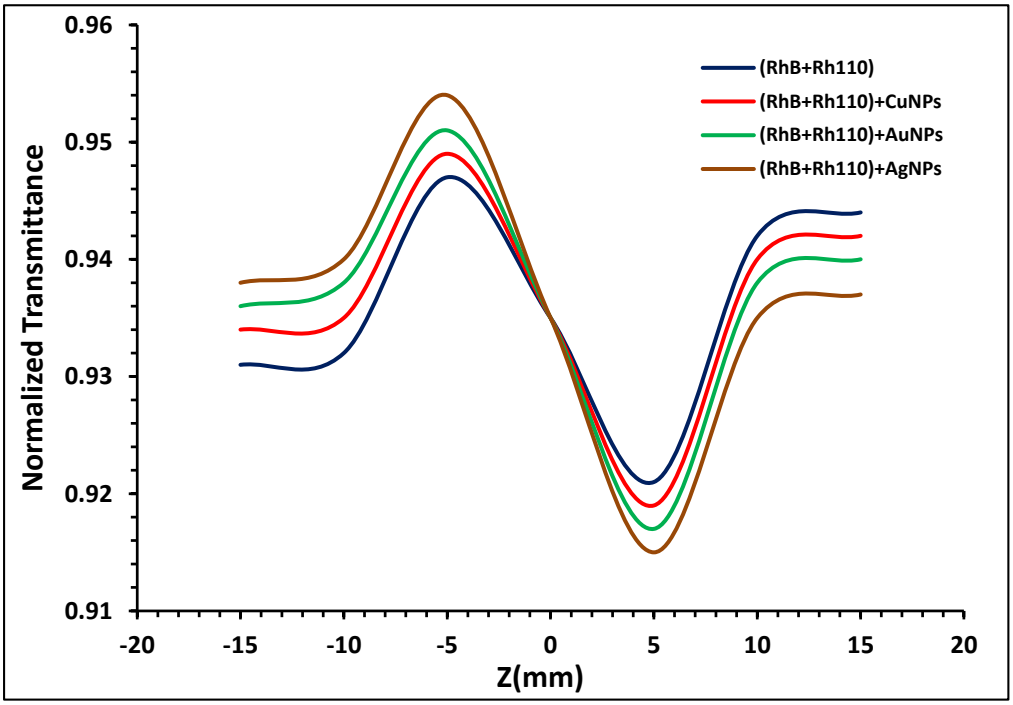

Figure (4.33): The normalized transmittance of closed-aperture Z-Scan measurements as a function of distance for Rh mix dye solutions dissolved in Ethanol solvent with different nanoparticles.

Table (4.5) shows the nonlinear refractive index properties of organic dye solutions and their mixture dissolved in ethanol solvent with different nanoparticles used in this study. It is noted from this Table that the highest values of the nonlinear refractive index (n_2) for all dye solutions are by adding (Ag NPs), the reason for this is due to the increase of the difference between peak and valley of transmittance (ΔT_{p-v}) and thus the increase of nonlinear phase shift $\Delta\Phi$.

Table (4.5): The nonlinear refractive index properties of organic dye solutions and their mixture dissolved in ethanol solvent with different nanoparticles used in this study.

Samples	ΔT_{P-V}	$\Delta\Phi_o$	n_2 (cm^2/mW) $\times 10^{-10}$
Rh B Pure	**0.031**	**0.076**	**2.19**
Rh B+Cu NPs	**0.036**	**0.087**	**2.43**
Rh B+Au NPs	**0.040**	**0.099**	**3.21**
RhB+Ag NPs	**0.045**	**0.110**	**3.68**
Rh 110 Pure	**0.023**	**0.056**	**1.29**
Rh 110+Cu NPs	**0.027**	**0.067**	**1.34**
Rh 110+Au NPs	**0.031**	**0.076**	**1.48**
Rh 110+Ag NPs	**0.035**	**0.087**	**1.65**
Rh mix	**0.026**	**0.064**	**1.52**
Rh mix + Cu NPs	**0.030**	**0.074**	**1.91**
Rh mix +Au NPs	**0.034**	**0.083**	**2.75**
Rh mix +Ag NPs	**0.039**	**0.096**	**3.25**

4.4.2 The nonlinear absorption coefficient of (Rh B, Rh 110 and Rh mix) dyes solutions dissolved in Ethanol solvent with nanoparticles.

The nonlinear absorption coefficient of Rh B, Rh 110 and Rh mix organic dyes solutions dissolved in Ethanol solvent at (0.05 mM) with different nanoparticles (Cu , Au and Ag) NPs, at volumetric ratio (1:3) were measured by open-aperture Z-Scan technique.

The normalized transmittance of Open-aperture Z-Scan measurements as a function of distance for prepared samples dissolved in Ethanol solvent is shown in Figures (4.34 , 4.35 and 4.36). It is noted from these Figures that the nonlinear absorption is two photon absorption. The behavior of transmittance starts linearly at different distances from the far field of the sample position (-Z).At the near field, the transmittance curve begins to decrease until it reaches the minimum value of T(z) at the focal point (Z=0). The nonlinear absorption coefficient (β) can be calculate by using equation (2.22).

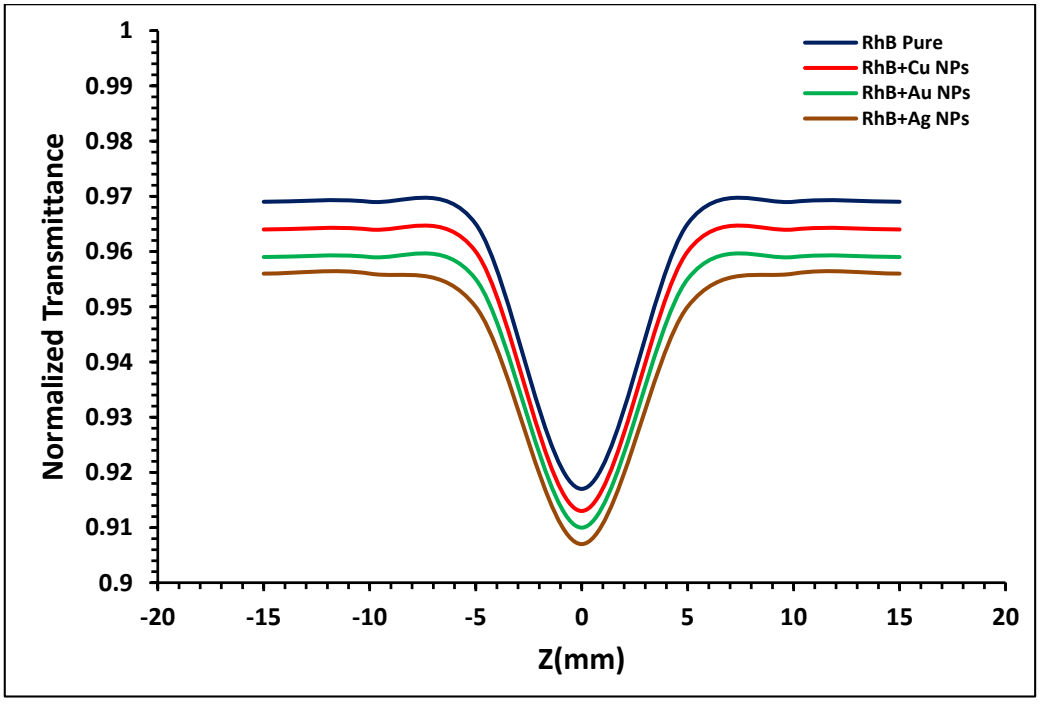

Figure (4.34): The normalized transmittance of open-aperture Z-Scan measurements as a function of distance for Rh B dye solutions dissolved in Ethanol solvent with different nanoparticles.

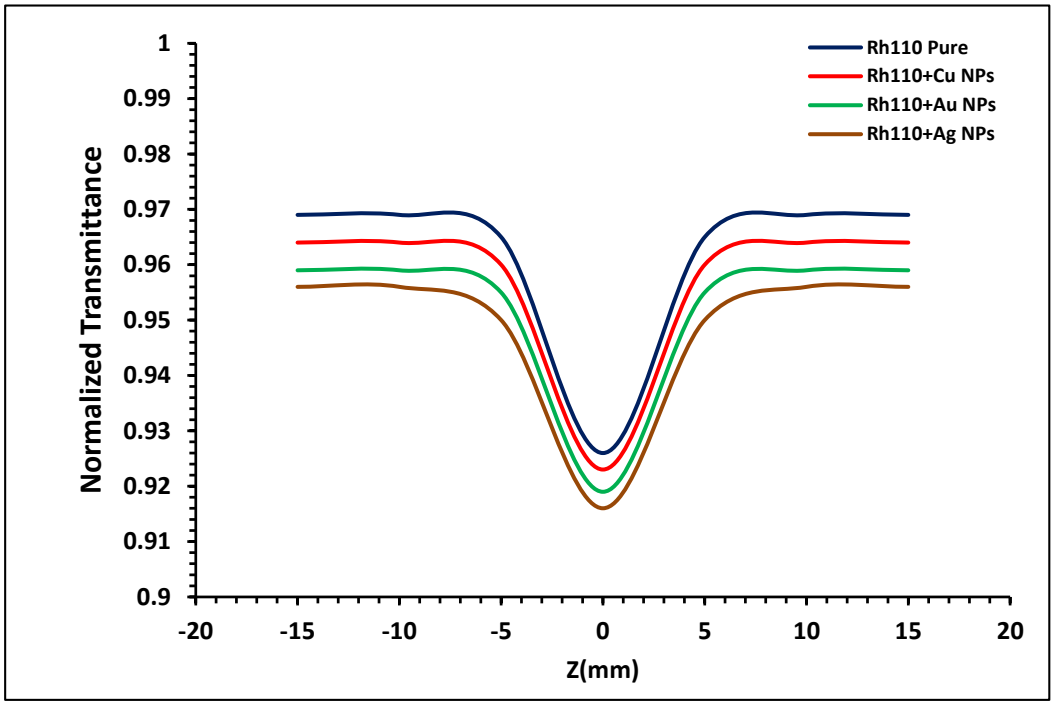

Figure (4.35): The normalized transmittance of open-aperture Z-Scan measurements as a function of distance for Rh 110 dye solutions dissolved in Ethanol solvent with different nanoparticles

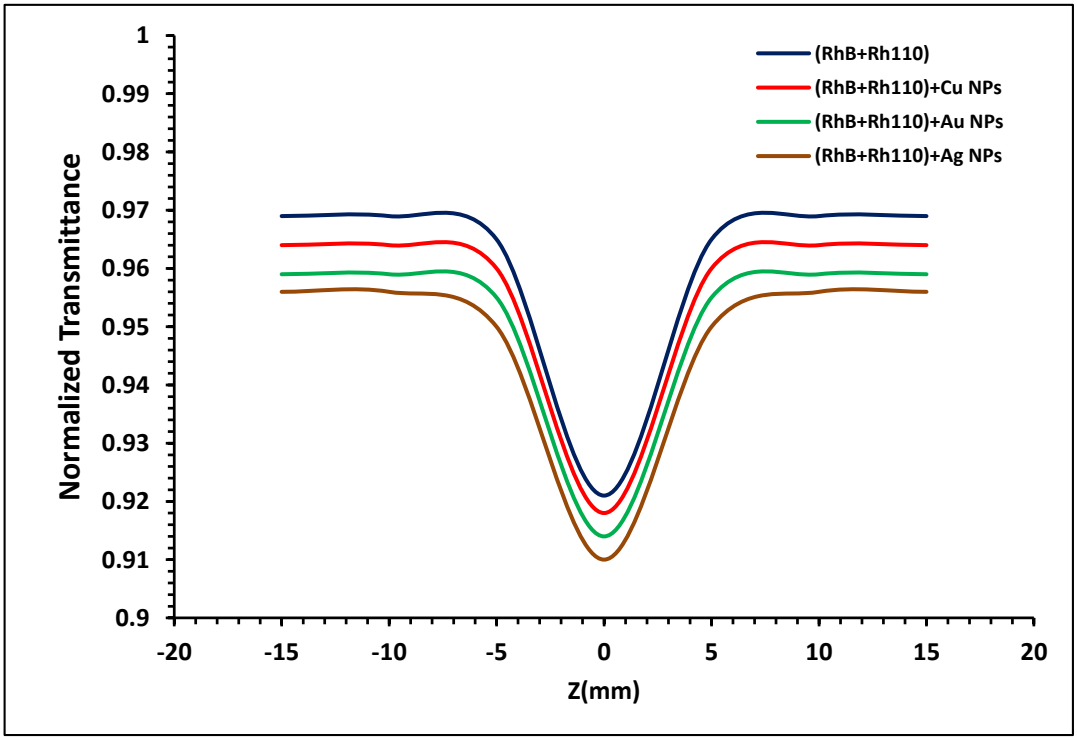

Figure (4.36): The normalized transmittance of open-aperture Z-Scan measurements as a function of distance for Rh mix dye solutions dissolved in Ethanol solvent with different nanoparticles.

Table (4.6): The nonlinear absorption coefficient Properties of organic dye solutions and their mixtures dissolved in Ethanol solvent with different nanoparticles at λ=532nm

Samples	T(z)	β (cm/mW)
Rh B Pure	0.917	3.17×10^{-3}
Rh B+Cu NPs	0.913	2.83×10^{-3}
Rh B+Au NPs	0.910	2.57×10^{-3}
Rh B+Ag NPs	0.907	2.39×10^{-3}
Rh 110 Pure	0.926	3.65×10^{-3}
Rh 110+Cu NPs	0.923	3.36×10^{-3}
Rh 110+Au NPs	0.919	3.22×10^{-3}
Rh 110+Ag NPs	0.916	2.94×10^{-3}
Rh mix	0.921	3.35×10^{-3}
Rh mix + Cu NPs	0.918	3.13×10^{-3}
Rh mix +Au NPs	0.914	2.86×10^{-3}
Rh mix +Ag NPs	0.910	2.54×10^{-3}

4.4.3 The nonlinear refractive index of (Rh B, Rh 110 and Rh mix) dyes solutions dissolved in Methanol solvent with nanoparticles.

The nonlinear refractive index of Rh B, Rh 110 and Rh mix organic dyes solutions dissolved in Methanol solvent at (0.05 mM) with different nanoparticles (Cu, Au and Ag) NPs were measured by closed-aperture Z-Scan technique. The normalized transmittance of closed-aperture Z-Scan measurements as a function of distance for prepared samples dissolved in Methanol solvent is shown in Figures (4.37, 4.38 and 4.39) . The transmittance curves from peak to a valley obtained from the closed-aperture Z-Scan data indicates that the sign of the refraction nonlinearity is negative ($n_2 < 0$), leading to self-defocusing lensing in these samples.

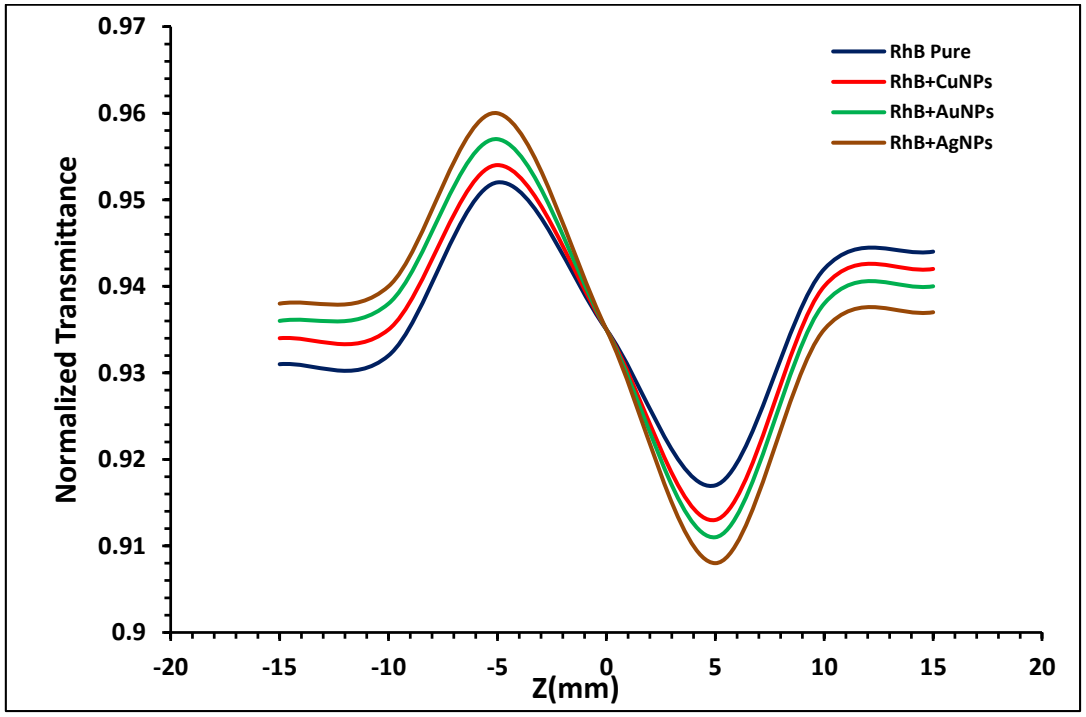

Figure (4.37): The normalized transmittance of closed-aperture Z-Scan measurements as a function of distance for Rh B dye solutions dissolved in Methanol solvent with different nanoparticles

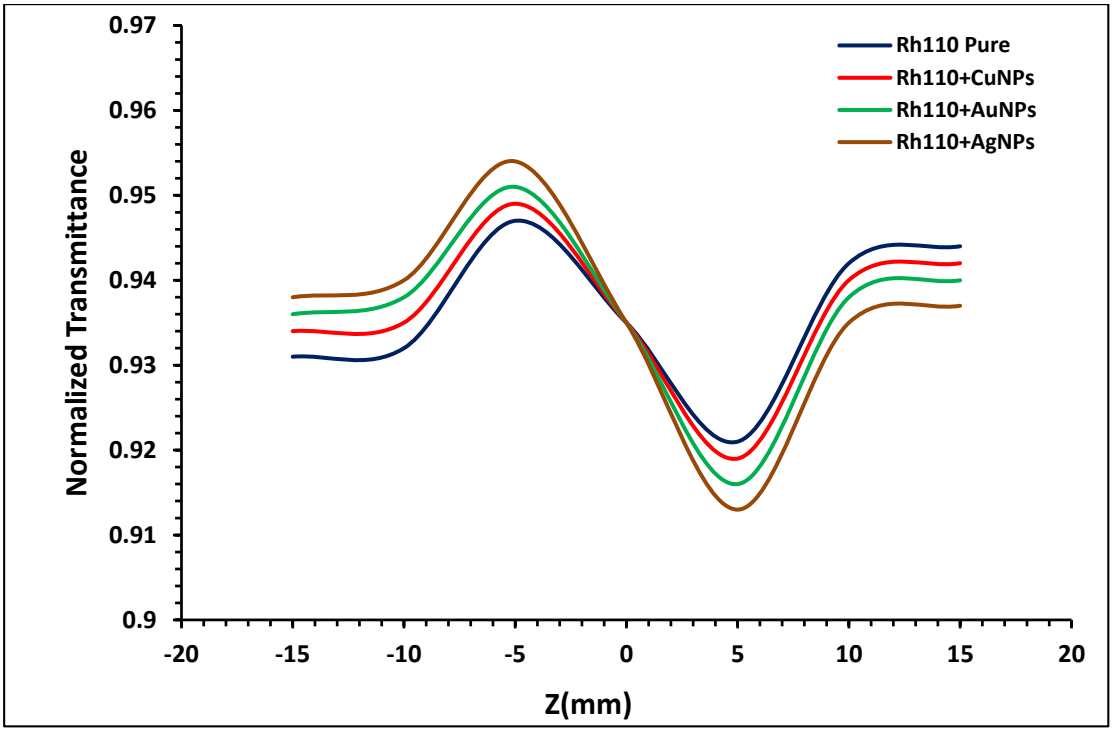

Figure (4.38): The normalized transmittance of closed-aperture Z-Scan measurements as a function of distance for Rh 110 dye solutions dissolved in Methanol solvent with different nanoparticles

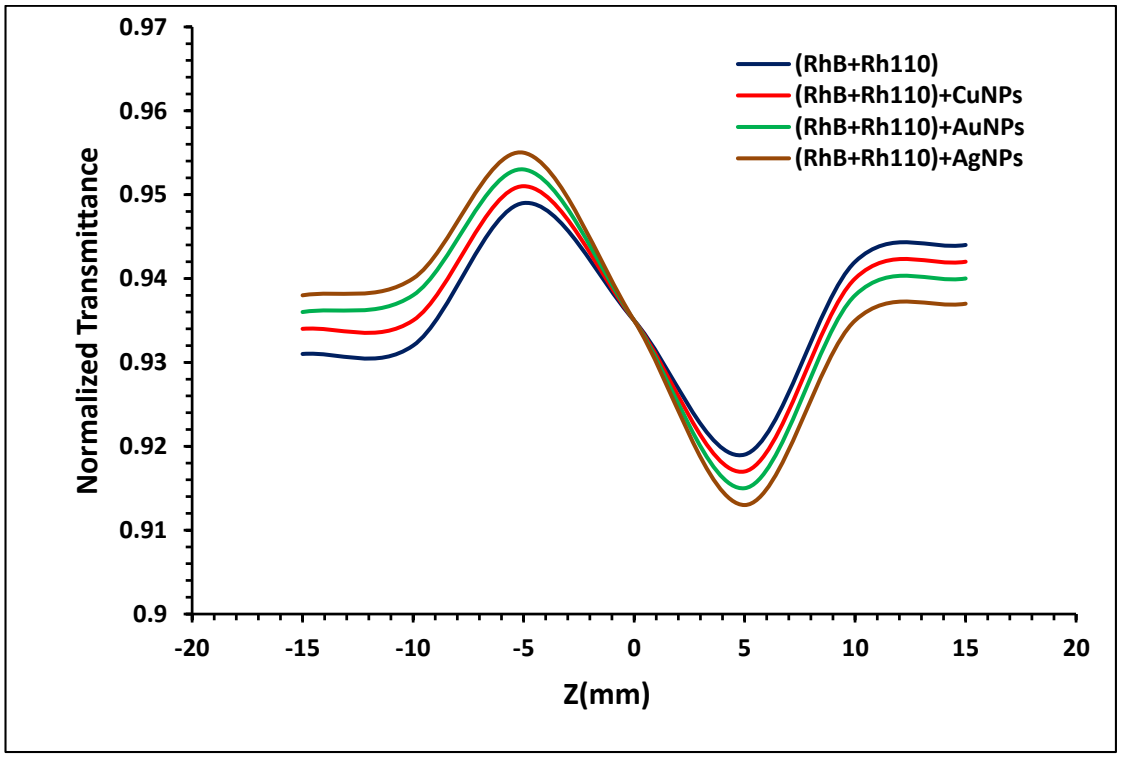

Figure (4.39): The normalized transmittance of closed-aperture Z-Scan measurements as a function of distance for Rh mix dye solutions dissolved in Methanol solvent with different nanoparticles

Table (4.7) shows the nonlinear refractive index properties of organic dye solutions and their mixture dissolved in Methanol solvent with different nanoparticles. It is noted from this table that the highest values of the nonlinear refractive index (n_2) for all dye solutions are by adding (Ag NPs), It is also noted that the values of the nonlinear refractive index (n_2) for all the prepared samples are larger compared to the solutions dissolved in the Ethanol solvent, and the reason for this is due to the polarity of the Methanol solvent.

Table(4.7): The nonlinear refractive index properties of organic dye solutions and their mixtures dissolved in Methanol solvent with different nanoparticles at λ=532nm

Samples	ΔT_{P-V}	$\Delta\Phi_o$	$n_2 \times 10^{-10}$ (cm^2/mW)
Rh B Pure	**0.035**	**0.086**	**2.43**
Rh B+Cu NPs	**0.041**	**0.101**	**2.71**
Rh B+Au NPs	**0.046**	**0.113**	**3.56**
RhB+Ag NPs	**0.052**	**0.128**	**3.92**
Rh 110 Pure	**0.026**	**0.064**	**1.52**
Rh 110+Cu NPs	**0.030**	**0.074**	**1.77**
Rh 110+Au NPs	**0.035**	**0.086**	**1.91**
Rh 110+Ag NPs	**0.041**	**0.101**	**2.43**
Rh mix	**0.031**	**0.073**	**1.86**
Rh mix + Cu NPs	**0.035**	**0.084**	**2.44**
Rh mix +Au NPs	**0.038**	**0.093**	**3.15**
Rh mix +Ag NPs	**0.043**	**0.105**	**3.53**

4.4.4 The nonlinear absorption coefficient of (Rh B, Rh 110 and Rh mix) dyes solutions dissolved in Methanol solvent with nanoparticles.

The nonlinear absorption coefficient of Rh B, Rh 110 and Rh mix organic dyes solutions dissolved in Methanol solvent at (0.05 mM) with different nanoparticles (Cu, Au and Ag) NPs were measured by open aperture Z-Scan technique The normalized transmittance of Open-aperture Z-Scan measurements as a function of distance for prepared samples dissolved in Ethanol solvent is shown in Figures (4.40 , 4.41 and 4.42). It is noted from these Figures that the nonlinear absorption is two photon absorption.

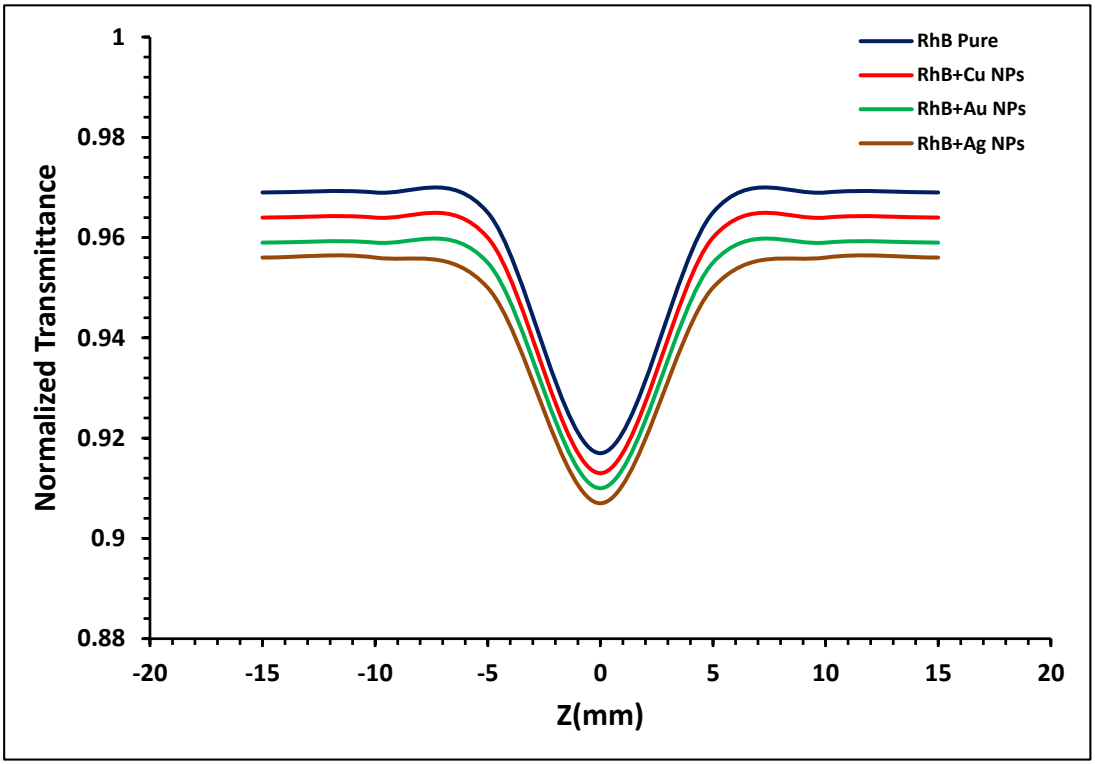

Figure (4.40): The normalized transmittance of open-aperture Z-Scan measurements as a function of distance for RhB dye solutions dissolved in Methanol solvent with different nanoparticles

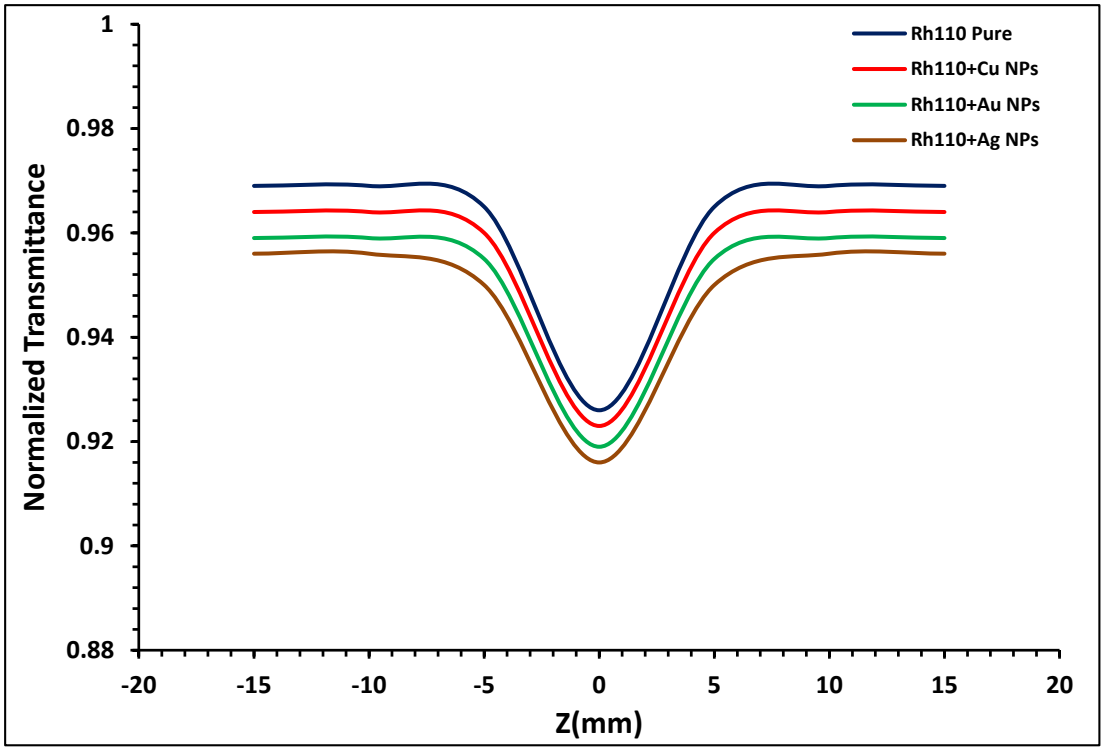

Figure (4.41): The normalized transmittance of open-aperture Z-Scan measurements as a function of distance for Rh 110 dye solutions dissolved in Methanol solvent with different nanoparticles

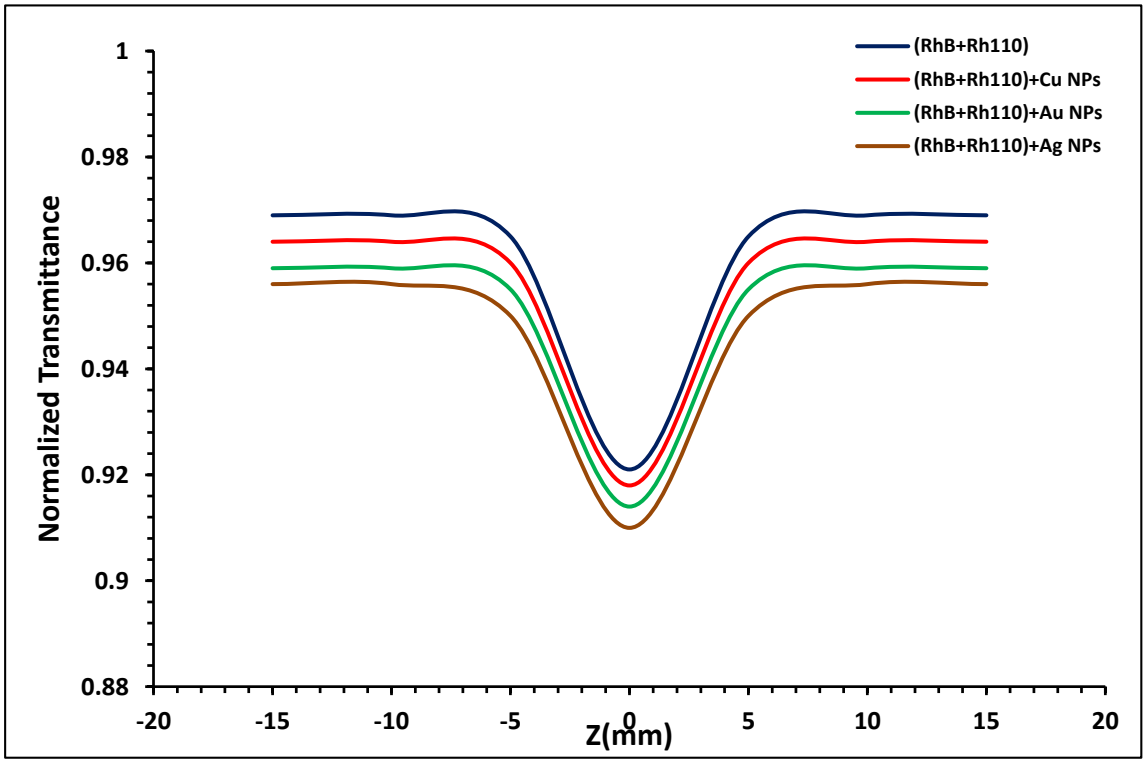

Figure (4.42): The normalized transmittance of open-aperture Z-Scan measurements as a function of distance for Rh mix dye solutions dissolved in Methanol solvent with different nanoparticles

Table (4.8) shows the nonlinear absorption coefficient properties of organic dye solutions and their mixtures dissolved in methanol solvent with different nanoparticles. It is noted from the table that the highest value of the nonlinear absorption coefficient (β) is for pure organic dye solutions and their mixtures without adding nanoparticles, It is also noted that the values of the nonlinear absorption coefficient for all the prepared solutions are lower compared to the solutions dissolved in the Ethanol solvent, and the reason for this is due to the polarity of the Methanol solvent.

Table (4.8): The nonlinear absorption coefficient Properties of organic dye solutions and their mixtures dissolved in Methanol solvent with different nanoparticles at λ=532nm

Samples	T(z)	β (cm/mW)
Rh B Pure	0.917	2.31×10^{-3}
Rh B+Cu NPs	0.913	2.23×10^{-3}
Rh B+Au NPs	0.910	2.16×10^{-3}
Rh B+Ag NPs	0.907	2.12×10^{-3}
Rh 110 Pure	0.926	2.63×10^{-3}
Rh 110+Cu NPs	0.923	2.44×10^{-3}
Rh 110+Au NPs	0.919	2.36×10^{-3}
Rh 110+Ag NPs	0.916	2.25×10^{-3}
Rh mix	0.921	2.52×10^{-3}
Rh mix + Cu NPs	0.918	2.31×10^{-3}
Rh mix +Au NPs	0.914	2.24×10^{-3}
Rh mix +Ag NPs	0.910	2.16×10^{-3}

4.5 Optical Limiting Behavior

The optical limiting behavior of Rh B, Rh 110 and Rh mix organic dyes solutions dissolved in Ethanol and Methanol solvents at (0.05 mM) with different nanoparticles (Cu, Au and Ag) NPs were measured by optical limiting setup. Figures (4.43 - 4.48) shows the optical limiting characteristics at room temperature for all samples were dissolved in (Ethanol and Methanol) solvents respectively.

From these Figures, it is noted that each prepared sample has a threshold intensity that depends on the values of the nonlinear refractive index and is inversely proportional to it, so the highest value of the threshold intensity was for Pure dyes solutions, in addition to that solutions dissolved in Ethanol solvent give the highest threshold intensity compared to solutions dissolved in solvent Methanol.

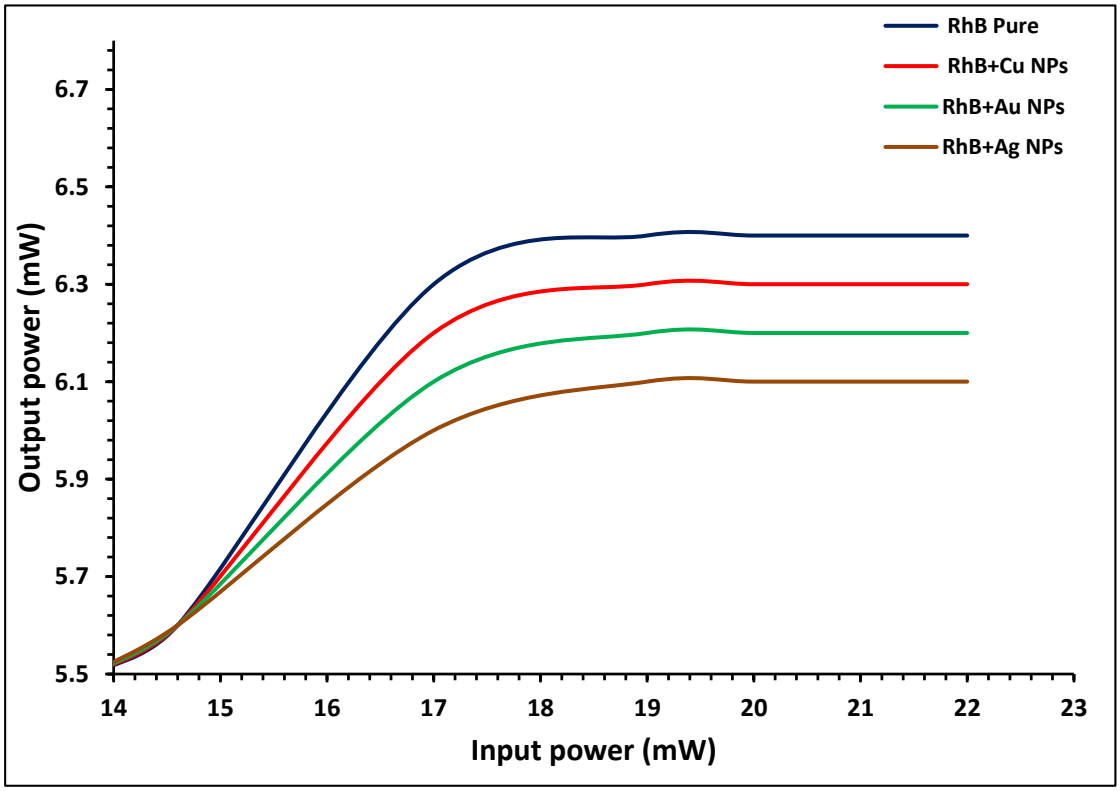

Figure (4.43): The optical limiting response for Rh B dye solutions dissolved in Ethanol solvent with different nanoparticles

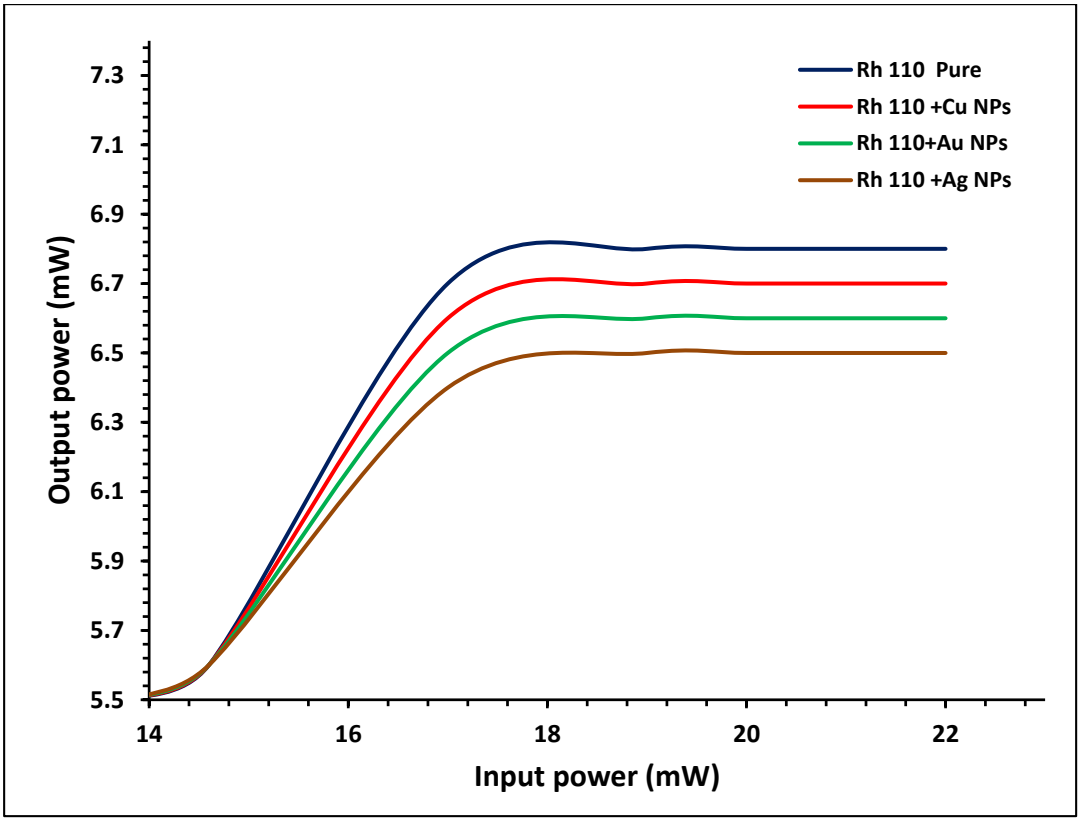

Figure (4.44): The optical limiting response for Rh 110 dye solutions dissolved in Ethanol solvent with different nanoparticles.

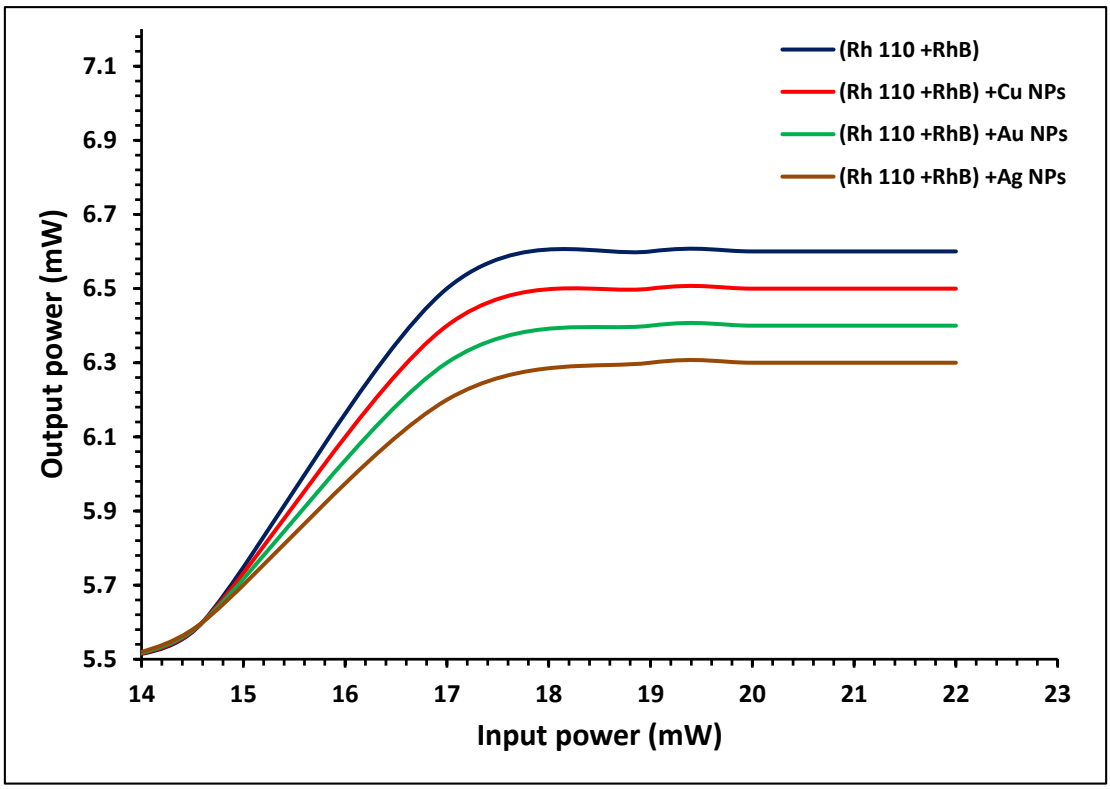

Figure (4.45): The optical limiting response Rh mix dye solutions dissolved in Ethanol solvent with different nanoparticles.

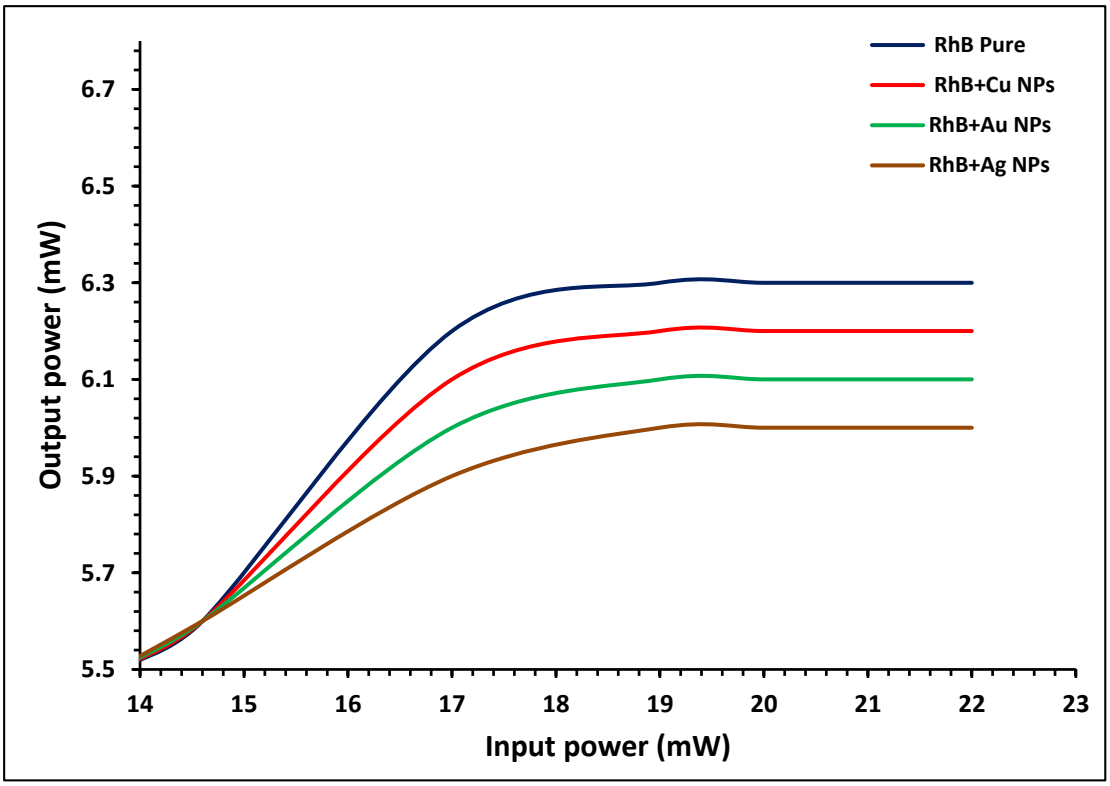

Figure (4.46): The optical limiting response for Rh B dye solutions dissolved in Methanol solvent with different nanoparticles

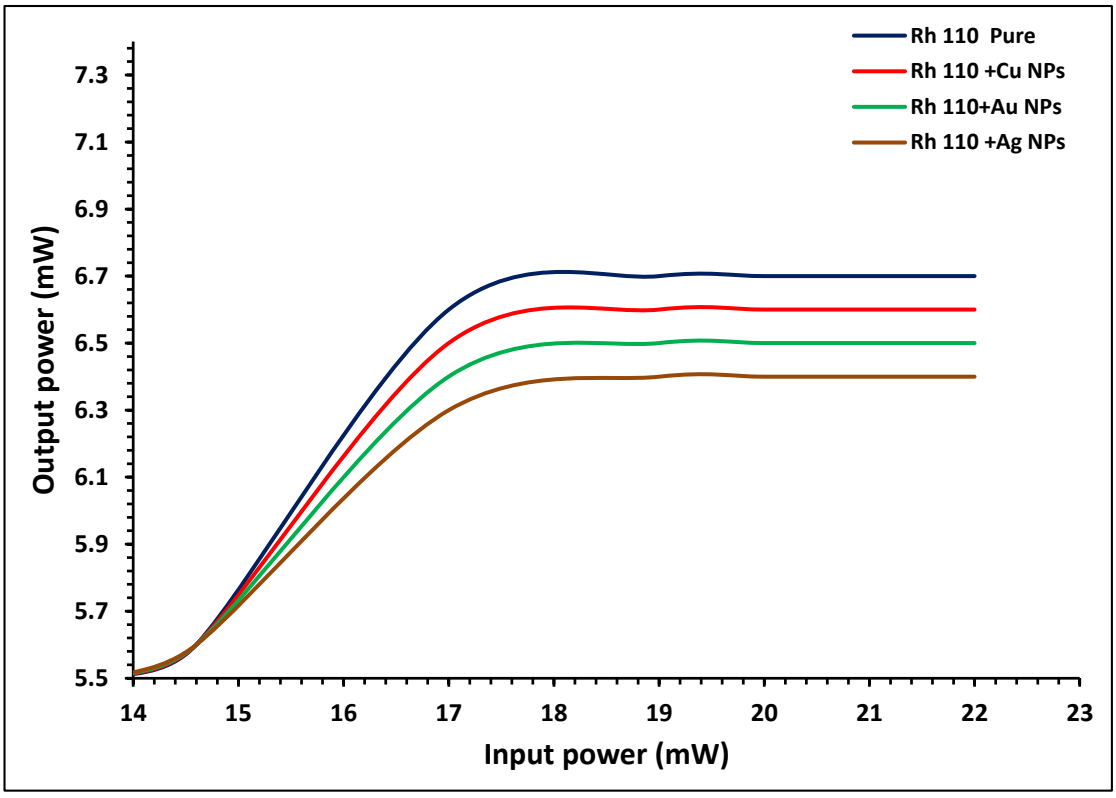

Figure (4.47): The optical limiting response for Rh 110 dye solutions dissolved in Methanol solvent with different nanoparticles.

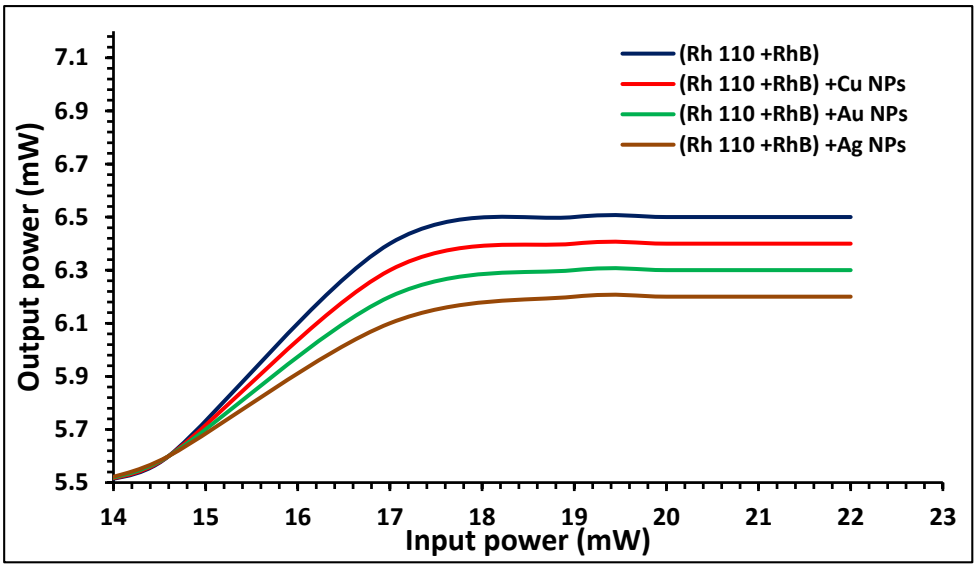

Figure (4.48): The optical limiting response Rh mix dye solutions dissolved in Methanol solvent with different nanoparticles.

Table (4.9): The optical limiting response of Rh B ,Rh 110 and Rh mix organic laser dyes in ethanol solved

Sample	Concentration(Mm)	Limiting Threshold	Limiting Amplitude
RhB pure	0.05	6.4	22
Rh B +Cu Nps	0.05	6.3	21
Rh B +Au Nps	0.05	6.2	20
Rh B +Ag Nps	0.05	6.1	19
Rh110 pure	0.05	6.8	24
Rh 110 +Cu Nps	0.05	6.7	23
Rh 110 +Au Nps	0.05	6.5	22
Rh 110 +Ag Nps	0.05	6.5	21
Rh mix pure	0.05	6.6	23
Rh mix +Cu Nps	0.05	6.5	22
Rh mix +Au Nps	0.05	6.4	21
Rh mix +Ag Nps	0.05	6.3	20

Table (4.10): The optical limiting response of Rh B ,Rh 110 and Rh mix organic laser dyes in methanol solved

Sample	Concentration(Mm)	Limiting Threshold	Limiting Amplitude
RhB pure	0.05	6.3	19
Rh B +Cu Nps	0.05	6.2	18
Rh B +Au Nps	0.05	6.1	17
Rh B +Ag Nps	0.05	6	16
Rh110 pure	0.05	6.6	21
Rh 110 +Cu Nps	0.05	6.5	20
Rh 110 +Au Nps	0.05	6.5	19
Rh 110 +Ag Nps	0.05	6.4	18
Rh mix pure	0.05	6.5	20
Rh mix +Cu Nps	0.05	6.4	19
Rh mix +Au Nps	0.05	6.3	18
Rh mix +Ag Nps	0.05	6.2	17

4.6 Conclusions

The main conclusions that are obtained in this work:

1. The absorbance values and the linear optical coefficients (linear absorption coefficient and linear refractive index) increase with the increase in the concentration of the dyes and their mixture. Rhodamine B dye gives the highest values compared to the other dye and the mixture. Also, these values are higher for the dyes dissolved in methanol solvent compared to the ethanol solvent.
2. The possibility of preparing nanoparticles (Cu, Au and Ag) NPs by liquid pulsed laser ablation and using them as a mixture with organic dyes in some optical applications.
3. The values of absorbance and linear optical coefficients at the wavelength used increase by adding the prepared nanoparticles, and the highest of these values are for the mixture of Rhodamine B dye dissolved in methanol solvent with Ag NPs prepared with the same type of solvent.
4. The nonlinear optical properties of laser organic dye mixture solutions with nanoparticles prepared in this study showed that all these solutions give nonlinear absorption (absorption of two photons), and also that these solutions are considered nonlinear materials as a de-focusing medium.
5. The possibility of using all samples of pure and grafted dyes and their mixtures in various electro-optical applications as optical limiting.

4.7 The Suggestions and Future Works

In this context, a further investigation can be suggested as future works:

1. Studying spectral linear and nonlinear optical properties of mixture dyes solutions with another types of solvents at different concentrations.
2. Studying nonlinear optical properties of dyes using lasers with different wave lengths and different powers.
3. Studying effect for adding another type of nanoparticles on spectral, linear and non-linear of new mixture of other laser dyes.
4. Studying effect for adding types of polymers on spectral, linear and non-linear of new mixture of other laser dyes.

References

[1] Corless, J. D., West, J. A., Bromage, J., & Stroud Jr, C. R. (1997). Pulsed single-mode dye laser for coherent control experiments. Review of scientific instruments, 68(6), 2259-2264.

[2] Burlamacchi, P., & Pratesi, R. (1976). GHz tuning of a planar dye laser with single dispersive element. Applied Physics Letters, 28(3), 124-126.

[3] Burlamacchi, P., & Pratesi, R. (1976). GHz tuning of a planar dye laser with single dispersive element. Applied Physics Letters, 28(3), 124-126.

[5] Lambda physik, Wall chart, 3rd edition,(1996).

[6] Singh, S., Kanetkar, V. R., Sridhar, G., Muthuswamy, V., & Raja, K. (2003). Solid-state polymeric dye lasers. Journal of Luminescence, 101(4), 285-291.

[7] Feng, W., Yi, W., Wu, H., Ozaki, M., & Yoshino, K. (2005). Enhancement of third-order optical nonlinearities by conjugated polymer-bonded carbon nanotubes. Journal of applied physics, 98(3).

[8] Jaber, W. (2015). A Study of Optical Properties of Acridine Dye and Alumina Nanoparticles Doped in PMMA Polymer (Doctoral dissertation, University of Babylon,).

[9] Jaffar, A. F., Akram, I. N., Salman, A. M., & Al-Taai, Q. A. (2020). Nonlinear properties of olive oil films doped with poly (methyl methacrylate), polystyrene and their blend by using z-scan technique. International Journal.

[10] Radhi, F. S. (2012). Nonlinear responses and optical limiting behavior of 2-Chloro-5-nitroanisole dye under CW laser illumination. Journal of Kerbala University, 10(4).

References

[11] F. Radhi, *" Nonlinear Responses and Optical Limiting Behavior of 2-Chloro-5-Nitroanisole Dye Under CW Laser Illumination"* ,Journal of Kerbala University,10, 4,181 – 186, (2012).

[12] Mahdi, Z. F. (2010). Improvement of nonlinear optical properties for mixture laser dyes doped PMMA. Iraqi J. Laser, 9(2), 9-14.

[13] Balaji, G., Rekha, R., & Ramalingam, A. (2011). Nonlinear characterization of safranin O dye for application in optical limiting. Acta Physica Polonica A, 119(3), 359-363.

[14] Ali, R. A., Abdul-Munem, O. M., & Abd, A. N. (2012). Study the spectroscopic characteristics of Rhodamine B Dye in Ethanol and Methanol mixture and Calculation the Quantum Efficiency. Baghdad Science Journal, 9(2), 352-358.

[15] Hajiesmaeilbaigi, F., Motamedi, A., Golian, Y., & Nik, E. B. (2012, November). Linear and nonlinear optical properties of Rhodamine B dye solution with Au nanoparticles. In Quantum and Nonlinear Optics II (Vol. 8554, pp. 146-151). SPIE.

[16] Al-Hamdani Ali, H., Rajaa, N., & Rafah, A. H. (2014). Spectral Properties of Rodamine B dissolved in Chloroform. IOSR Journal of Research & Method in Education (IOSR-JRME), 4(6), 68-7.

[17] Kitching, H., Kenyon, A. J., & Parkin, I. P. (2014). The interaction of gold and silver nanoparticles with a range of anionic and cationic dyes. Physical Chemistry Chemical Physics, 16(13), 6050-6059.

[18] Parvin, U. M., & Ahamed, M. B. (2015). Nonlinear optical properties of methyl blue dye by Z-scan technique. Optik, 126(5), 551-553.

[19] Boudebs, G., Wang, H., Cassagne, C., & Chniti, M. (2016, July). Dark-field Z-scan imaging technique and application to optical nonlinear

refraction measurement. In 2016 18th International Conference on Transparent Optical Networks (ICTON) (pp. 1-4). IEEE. [20] Jeyaram, S., and T. Geethakrishnan. "Third-order nonlinear optical properties of acid green 25 dye by Z─ scan method." Optics & Laser Technology 89,PP. 179-185, 2017.

[21] Khlaif, L. G. (2017). The study of nonlinear optical properties of rhodamine B dye and TiO2 nanoparticles doped in PMMA polymer. Iraqi Journal of Physics, 15(33), 96-100.

[22] Al-Hamdani, A. H. (2018). Third Order Nonlinear Properties of Rhodamine B Dye Doped PVA Polymer Determined by Eclipsing Scan Technique. International Journal of Nanoelectronics and Materials, 11(2), 135-142.

[23] Dong, J., Carpinone, P. L., Pyrgiotakis, G., Demokritou, P., & Moudgil, B. M. (2020). Synthesis of precision gold nanoparticles using Turkevich method. KONA Powder and Particle Journal, 37, 224-232.

[24] Prakash, A., Pathrose, B. P., Radhakrishnan, P., & Mujeeb, A. (2020). Nonlinear optical properties of neutral red dye: Enhancement using laser ablated gold nanoparticles. Optics & Laser Technology, 130, 106338.

[25] Prakash, Anitha, Bini P. Pathrose, P. Radhakrishnan, and A. Mujeeb. "Nonlinear optical properties of neutral red dye: Enhancement using laser ablated gold nanoparticles." Optics & Laser Technology 130: 106338, 2020.

[26] Habeeba, A. U., Saravanan, M., Girisun, T. S., & Anandan, S. (2021). Nonlinear optical studies of conjugated organic dyes for optical limiting applications. Journal of Molecular Structure, 1240, 130559.

References

[27] Ali, F.H. and Naser, B.A., 2022, November. Optical nonlinearities and optical limiting behaviors for mixture of organic laser dyes. In AIP Conference Proceedings (Vol. 2394, No. 1). AIP Publishing.

[28] Silva, E., Vilchis-Nestor, A. R., De La Cruz, W., Regalado-Contreras, A., Castro-Beltran, A., & Luque, P. A. (2023). Analysis of the structural, morphological, and optical properties of Selaginella lepidophylla-mediated ZnO semiconductor nanoparticles and their influence on the photocatalytic removal of Rhodamine B dye. Journal of Materials Science: Materials in Electronics, 34(17), 1330.

[29] Maeda, M. (1984). Laser Dyes Academic Press. New York.

[30] Förster, "Handbook of Chemistry and Physics," Zeitschrift fur Phys. Chemie, vol. 8, no. 5–6, p. 394, 1956.(1984)

[31] Crenshaw, B. R., Kunzelman, J., Sing, C. E., Ander, C., & Weder, C. (2007). Threshold temperature sensors with tunable properties. Macromolecular Chemistry and Physics, 208(6), 572-580.

[32] Bosshard, C., Canva, M., Dalton, L., Gubler, U., Jin, J. I., Shim, H. K., & Stegeman, G. I. (2002). Polymers for photonics applications I (Vol. 158). Springer Science & Business Media.

[33] Singh, S., Kanetkar, V. R., Sridhar, G., Muthuswamy, V., & Raja, K. (2003). Solid-state polymeric dye lasers. Journal of Luminescence, 101(4), 285-291.

[34] Paul, D. R., & Robeson, L. M. (2008). Polymer nanotechnology: nanocomposites. Polymer, 49(15), 3187-3204.

[35] Mirza, I., & Lunney, J. G. (2011). Fabrication of metal nanoparticle films using pulsed laser deposition. 30th ICPIG, Belfast, Northern Ireland, UK (Aug. 28–Sept. 2, 2011).

References

[36] Shankarling, G. S., & Jarag, K. J. (2010). Laser dyes. Resonance, 15, 804-818.

[37] Raikar, U. S., Tangod, V. B., Mastiholi, B. M., & Sreenivasa, S. (2010). Solvent effects and photophysical studies of ADS560EI laser dye. African Journal of Pure and Applied Chemistry, 4(9), 188-197.

[39] Ali, Q. R. (2013). Photobleaching Spectroscopic Studies and Lifetime Measurements of Fluorescent Organic Dyes. a thesis, University of Baghdad, College of Science.

[40] Nagachandra, K. H., Mannekutla, J. R., Amarayya, S. M., & Inamdar, S. R. (2012). Solvent effect on the spectral properties of dipolar laser dyes: Evaluation of ground and excited state dipole moments. European Journal of Chemistry, 3(2), 163-171.

[41] Mannekutla, J. R., Mulimani, B. G., & Inamdar, S. R. (2008). Solvent effect on absorption and fluorescence spectra of coumarin laser dyes: evaluation of ground and excited state dipole moments. Spectrochimica Acta Part A: Molecular and Biomolecular Spectroscopy, 69(2), 419-426.

[42] Schäfer, F. P. (Ed.). (2013). Dye lasers (Vol. 1). Springer Science & Business Media.

[43] Yahia, I. S., Rammah, Y. S., & Khaled, K. F. (2013). Fabrication of an electrochemical cell based on Rhodamine B Dye for low power applications. Journal of Materials and Environmental Science, 4(3), 442-47.

[44] Sharifzade, G., Asghari, A., & Rajabi, M. (2017). Highly effective adsorption of xanthene dyes (rhodamine B and erythrosine B) from aqueous solutions onto lemon citrus peel active carbon: characterization, resolving analysis, optimization and mechanistic studies. RSC advances, 7(9), 5362-5371.

References

[45] Arbeloa, F. L., Costela, A., & Arbeloa, I. L. (1990). Molecular structure effects on the lasing properties of rhodamines. Journal of Photochemistry and Photobiology A: Chemistry, 55(1), 97-103.

[46] Lide, D. R. (Ed.). (2004). CRC handbook of chemistry and physics (Vol. 85). CRC press.

[47] Windholz, M., Budavari, S., Stroumtsos, L. Y., & Fertig, M. N. (1976). The Merck index. An encyclopedia of chemicals and drugs (No. 9th edition).

[48] Barbero, N., Barni, E., Barolo, C., Quagliotto, P., Viscardi, G., Napione, L., ... & Bussolino, F. (2009). A study of the interaction between fluorescein sodium salt and bovine serum albumin by steady-state fluorescence. Dyes and pigments, 80(3), 307-313.

[49] Elvers, B. (1991). Ullmann's encyclopedia of industrial chemistry (Vol. 17, pp. 363-376). Hoboken, NJ: Verlag Chemie.

[50] Timmermans, J. (1950). Physico-Chemical Constants of Pure Organic Compounds Elsevier Publ. Co. Inc.[New York 1950] S, 39.

[51]El-Sayed, M. A. (2004). Small is different: shape-, size-, and composition-dependent properties of some colloidal semiconductor nanocrystals. Accounts of chemical research, 37(5), 326-333.

[52] Okubo, T. (2008). Nanoparticles: syntheses, stabilization, passivation and functionalization. Nagarajan R, Hatton TA (eds), 256.

[53] Miraz, I. and Lunney, J.G. Fabrication of metal nanoparticle films using pulsed laser deposition. 30th ICPIG, Belfast, Northern Ireland, UK.2011

[54] Ali, A. K., & Raouf, D. N. (2011). Preparation of silver nanoparticles by pulsed laser ablation in liquid medium. Eng. & Tech. Journal, 29(15).

[55] Lazarides, A. A., & Schatz, G. C. (2000). DNA-linked metal nanosphere materials: Fourier-transform solutions for the optical response. The Journal of Chemical Physics, 112(6), 2987-2993.

References

[56] Drukker, K., Wu, G., & Schatz, G. C. (2001). Model simulations of DNA denaturation dynamics. The Journal of Chemical Physics, 114(1), 579-590.

[57] El-Sayed, M. A. (2001). Some interesting properties of metals confined in time and nanometer space of different shapes. Accounts of chemical research, 34(4), 257-264.

[58] Alagarasi, A. (2013). Chapter-introduction to nanomaterials. Indian Institute of Technology Madras, 1-24.

[59] Wheeb, A. H., Mahdi, Z. F., & Faris, R. A. (2012). The nonlinear optical properties of Epoxy/Alumina Nanocomposites. Iraqi Journal of Laser, 11(A), 29-38.

[60] Contreras, J. E., Rodriguez, E. A., & Taha-Tijerina, J. (2017). Nanotechnology applications for electrical transformers—A review. Electric Power Systems Research, 143, 573-584.

[61] Berube, D., Cummings, C., Cacciatore, M., Scheufele, D., & Kalin, J. (2011). Characteristics and classification of nanoparticles: expert Delphi survey. Nanotoxicology, 5(2), 236-243.

[62] Tiwari, J. N., Tiwari, R. N., & Kim, K. S. (2012). Zero-dimensional, one-dimensional, two-dimensional and three-dimensional nanostructured materials for advanced electrochemical energy devices. Progress in Materials Science, 57(4), 724-803.

[63] Piquemal, J. Y., Briot, E., & Brégeault, J. M. (2013). Preparation of materials in the presence of hydrogen peroxide: from discrete or “zero-dimensional” objects to bulk materials. Dalton Transactions, 42(1), 29-45.

[64]Yeap, S. P. (2018). Permanent agglomerates in powdered nanoparticles: Formation and future prospects. Powder Technology, 323, 51-59.

References

[65] Gubicza, J. Defect structure and properties of nanomaterials. Woodhead Publishing.2017

[66] Zhang, H., Toshima, N., Takasaki, K., & Okumura, M. (2014). Preparation of Agcore/Aushell bimetallic nanoparticles from physical mixtures of Au clusters and Ag ions under dark conditions and their catalytic activity for aerobic glucose oxidation. Journal of alloys and compounds, 586, 462-468.

[67] Sun, B., Jiang, X., Dai, S., & Du, Z. (2009). Single-crystal silver nanowires: preparation and surface-enhanced Raman scattering (SERS) property. Materials letters, 63(29), 2570-2573.

[68] Biener, J., Wittstock, A., Baumann, T. F., Weissmüller, J., Bäumer, M., & Hamza, A. V. (2009). Surface chemistry in nanoscale materials. Materials, 2(4), 2404-2428.

[69] Kumar, P., Robins, A., Vardoulakis, S., & Britter, R. (2010). A review of the characteristics of nanoparticles in the urban atmosphere and the prospects for developing regulatory controls. Atmospheric Environment, 44(39), 5035-5052.

[70] Birks, J. B. (1976). Organic molecular photophysics, Vol. 2.

[71] Alarcon, E. I., Griffith, M., & Udekwu, K. I. (2015). Silver nanoparticle applications. Springer International Publishing. doi, 10, 978-

[72] Ogarev, V. A., Rudoi, V. M., & Dement'eva, O. V. (2018). Gold nanoparticles: synthesis, optical properties, and application. Inorganic Materials: Applied Research, 9, 134-140.

[73] Hu, M., Chen, J., Li, Z. Y., Au, L., Hartland, G. V., Li, X., ... & Xia, Y. (2006). Gold nanostructures: engineering their plasmonic properties for biomedical applications. Chemical Society Reviews, 35(11), 1084-1094.

References

[74] Lan, T., Dong, C., Huang, X., & Ren, J. (2011). Single particle technique for one-step homogeneous detection of cancer marker using gold nanoparticle probes. Analyst, 136(20), 4247-4253.

[75]Dudley, C. (2004). Absorption, fluorescence and amplified spontaneous emission of blue-emitting dyes (Doctoral dissertation, Washington State University).

[76] Lan, T., Dong, C., Huang, X., & Ren, J. (2011). Single particle technique for one-step homogeneous detection of cancer marker using gold nanoparticle probes. Analyst, 136(20), 4247-4253.

[77] Maslyukov, A., Sokolov, S., Kaivola, M., Nyholm, K., & Popov, S. (1995). Solid-state dye laser with modified poly (methyl methacrylate)-doped active elements. Applied optics, 34(9), 1516-1518.

[78] Turrell, G., & Corset, J. (Eds.). (1996). Raman microscopy: developments and applications. Academic Press.

[79] Demtröder, W. (1982). Laser spectroscopy (Vol. 2). Berlin, Heidelberg: springer.

[80] Alda, J. (2003). Laser and Gaussian beam propagation and transformation. Encyclopedia of optical engineering, 999, 1013-1013.

[81] Millar, V. (1993). New extended methine dyes for application in laser technology (Doctoral dissertation, University of Leeds).

[82] Ban A. Naser, Asim A. Balakit, Alhak A. Muslim and Abdulazeez O. Mousa, 2018. Study of the Nonlinear Optical Properties of New Diarylethene Perfluorocyclopentene Derivative by Using Z-scan Technique. Journal of Engineering and Applied Sciences, 13: 9597-9601

[83] Yakop, N. A. H. S., & Badran, H. A. (2014). Single-beam Z-scan measurement of the third-order optical nonlinearities of ethidium bromide. J. Eng. Res. Appl, 4(1), 727-731.

[84] Faris, R. A., & Al-Bawi, Z. F. (2017). Investigation of Some Optical Properties for Prepared Silver Nanoparticles embedded in polymer film.

References

[85] Wooten, F., (1973). Optical properties of solids. American Journal of Physics, 41(7)939-940.2017

[86] Fox, M. (2002). Optical properties of solids.

[87] Kittel, C. (2005). Introduction to solid state physics. John Wiley & sons, inc.

[88] Khalaf, R. Manshad. (2001). Studing of Nonlinear Optical Properties for Organic Dye (Doctoral dissertation, thesis, University of Basrah).2013

[89] Hemerik, M. M. (2001). Design of a mid-infrared cavity ring down spectrometer.

[90] Turner, D. B., Wilk, K. E., Curmi, P. M., & Scholes, G. D. (2011). Comparison of electronic and vibrational coherence measured by two-dimensional electronic spectroscopy. The Journal of Physical Chemistry Letters, 2(15), 1904-1911.

[91] Arbeloa, F. L., Costela, A., & Arbeloa, I. L. (1990). Molecular structure effects on the lasing properties of rhodamines. Journal of Photochemistry and Photobiology A: Chemistry, 55(1), 97-103.

[92] Saleh, B. E., & Teich, M. C. (2008). Fundamentals of photonics (Vol. 332). New York: Wiley.

[93] Kabashin, A. V., & Meunier, M. (2003). Synthesis of colloidal nanoparticles during femtosecond laser ablation of gold in water. Journal of Applied Physics, 94(12), 7941-7943.

[94] Arbeloa, F. L., Costela, A., & Arbeloa, I. L. (1990). Molecular structure effects on the lasing properties of rhodamines. Journal of Photochemistry and Photobiology A: Chemistry, 55(1), 97-103.

[95] McWeeny, R. (2007). Atoms, molecules, matter–the stuff of chemistry.

References

[96] Lazzeretti, P. (2019). Continuity equations for electron charge densities and current densities induced in molecules by electric and magnetic fields. The Journal of Chemical Physics, 151(11).

[97] Atkins, P. W., & Friedman, R. S. (2011). Molecular quantum mechanics. Oxford university press.

[98] Abdul-Zahra, A. (2008). Investigation of nonlinear optical properties for laser dyes-doped polymer thin film", Thesis, University of Baghdad Institute of Laser for Postgraduate Studies.

[99] Loicq, J., Renotte, Y., Delplancke, J. L., & Lion, Y. (2004). Non-linear optical measurements and crystalline characterization of CdTe nanoparticles produced by the 'electropulse'technique. New Journal of Physics, 6(1), 32.

[100] S Radhi, F. (2012). Nonlinear responses and optical limiting behavior of 2-Chloro-5-nitroanisole dye under CW laser illumination. journal of kerbala university, 8(2), 181-186.

[101] Fuh, A. Y. G., Lin, H. C., Mo, T. S., & Chen, C. H. (2005). Nonlinear optical property of azo-dye doped liquid crystals determined by biphotonic Z-scan technique. Optics express, 13(26), 10634-10641.

[102] Patil, P. S., Maidur, S. R., Rao, S. V., & Dharmaprakash, S. M. (2016). Crystalline perfection, third-order nonlinear optical properties and optical limiting studies of 3, 4-Dimethoxy-4′-methoxychalcone single crystal. Optics & Laser Technology, 81, 70-76.

[103] Jeyaram, S., & Geethakrishnan, T. (2017). Third-order nonlinear optical properties of acid green 25 dye by Z─ scan method. Optics & Laser Technology, 89, 179-185.

[104] Jasim, K. E. (2019). Third-order nonlinear optical properties of quantum dots. Standards, methods and solutions of metrology.

[105] Medhekar, S., Kumar, R., Mukherjee, S. and Choubey, R.K., February. Study of nonlinear refraction of organic dye by Z-scan technique

using He–Ne laser. In AIP conference proceedings (Vol. 1512, No. 1, pp. 470-471). American Institute of Physics.2013

[106] Henari, F. Z., & Patil, P. S. (2014). Nonlinear optical properties and optical limiting measurements of {(1Z)-[4-(dimethylamino) phenyl] methylene} 4-nitrobenzocarboxy hydrazone monohydrate under CW laser regime. Optics and Photonics Journal, 2014.

[107] Nooraldeen, A. Y., Palanichant, M., & Palanisamy, P. K. (2009). Influence of solvents polarity on NLO properties of fluorone dye. International journal of nonlinear Science, 7(3), 290-300.

[108] Abd AL-Adel, K., & Badran, H. A. (2012). The Study of the Nonlinear Optical Properties of Solutions under CW Laser Illumination. Journal of Basrah Researches (Sciences), 38(4), 73-79.

[109] Abd AL-Adel, K., & Badran, H. A. (2012). The Study of the Nonlinear Optical Properties of Solutions under CW Laser Illumination. Journal of Basrah Researches (Sciences), 38(4), 73-79.

[110] Gamernyk, R. V., Periv, M. V., Malynych, S. Z., & Zaichenko, O. S. (2016). Spatial coherency of light and nonlinear optical properties of colloidal gold studied by CW Z-scan technique. NanoWorld Journal, 1(2).

[111] Razook, Z. N. (2011). Study of Spectral Properties of Eosiny Dye Dope Polymer PMMA", M.Sc. thesis, AL-Mustansiriyah University, college of science.

[112] Muncheryan, H. M. (1983). Principles and practice of laser technology.

[114] Ladoulis, C. T., & Gill III, T. J. (1970). Physical chemical studies on the specific interaction of an acriflavine-phosphotungstic Acid complex with double-stranded nucleic acids. The Journal of cell biology, 47(2), 500-511.

[115] Bhushan, B. (Ed.). (2017). Springer handbook of nanotechnology. Springer.

References

[116] Winter, C. S., Manning, R. J., Oliver, S. N., & Hill, C. A. S. (1992). Measurement of the large optical nonlinearity of nickel dithiolene doped polymers. Optics communications, 90(1-3), 139-143.

[117] Li, X. D., Zhai, Q. Z., & Zou, M. Q. (2010). Optical properties of (nanometer MCM-41)–(malachite green) composite materials. Applied Surface Science, 257(3), 1134-1140.

[118] Jaffar, A. F. (2012). Optical Nonlinearity of Oxazine Dye Doped PMMA Films by Z-Scan Techniques. Al-Nahrain Journal of Science, 15(2), 106-112.

[119] Li, Y., & Luo, D. (2016). Fabrication and application of 1D micro-cavity film made by cholesteric liquid crystal and reactive mesogen. Optical Materials Express, 6(2), 691-696.

[120] Saini, G. S. S., Kaur, S., Tripathi, S. K., Mahajan, C. G., Thanga, H. H., & Verma, A. L. (2005). Spectroscopic studies of rhodamine 6G dispersed in polymethylcyanoacrylate. Spectrochimica Acta Part A: Molecular and Biomolecular Spectroscopy, 61(4), 653-658.

[121] Badran, H. A., Al-Ahmad, A. Y., & Al-Mudhaffer, M. F. (2011). Study of the linear and nonlinear optical properties of Neutral Red doped Polyvinylpyrrolidone film. Journal of Basrah Researches ((Sciences)), 37(2).

[122] Dancus, I., Vlad, V. I., Petris, A., Frunza, S., Beica, T., Zgura, I., ... & Vuluga, D. M. (2010). Low power laser induced optical nonlinearities in organic molecules. Romanian Reports in Physics, 62(3), 567-580.

[123] Khilkhal, W. M., Al-Dahash, G. A., & Wahid, S. N. A. (2015). Study the effect of the aqueous media on the properties of produced copper nanoparticles colloidal by using laser ablation technique. J. Eng. Technol, 33(5), 830-837.

References

[124] Al Hussainey, A. M., & Naser, B. A. (2021). Non-linear optical properties of organic laser dye. Annals of the Romanian Society for Cell Biology, 25(6), 11556-11567.

[125] Arbeloa, F. L., Costela, A., & Arbeloa, I. L. (1990). Molecular structure effects on the lasing properties of rhodamines. Journal of Photochemistry and Photobiology A: Chemistry, 55(1), 97-103.

[126] Barbero, N., Barni, E., Barolo, C., Quagliotto, P., Viscardi, G., Napione, L., ... & Bussolino, F. (2009). A study of the interaction between fluorescein sodium salt and bovine serum albumin by steady-state fluorescence. Dyes and pigments, 80(3), 307-313.

[127] Timmermans, J. (1950). Physico-chemical constants of pure organic compounds. Elsevier Publishing.

[128] Speight, J. (2005). Lange's handbook of chemistry. McGraw-Hill Education.

[129] Ali, Q. R. (2013). Photobleaching Spectroscopic Studies and Lifetime Measurements of Fluorescent Organic Dyes. a thesis, University of Baghdad, College of Science.

[130] Dijkkamp, D., Venkatesan, T., Wu, X. D., Shaheen, S. A., Jisrawi, N., Min-Lee, Y. H., ... & Croft, M. (1987). Preparation of Y-Ba-Cu oxide superconductor thin films using pulsed laser evaporation from high T c bulk material. Applied Physics Letters, 51(8), 619-621.

[132] Ogale, S. B., Patil, P. P., Phase, D. M., Bhandarkar, Y. V., Kulkarni, S. K., Kulkarni, S., ... & Guha, S. (1987). Synthesis of metastable phases via pulsed-laser-induced reactive quenching at liquid-solid interfaces. Physical Review B, 36(16), 8237.

[133] Fultz, B., & Howe, J. M. (2012). Transmission electron microscopy and diffractometry of materials. Springer Science & Business Media.

References

[135] Raikar, U. S., Tangod, V. B., Mastiholi, B. M., & Sreenivasa, S. (2010). Solvent effects and photophysical studies of ADS560EI laser dye. African Journal of Pure and Applied Chemistry, 4(9), 188-197.

[136] Zhang, H., Toshima, N., Takasaki, K., & Okumura, M. (2014). Preparation of Agcore/Aushell bimetallic nanoparticles from physical mixtures of Au clusters and Ag ions under dark conditions and their catalytic activity for aerobic glucose oxidation. Journal of alloys and compounds, 586, 462-468.

[137] Jeyaram, S., & Geethakrishnan, T. (2017). Third-order nonlinear optical properties of acid green 25 dye by Z─ scan method. Optics & Laser Technology, 89, 179-185.

[138] Alnayli, R. S., Shanon, Z. S., & Hadi, A. S. (2019, July). Study the linear and nonlinear optical properties for laser dye Rhodamine B. In Journal of Physics: Conference Series (Vol. 1234, No. 1, p. 012022). IOP Publishing.

[139] Gawande, M. B., Goswami, A., Felpin, F. X., Asefa, T., Huang, X., Silva, R., ... & Varma, R. S. (2016). Cu and Cu-based nanoparticles: synthesis and applications in catalysis. Chemical reviews, 116(6), 3722-3811.

الخلاصة

في هذا العمل حُضرت محاليل صبغات عضوية ليزرية (صبغة الرودامين 110 ، صبغة الرودامين B) وخليطهما المذابة بمذيبات عضوية (الايثانول والميثانول) وبتراكيز مختلفة (0.01,0.03,0.05) ملي مولاري .دُرست الخصائص البصرية الخطية لجميع المحاليل المحضرة وذلك باستخدام مطياف الاشعة المرئية-الفوق البنفسجية، بينت النتائج ان قيم الامتصاصية وقيم المعاملات البصرية الخطية (معامل الامتصاص الخطي ومعامل الانكسار الخطي) تزداد بزيادة التركيز وان اعلى هذه القيم هي للصبغات المذابة بمذيب الميثانول وان صبغة الرودامين B تعطي اعلى القيم مقارنة بالصبغة الاخرى والخليط.

حُضرت بعض المواد النانوية المعدنية (Cu,Au,and Ag)NPs بطريقة الاستئصال بالليزر النبضي بالسوائل وذلك باستخدام ليزر الانديوم- ياك ذات الطول الموجي (1064 nm) يطلق حزمة ليزرية بطاقة (300 mJ) على اهداف من هذه المواد موضوعة في مذيب معين وذلك للحصول على سائل غروي حجمه (10 ml) يحتوي على المواد النانوية. بعد ذلك تم فحص عينات المواد النانوية باستخدام صور المجهر الالكتروني النفاذ (TEM) وصور المجهر الالكتروني الماسح (SEM) وذلك للتاكد من ابعادها النانوية وتوزيعها المتجانس داخل المحلول الغروي.

حُضرت محاليل من الصبغات العضوية الليزرية وخليطهم عند تركيز ثابت (0.05) ملي مولاري وخلط هذه المحاليل مع محاليل المواد النانوية وبنسبة (1:3) وذلك لدراسة تأثير هذه المواد على الخصائص البصرية الخطية واللاخطية لهذه الصبغات وذلك للاستفادة منها في مجال البصريات اللاخطية.

بينت نتائج الخصائص البصرية الخطية لمحاليل خليط الصبغات المستخدمة في هذه الدراسة مع المواد النانوية المحضرة ان قيم الامتصاصية والمعاملات البصرية الخطية وعند الطول الموجي المستخدم (532 nm) تزداد بإضافة المواد النانوية ، وان اعلى هذه القيم هي لمحلول خليط صبغة الرودامين B المذابة بمذيب الميثانول مع Ag NPs المحضرة بنفس نوع المذيب.

تضمنت الفحوصات اللاخطية استخدام تقنية Z-Scan في حالتي الفتحة المفتوحة و الفتحة المغلقة للحصول على معامل الامتصاص اللاخطي (β) ومعامل الانكسار اللاخطي (n_2) على التوالي. تم اداء القياسات باستخدام ليزر الحالة الصلبة ذو الطول الموجي (532) نانومتر وقدرة (50 mW) . تبين نتائج الخصائص البصرية اللاخطية لمحاليل خليط الصبغات العضوية الليزرية مع المواد النانوية المحضرة في هذه الدراسة ان جميع هذه المحاليل تعطى امتصاص لاخطي (امتصاص فوتونين) ، وان افضل قيمة لمعامل الامتصاص اللاخطي (β) هي لمحلول صبغة الرودامين ١١٠ النقية المذابة بمذيب الايثانول وهي (3.65×10^{-3} cm/mW) .كذلك تبين النتائج ايضا ان هذه المحاليل تعد من المواد اللاخطية كوسط مفرق ، وان افضل قيمة لمعامل الانكسار اللاخطي (n_2) هي (3.92×10^{-10} cm_2/mW) هي لمحلول خليط صبغة الرودامين B المذابة بمذيب الميثانول مع Ag NPs .

بينت نتائج هذه الدراسة امكانية استخدام جميع نماذج الصبغات المطعمة والنقية وخليطها في مختلف التطبيقات الكهروبصرية كمحددات للقدرة البصرية اذ تعد الصبغات العضوية الليزرية (النقية والمطعمة) من المواد الجيدة في مجال البصريات اللاخطية وتطبيقاتها وذلك لاستجابتها اللاخطية العالية التي تعمل عند مدى طيفي واسع.

جمهورية العراق
وزارة التعليم العـــالي والبحث العلـمي
جامـــعة بابـــل
كليـــة التربية للعلوم الصرفة
قســـم الفيزيـــاء

الخواص الخطية واللاخطية لصبغات ليزرية مطعمة بالجسيمات النانوية المعدنية المحضرة بطريقة الاستئصال بالليزر النبضي بالسوائل

رسالة مقدمة
الى مجلس كلية التربية للعلوم الصرفة جامعة بابل
كجزء من متطلبات نيل درجة الدكتوراه
فلسفة في التربية / الفيزياء

من قبل الطالبة

رسل كاظم محمود كاظم

بكالوريوس تربية فيزياء / جامعة بابل 2013م
ماجستير تربية فيزياء / جامعة بابل 2017 م

بأشراف

أ. د. طالب محسن عباس الشافعي

1445هـ **2023 م**